

**Aus der Medizinischen Universitätsklinik und Poliklinik Tübingen
Abteilung Innere Medizin VIII
(Schwerpunkt: Klinische Tumorbiologie)**

**Combination of the oral histone deacetylase inhibitor
resminostat with oncolytic measles vaccine virus as a
new option for epi-virotherapeutic treatment of
hepatocellular carcinoma**

**Inaugural-Dissertation
zur Erlangung des Doktorgrades
der Medizin**

**der Medizinischen Fakultät
der Eberhard Karls Universität
zu Tübingen**

**vorgelegt von
Ruf, Benjamin**

2017

Dekan:	Professor Dr. I. B. Autenrieth
1. Berichterstatter:	Professor Dr. U. M. Lauer
2. Berichterstatter:	Prof. Dr. S. Beckert
3. Berichterstatter:	Prof. Dr. J. Rommelaere

Tag der Disputation: 10.01.2017

Meiner Familie

Table of content

1	Introduction	1
1.1	Hepatocellular carcinoma	1
1.1.1	Epidemiology	1
1.1.2	Current state-of-the-art treatment options for liver cancer	2
1.2	Oncolytic virotherapy as an innovative approach in cancer treatment	2
1.2.1	History of oncolytic viruses	3
1.2.2	Principles of oncolytic virotherapy	3
1.2.3	Oncolytic virus families in clinical testing	5
1.2.4	“Assessment of current virotherapeutic application schemes” [27]	9
1.3	Oncolytic measles vaccine viruses	13
1.3.1	Virus biology	13
1.3.2	Suicide transgene expressing MeV-SCD	14
1.3.3	Measles vaccine viruses (MeV)-based oncolytic monotherapy in selected clinical trials	16
1.4	Limitations to oncolytic virotherapy	20
1.5	Innate immunity signaling following oncolytic virus infection	21
1.6	Inhibitors of histone deacetylases (HDACi)	22
1.6.1	Principles of HDACi-based cancer therapy	22
1.6.2	Resminostat, a novel histone deacetylase inhibitor	24
1.7	Epi-virotherapeutic combination therapies	27
1.8	Objective	28
2	Materials and Methods	30
2.1	Safety	30
2.2	Cell biology methods	31
2.2.1	Cell lines	31
2.2.2	General cell culture	31
2.2.3	Cryoconservation of cultured cells	32
2.2.4	Thawing of cell lines	32
2.2.5	Cell counting using a Neubauer haemocytometer	33
2.2.6	Infection with MeV-SCD/MeV-GFP and/or treatment with resminostat	34
2.3	Virological methods	35
2.3.1	Titration of measles vaccine virus	35
2.3.2	Viral growth curves	37
2.3.3	Fluorescence microscopy on MeV-GFP infected cells	39

2.4	Flow Cytometry.....	40
2.4.1	Analysis of altered primary infection rates by fluorescence-activated cell sorting (FACS) using MeV-GFP	40
2.4.2	Quantitative analysis of CD46 receptor expression using flow cytometry	41
2.4.3	“Analysis of cell cycle profiles by flow cytometry	42
2.5	Cell Mass and Viability Assays	43
2.5.1	Sulforhodamine B (SRB) cytotoxicity assay	43
2.5.2	CellTiter-Blue® Cell Viability Assay.....	44
2.6	Molecular Biology Methods	45
2.6.1	Immunoblotting.....	45
2.6.2	“Real-time-quantitative Polymerase Chain Reaction (qPCR).....	50
3	Results	51
3.1	Preliminary experiments	51
3.1.1	Cytotoxic effect of MeV-SCD monotherapy.....	51
3.1.2	Anti-tumor activities of resminostat on human hepatoma cell lines	52
3.2	Resminostat + MeV-SCD-based combination treatment settings	54
3.2.1	Boosted cytotoxic/oncolytic effect of the epi-virotherapeutic combination treatment.....	54
3.2.2	Other application settings in MeV-SCD/resminostat co-treatment	57
3.2.3	Triple-therapy: Addition of prodrug 5-FC to the MeV/Res combination setting	59
3.3	Influences of resminostat on biological activity/growth characteristics of measles vaccine virus	61
3.3.1	Examination of measles virus growth kinetics under the co-treatment with resminostat.....	61
3.3.2	“Resminostat-mediated enhancement of primary infection rates in hepatoma cell lines	64
3.3.3	Enhanced primary infection rates are independent of measles receptor (CD46) expression levels.....	65
3.3.4	“Addition of resminostat does not impair MeV replication and spread.....	66
3.4	“Resminostat-induced downregulation of zfp64 in MeV infected hepatoma cells	68
3.5	“Epi-virotherapeutic treatment (MeV + Res) enlarges apoptosis of hepatoma cells	69
3.6	“Resminostat impedes IFIT-1 expression after exogenous IFN- β stimulation.....	71
4	Discussion	73

4.1	Boosted cytotoxic effects in the epi-virotherapeutic approach.....	73
4.2	HDACi + OV treatment: is apoptosis the answer?	74
4.3	Influences on virus biology by epigenetic manipulation	75
4.3.1	MeV-SCD replication and spread is hardly affected by resminostat....	75
4.3.2	Resminostat does not alter measles entry receptor CD46 expression levels	77
4.4	Resminostat functions as an immunomodulator in hepatoma cells	78
4.4.1	Interference with the host cell interferon system	78
4.4.2	Additional immunomodulating functions by down-regulation of zfp64	81
4.5	Future directions of immunovirotherapy	81
4.6	Perspectives	84
5	Summary.....	86
6	Zusammenfassung.....	88
Appendix	90
	List of equations.....	90
	List of figures	90
	List of tables	92
	Index of abbreviations.....	93
References	97
Publication list	112
Erklärungen zum Eigenanteil	114
Danksagung	117

1 Introduction

1.1 Hepatocellular carcinoma

1.1.1 Epidemiology

According to the World Health Organization's (WHO) *GLOBOCAN* report on estimated cancer incidences, there were 14.1 million cases of new occurrences of malignant diseases with 8.2 million cancer-related deaths in 2012 [1]. Therefore, cancer is the leading cause of death in the world. The WHO's *World Cancer Report* [2] states that hepatocellular carcinoma (HCC) has been the second most common cause of cancer mortality worldwide with a total of about 0.8 million reported deaths in 2012 (see Figure 1.1).

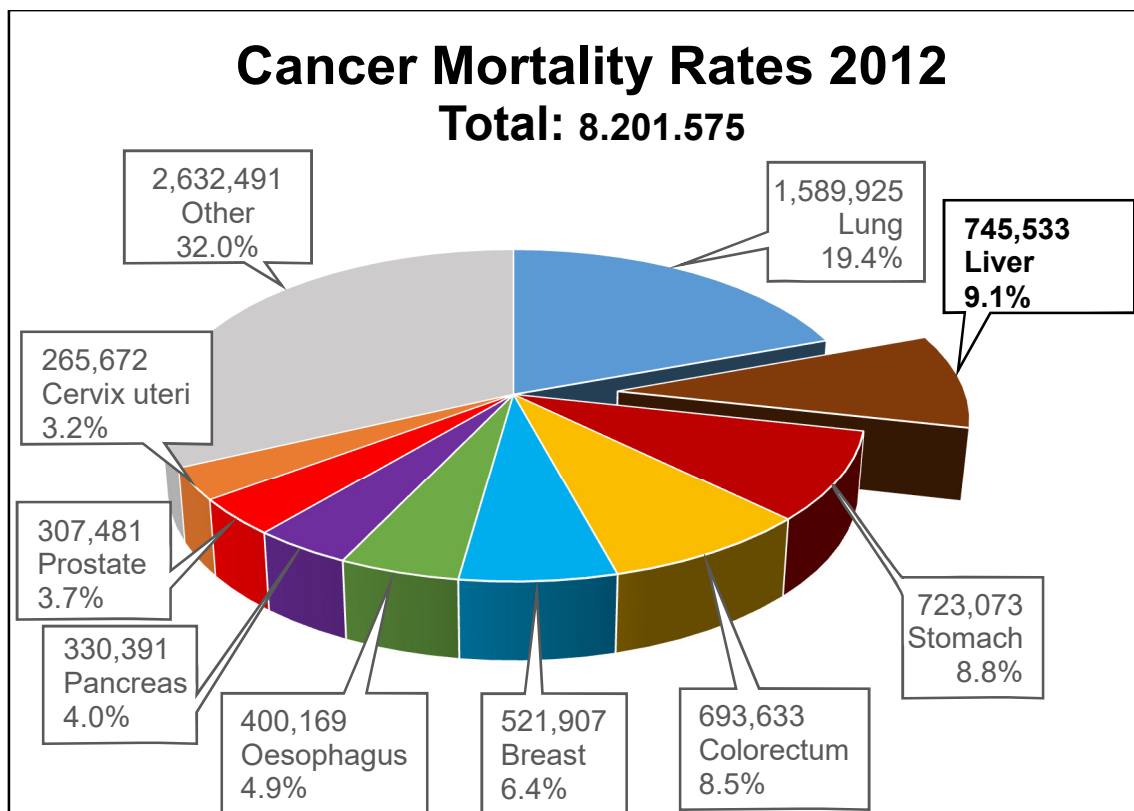


Figure 1.1: Cancer-related deaths 2012

Estimated percentage distribution [%] and number of cancer-related deaths (total: 8,201,575) worldwide in 2012 for both sexes and all ages. Generated at: <http://globocan.iarc.fr/Pages/online.aspx>, retrieved: 06.03.2015, data based on WHO, Globocan, IARC, 2012 [1]

Persistent HBV (Hepatitis B Virus) and HCV infections (Hepatitis C Virus) are predominant risk factors for the development of primary liver cancer, especially

in regions of the world with high incidences of infections (i.e. Africa, Eastern Asia). In industrial nations, liver cirrhosis based on ethanol abuse, intoxications (e.g. aflatoxin) and on grounds of a metabolic syndrome are relevant etiologic factors for the occurrence of hepatocellular carcinoma [3].

1.1.2 Current state-of-the-art treatment options for liver cancer

Traditionally potentially curative treatment options for this heterogeneous malignant tumor are resection of small tumors, percutaneous ablation or liver transplantation, which all are subject to (i) a very early-stage disease at diagnosis and (ii) surgical inclusion criteria like whether or not the vascular system is infiltrated or residual functional capacity of remaining liver (most recently reviewed in [4]). Despite substantial efforts to improve median survival of patients with advanced stage HCC, prognosis of this type of cancer is still dismal (recently reviewed in [5]). In most cases, progression of the disease can be delayed only transiently and long-term disease suppression or even cure cannot be achieved by current pharmacological therapies. Thus, treatment with sorafenib (Nexavar®), the only approved first-line systemic therapy for patients with advanced stage HCC, results in only a modest prolongation of median survival of about three months [6]. Several late-stage (II/III) clinical trials employing drugs with distinct mechanisms of action (e.g. tyrosine kinase inhibitors, Epidermal Growth Factor Receptor (EGFR) blockers, Vascular Endothelial Growth Factor (VEGF)-Receptor blocker etc.) yet failed to prove superiority compared to the current first-line treatment option for advanced HCC. Accordingly, further improvements in the treatment of late-stage HCC are desperately needed.

1.2 Oncolytic virotherapy as an innovative approach in cancer treatment

Oncolytic viruses (OVs) represent a novel therapeutic approach (so-called virotherapy) in the treatment of various malignant neoplasia, employing their ability to selectively infect, replicate in and (onco-)lyse tumor cells, without affecting normal tissues. In this chapter, a brief reflection on the history of oncolytic viruses will be given, along with the introduction of general

virotherapeutic principles and a short summary of viruses being tested in the clinical setting on cancer patients.

1.2.1 History of oncolytic viruses

The idea of employing natural occurring pathogenic viruses as anti-cancer agents was initially based on several observations of tumor regression in patients with coincidental natural virus infections [7] or subsequent to vaccinations with live attenuated viruses [8, 9]. Early anecdotes of spontaneous disease remission following infection were made even before the “discovery” of viruses as contagious agents [10]. Contagion with wild-type measles virus was reported to be coincidental with regressions of leukemia [11, 12], Morbus Hodgkin [13, 14] and a well-documented case of Burkitt’s lymphoma [15]. Early clinical trials used primitive techniques for administration of naturally occurring viruses, as infectious body fluids or infected tissue samples were applied to tumor patients. Unsurprisingly, adverse events were serious and unpredictable [7] and therefore early enthusiasm for virotherapy abated until technical advantages allowed to engineer viruses with beneficial tissue tropism and restricted replication-competence to malignant tissue.

1.2.2 Principles of oncolytic virotherapy

Oncolytic virotherapy is an emerging novel approach in treating malignant diseases using live attenuated, naturally occurring or genetically modified virus vectors with selective tropism for neoplastic cells. This oncotropism is a result of epigenetic and genetic alterations in the process of malignant transformation (e.g. [17]), as tumors acquire the potency to dampen innate and adaptive immune responses by hiding immunogenic tumor neo-antigens and escaping immune effector cells [18], which in turn creates an ideal niche for viral particles that are otherwise unable to infect healthy cells (see Figure 1.2).

“The field of oncolytic virotherapy undoubtedly has made formidable progress since first ever replication-competent, genetically engineered viruses have entered preclinical & clinical testing in the 1990s [19]. The first clinical trials with such modified/attenuated virus pathogens used as oncolytic vectors primarily had to address numerous safety concerns. But ever since, oncolytic viruses have

proven to constitute generally well-tolerated novel biological anti-cancer drugs [20].

However, when coming to the efficiency of the oncolytic paradigm, many limitations of those first-generation virotherapeutics regarding anti-tumor efficacy became obvious [21]. Accordingly, next generation oncolytics were designed (i) to enhance tumor specificity, (ii) to express efficiency-boosting transgenes, such as suicide genes or immunomodulatory cytokines, or (iii) to coat viruses as camouflage (to avoid rapid neutralization when getting in contact with the highly effective anti-viral host immune response) [22]. Latest evidence suggests that anti-tumor activity of oncolytic viruses is not solely dependent on pathogen-mediated direct/specific infection and (onco-)lysis of malignant cells but is also capable of triggering an adaptive anti-tumor immune response. In this context, current evidence suggests that the mechanisms of action of virotherapeutics can be attributed at least partly (i) to a profound exposure of antigenic tumor epitopes being released in huge amounts throughout the oncolytic process, (ii) to a subsequent inflammatory tumor infiltration as well as (iii) to the induction of a T-cell-mediated anti-tumor immune response (see original work [23-26] as well as data reviewed in [18]).” [27]

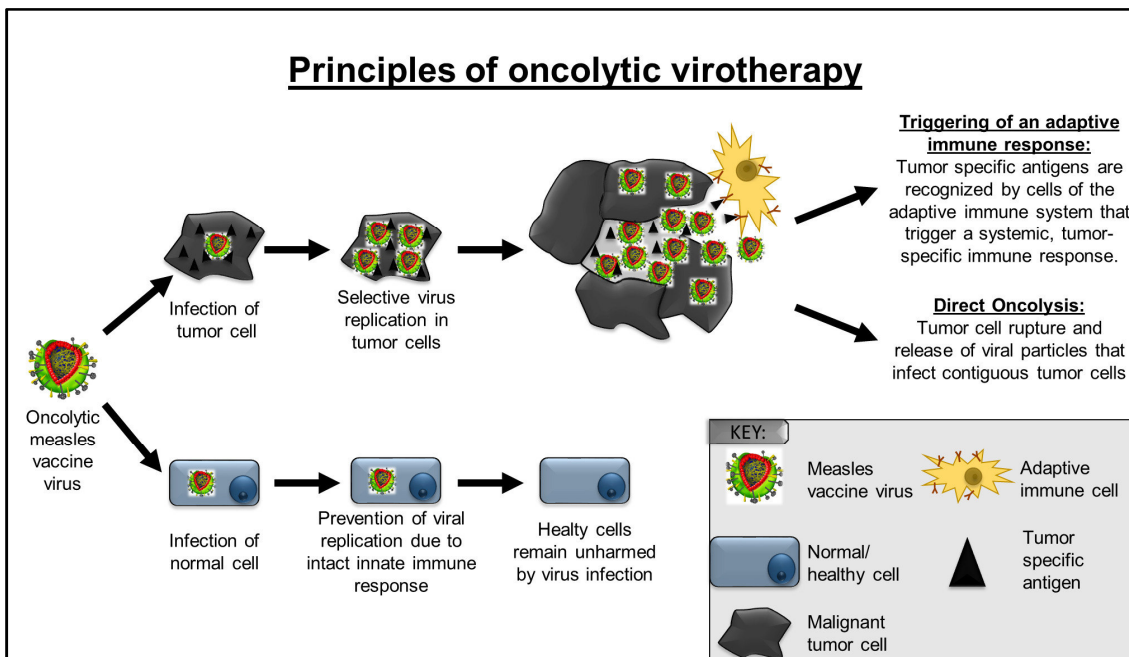


Figure 1.2: Principles of oncolytic virotherapy using the example of oncolytic measles vaccines. Modified from Kirn D et al. [16]

1.2.3 Oncolytic virus families in clinical testing

Several oncolytic viruses are currently under investigation in various clinical trials as biological treatment options for a wide array of tumor entities. The catalogue of ongoing or finalized clinical trials comprises a plethora of different viral vectors, e.g. Adenovirus (notably, in 2006, the ONYX-015 derivative Adenovirus H101 was the first approved oncolytic vector for tumor therapy in China [28]), Coxsackievirus, Herpes Simplex Virus (HSV), Measles Vaccine Virus (Edmonston Strain), Newcastle Disease Virus, Parvovirus, Poliovirus (Sabin Strain), Reovirus (Dearing Strain), Seneca Valley Virus, Retrovirus, Vaccinia (strains Lister, Wyeth, Western Reserve) and Vesicular Stomatitis Virus (VSV), which are administered as single agents in monotherapeutic approaches or combined with chemo-/radiotherapy [29].

In late 2015, a first virotherapeutic compound received simultaneously approval by both U.S. Food and Drug Administration (FDA, see <http://www.fda.gov/NewsEvents/Newsroom/PressAnnouncements/ucm469571.htm>, retrieved 05.04.2016) as well as European Medicines Agency (EMA, see http://www.ema.europa.eu/ema/index.jsp?curl=pages/news_and_events/news/2015/10/news_detail_002421.jsp&mid=WC0b01ac058004d5c1, retrieved 05.04.2016), based on positive results of a Phase III clinical trial [30]: patients with late stage malignant melanoma (showing recurrence after initial surgical procedures) have now access to the first-in-market virotherapeutic agent IMLYGIC™ (AMGEN, Thousand Oaks, CA, USA), a genetically modified HSV-1 virus (also known as Talimogene Laherparepvec, T-Vec). Most interestingly, approval by regulatory authorities of this leading virotherapeutic vector was received although as primary endpoint a durable response rate (complete or partial response) of “only” 16.3% was achieved in patients receiving T-Vec/IMLYGIC™ (compared to 2.1 percent of patients in the control group ($p < 0.0001$)) for at least six months. On the contrary, improvement in overall survival (OS) within the patient group of this phase III trial ($n=292$ patients receiving virus dosages) could not be observed and effects on visceral metastases were likewise (statistically) non-detectable (see also section 1.2.4).

These results strongly indicate that the establishment of oncolytic virotherapy as a new pillar of cancer treatment started with the approval of IMLYGIC™ (the pioneering work in this field was therefore particularly acknowledged by FDA/EMA), but nevertheless efficacy of this innovative treatment option needs to be significantly improved. This could be achieved by introducing novel, more powerful vector systems (i.e. modified oncolytic viruses) and furthermore, reasonable combination strategies have to be established.

Table 1.1 presents a quick overview of current or completed clinical trials using viruses as monotherapeutic agents with their corresponding application scheme sorted by oncolytic vector platforms as well as by the respective identifiers provided by <http://clinicaltrials.gov/> (NCT).

Virus family	Vector	Route	Application scheme	References	
Adenovirus	ColoAd1 (enadenotucirev)	Intratumoral/ Intravenous	<u>Arm 1:</u> Single shot <u>Arm 2:</u> Triple-hit course (d1, d3, d5)	NCT02053220; [31]	
		Intravenous	One triple-hit course (d1, d3, d5)	NCT02028442	
	ICOVIR-5	Intravenous	Weekly intravenous infusions of bone-marrow derived autologous Mesenchymal Stem Cells (MSCs) infected with ICOVIR-5 (=CELYVIR)	NCT01844661	
		Intravenous	Single shot	NCT01864759	
	CG0070	Intravesical	Weekly intravesical administration (6 courses)	NCT01438112	
		Intravesical	<u>Arm 1:</u> Weekly intravesical administration (6 courses) <u>Arm 2:</u> Every 4 weeks (for up to 6 courses)	NCT00109655; [32]	
	DNX-2401 (Delta-24-RGD)	Intratumoral	Single shot	NCT00805376	
		Intraperitoneal	Triple-hit course (d1, d3, d5)	NCT00562003; [33]	
	Coxsackievirus	CAVATAK	Intratumoral	10 intratumoral injections over 18 weeks (d1, d3, d5, d8, d22, d43, d64, d86, d106 + d127)	NCT01227551; [34]
			Intratumoral	<u>Group 1:</u> Single shot <u>Group 2:</u> Three injections (d1, d3, d5) <u>Group 3:</u> Six injections (d1, d3, d5, d7, d9, d11)	NCT00832559
Intratumoral			Two injections (d1, d3)	NCT00438009	
Intratumoral			Single shot	NCT00235482	

Table 1.1: Selected clinical trials using oncolytic vector systems as monotherapeutic agents (Table published in [27]). d1, d2, d3: day 1, day 2, day 3; i.v.: intravenous; IP: intraperitoneal).
Table continued on next page.

Virus family	Vector	Route	Application scheme	References	
Herpes simplex virus	Talimogene Laherparepvec (T-Vec/IMLYGIC™)	Intratumoral	First injection on d1, second course 3 weeks from initial dose, all subsequent courses every 2 weeks	NCT02014441	
		Intratumoral	First injection on d1, second course 3 weeks from initial dose, all subsequent courses every 2 weeks	NCT00769704; [30]	
		Intratumoral	See above; up to 24 courses	NCT00289016; [35]	
		Intratumoral	Three injections every 3 weeks (plus max. three additional courses)	NCT00402025; [36]	
	M032	Intra-/Peritumoral	Single shot	NCT02062827	
		Intravenous/intratumoral	<u>Part 1:</u> Single shot <u>Part 2:</u> plus max. 3 additional courses	NCT00931931; [37]	
	Seprehvir (HSV 1716)	Intrapleural		<u>Part A:</u> Single shot <u>Part B:</u> <u>Group 1:</u> 2 courses at weekly intervals <u>Group 2:</u> 4 courses at weekly intervals	NCT01721018
			Intra-/Peritumoral	Single shot	NCT02031965
	HF10	Intratumoral		<u>Stage 1:</u> Single shot <u>Stage 2:</u> 4 courses (dosing interval ≥ 2 weeks)	NCT01017185; [38]
	rRp450	into hepatic artery		4 courses every 1-2 weeks	NCT01071941
Measles Vaccine virus (Edmonston strain)	MeV-CEA	Intratumoral/into resection bed	<u>Arm 1:</u> Single shot <u>Arm 2:</u> Two-hit-course (d1, d5)	NCT00390299	
		Intraperitoneal	Every 4 weeks for up to 6 courses	NCT00408590; [39]	
		Intrapleural	Every 4 weeks for up to 6 courses	NCT01503177	
	MeV-NIS	Intraperitoneal	Every 4 weeks for up to 6 courses	NCT00408590; [40]	
		Intraperitoneal	<u>Course 1:</u> Only MeV-NIS IP; <u>Subsequent courses:</u> MeV-NIS infected mesenchymal stem cells IP (every 4 weeks for up to 6 courses)	NCT02068794	
		Intratumoral	Single shot	NCT01846091	
		Intravenous	<u>Arm 1:</u> Single shot <u>Arm 2:</u> Single shot in combination with Cyclophosphamide	NCT00450814; [41]	
Parvovirus	ParvOryx	Intratumoral/ Intravenous	Two courses (d1, d10)	NCT01301430; [42]	
Polio-Virus (Sabin strain)	PVS-RIPO	Intratumoral	Single shot	NCT01491893; [43]	

Table 1.1: Continued

1 Introduction

Virus family	Vector	Route	Application scheme	References
Reovirus (Dearing strain)	Reolysin	Intratumoral	Single shot	NCT00528684; [44]
		Intravenous	Up to 12 quintuple-hit courses (d1-5) every 4 weeks	NCT00651157; [45]
		Intravenous	Quintuple-hit courses (d1-5) every 4 weeks	NCT00503295; [46]
		Intravenous/ Intraperitoneal	Administration i.v. as quintuple-hit courses (d1-5) every 4 weeks + additional IP administration on 2 consecutive days beginning with course 2	NCT00602277
		Intravenous	Up to 12 quintuple-hit courses (d1-5) every 4 weeks	NCT01533194
		Intravenous	Up to 12 quintuple-hit-courses (d1-5) every 4 weeks	NCT01240538
Senecca Valley virus	NTX-010	Intravenous	Single shot	NCT01017601; [47]
		Intravenous	Single shot	NCT00314925; [48]
Vaccinia virus (Lister strain)	GL-ONC1 (GLV-1h68)	Intraperitoneal	Every 4 weeks (4 courses)	NCT01443260; [49]
		Intraleural	Single shot	NCT01766739
		Intravenous	<u>Arm 1:</u> Every 4 weeks (up to 6 courses) <u>Arm 2:</u> Every 4 weeks (3 triple-hit-courses d1, d2, d3) <u>Arm 3:</u> Every 4 weeks (3 quintuple-hit-courses d1, d2, d3, d4, d5)	NCT00794131; [50]
Vaccinia virus (Western Reserve strain)	vvDD-CDSR (JX-929)	Intratumoral/ Intravenous	Single shot	NCT00574977; [51]
Vaccinia virus (Wyeth strain)	JX-594 (pexastimogene devacirepvec, Pexa-Vec)	Intratumoral	3 courses every 2 weeks	NCT00554372; [52]
		Intratumoral	Every 3 weeks (max. 8 courses)	NCT00629759; [53]
		Intratumoral	Weekly (up to 6 courses)	NCT00429312; [25]
		Intravenous	Single shot	NCT00625456; [54]
		Intravenous	Every 2 weeks (up to 4 courses)	NCT01380600; [55]
		Intravenous	Treatment on d1, d8, d22 and weeks 6, 12, 18	NCT01387555; [56]
		Intravenous	Weekly for 5 weeks (followed by up to 3 additional infusion boosts)	NCT01394939
		Intravenous	Weekly for 5 weeks, then every 3 weeks	NCT02017678
		Intravenous	Every 2 weeks Weekly for 5 weeks (treatment extension: i.v. infusion every 3 weeks in case of stable disease)	NCT01469611 NCT01636284
Vesicular Stomatitis Virus	VSV-IFN-beta	Intratumoral	Single shot	NCT01628640

Table 1.1: Continued

1.2.4 “Assessment of current virotherapeutic application schemes” [27]

Acknowledging the outstanding importance to (i) enhance efficiency of direct oncolysis-mediated tumor cyto-reduction and (ii) to maximize an anti-tumor immune response following virus infection, analysis of application schemes for virus administration in clinical trials is crucial to a successful oncolytic immunotherapy. “Prime examples for success achieved so far in virotherapy have to be discussed and correlated with the respective application regimes which might have fostered these (rare) success stories. This kind of analytic view quite stringently leads to the conclusion that not only one, but presumably two quite divergent application strategies could lead to success, i.e. “hit hard and early” and “killing softly”, reflecting also the two quite opposite paradigms of “single-shot” and “prime-boost” regimens (see Figure 1.3).

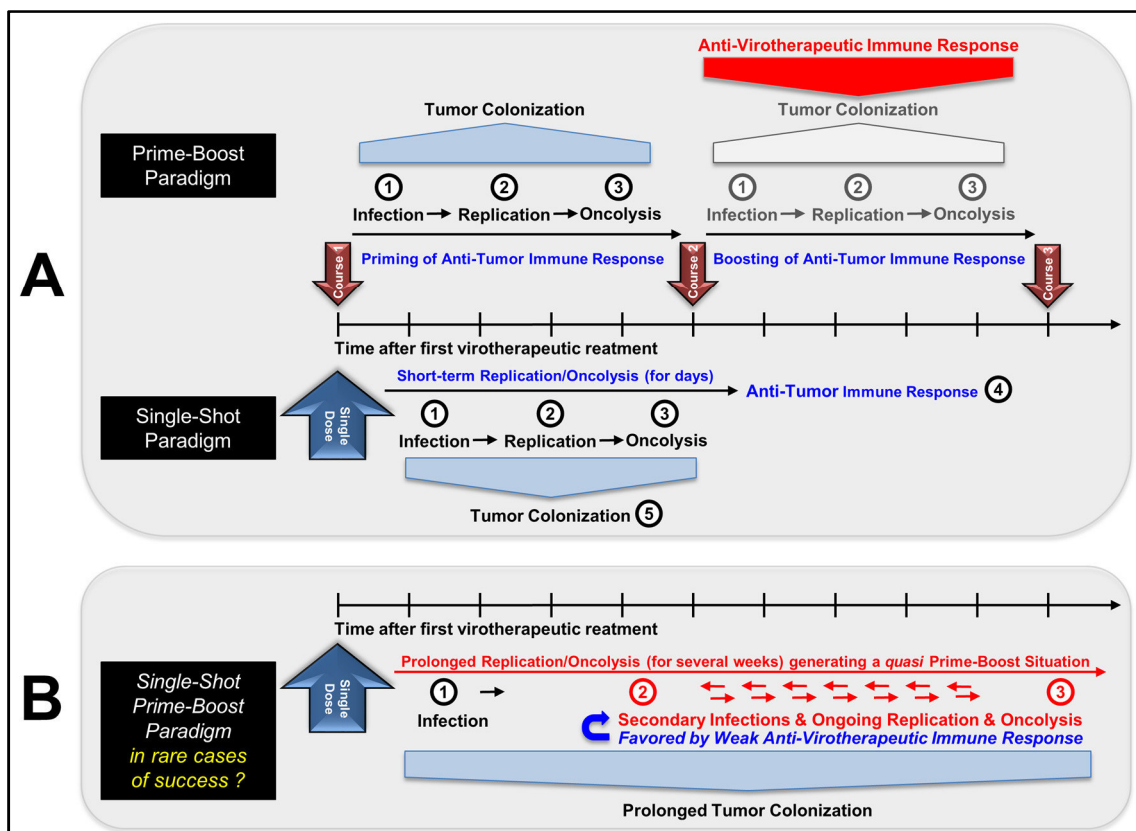


Figure 1.3: Prime-Boost / Single-Shot paradigms of virotherapeutic application schemes.
(Figure modified from published version [27])

The prime-boost paradigm (Figure 1.3 (A), upper panel) encompasses a huge variation in the number of application courses (see also Table 1.1) of oncolytic

viruses either applied as single-hit (d1 only) or multiple-hit courses (d1, d2, ..., dx). Here, priming of an anti-tumor immune response (depicted in the left part of the panel) is the result of initial tumor-cell infection and colonization [①], replication [②] and subsequent oncolysis [③]. After eventual decrease of this primary anti-tumor immune response, the second and every following course of repetitive virus application is used under the premise (i) to further debulk remaining tumors using once again mechanisms of direct virus-mediated oncolysis [①+②+③] and (ii) boosting the anti-tumor immune response (depicted in the right part of the panel) by releasing concealed tumor antigens within the meaning of an anti-tumor vaccination [21]. Preferential route of administration here is an intratumoral injection, as a rapid neutralization of viruses by a simultaneously triggered anti-viral immune response (depicted by a red arrow-type rectangle) can be avoided. In addition, multiple-hit courses in the prime-boost setting are limited by an anti-viral immune response as well, since the adaptive immune response is fully qualified often at the latest seven days after the first injection and thus further virus applications are considered as ineffective. Therefore, intervals between courses have to find a balance between attacking the tumor as soon as possible and simultaneously avoiding premature neutralization of the virotherapeutic vectors. The single-shot paradigm (see Figure 1.3 (A), lower panel) is in accordance with the initial understanding of the “oncolytic virotherapy paradigm” [29], as it is believed that a single systemic administration of oncolytic viruses leads to a systemic spread with subsequent selective primary infection [①] of the primary site of the tumor as well as of disseminated metastases. Self-amplification/ replication [②] of virotherapeutic vectors is followed by direct tumor-cell (onco-)lysis [③] and recognition of infected tumor cells by the innate host immune system with subsequent clearance of residual tumor masses through a tumor antigen triggered adaptive host-immune response [④]. Basic prerequisite for a successful utilization of the single-shot paradigm is to maximize the initial dosage of applied infectious particles as dose-dependent tumor colonization [⑤] and subsequent oncolysis of disseminated tumors is only achievable if a viremic threshold is passed [57]. Below this

threshold, systemically administered virus particles are immediately neutralized by preexisting antibodies or serum factors, such as complement [58].

The prime-boost paradigm in rare cases of success (Figure 1.3 (B)) addresses rare patient specific defects in the anti-viral immune response being so far undetected and clinically silent. Thereby, a prolonged replication/ oncolysis (for several weeks) generating quasi prime-boost situation is probably generated with the help of nature.

The “single-shot” paradigm (Figure 1.3 (A), lower panel) is best represented by the recent report on two measles-seronegative patients with relapsing drug-refractory myeloma being both treated by a single-shot intravenous infusion with a very high dosage of the measles vaccine virotherapeutic MeV-NIS leading in one patient to a durable complete remission at all disease sites [41]. Key factors postulated to have contributed to this successful outcome were mentioned as follows: (i) low pretreatment serum titers of anti-measles antibodies; (ii) usage of a very high virus dosage being sufficient to overcome a postulated dose-threshold required for successful tumor colonization; (iii) detection of measles virus transcripts (but not of live virus particles) in circulating cells even at 6 weeks after virus infusion, by which time there had been a substantial boost to the anti-measles antibody titer, suggesting the possibility of a continuing oncolytic activity even at that late time (Figure 1.3 (B)).

The “prime-boost” paradigm (Figure 1.3 (A), upper panel) is best represented by the recent OPTiM phase III virotherapy study in which the HSV-1 based, GM-CSF encoding virotherapeutic vector talimogene laherparepvec (T-Vec, IMLYGIC™) was applied intralesional/intratatumoral in unresected stage IIIB/C and IV melanomas [59].

Following an initial dose (functioning as a priming of the anti-tumor immune response; Figure 1.3 (A), upper panel, on the left), dosing of T-Vec/IMLYGIC™ was repeated every 2 weeks for up to 24 times defining a therapy intense “multiple-shot/long-term application” scenario, being in maximum contrast to any of the single-shot scenarios. Based on this application regime, T-Vec/IMLYGIC™ proved it could shrink tumors, keep them from regrowing and improve median

survival. However, T-Vec/IMLYGIC™ hit its primary endpoint of durable response but missed its second goal of boosting overall survival (p value of 0.051; see: [30]).

As premises for successful oncolytic virotherapy are multifactorial and multi-dimensional, several key factors contribute to an enhanced treatment efficacy which can be demonstrated using the example of T-Vec/IMLYGIC™ skin-cancer treatment: melanoma as a tumor entity seems to be highly vulnerable to oncolysis, as virotherapeutic treatment effects were also found following JX-594 vaccinia injections [24]. Both T-Vec/IMLYGIC™ and JX-594 were administered in conformance with the prime-boost paradigm, supporting to further cherish this application scheme in melanoma treatment. Both, T-Vec/IMLYGIC™ and JX-594 encode for human GM-CSF, an immunomodulating cytokine that is evaluated for the treatment of skin cancer as a monotherapeutic agent itself [60]. Therefore, this particular biology of vectors T-Vec/IMLYGIC™ and JX-594 seem to represent a qualified approach to this particular cancer biology.

Putatively, as mentioned above, such “multiple-shot/long-term application” scenarios only can be successful if the respective virotherapeutics are applied intratumoral. Otherwise, the anti-virotherapeutic immune response (depicted as a red arrow-type rectangle in Figure 1.3 (A), upper panel), which often is induced as early as seven days after the very first virotherapeutic treatment, would completely block with great efficiency any subsequent colonization of the respective tumor sites, although this would be required for a repetitive boosting of the anti-tumor immune response (Figure 1.3 (A), upper panel, on the right).

As to date no consent on either route of administration or preferential application scheme is established in the field and valuable data from clinical trials addressing those issues is still rare, it is not surprising that efficacy of clinical trials employing oncolytic viruses as monotherapeutics often fall short of expectations. Thus, to address those limitations of viral monotherapy (for details see also section 1.4), cunning combinational strategies are imploringly awaited for broad usage in clinical trials.

1.3 Oncolytic measles vaccine viruses

1.3.1 Virus biology

Measles virus (MeV) belongs to the group of negative-sense, single-stranded RNA viruses (-ssRNA), the family of *Paramyxoviridae*, and genus is classified as *Morbillivirus* (International Committee on Taxonomy of Viruses, ICTV, 2014). The highly contagious measles disease (clinical symptoms are fever, maculopapular exanthema, respiratory symptoms, conjunctivitis [61]) caused by MeV is an important cause of morbidity and mortality for children especially in developing countries, with an estimated global measles mortality of 139.300 in 2010 [62].

Six structural proteins are encoded by the negative-sense ssRNA (Figure 1.4): fusion protein F, hemagglutinin H, large protein L, phosphoprotein P, matrix protein M and the nucleocapsid protein N.

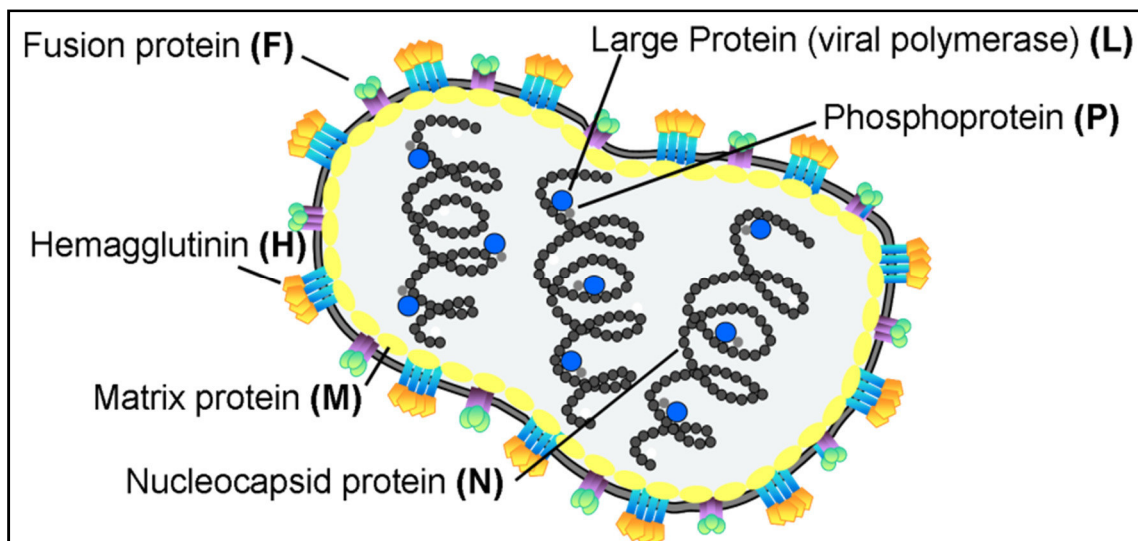


Figure 1.4: Schematic morphology of measles virus:

Measles virus is a negative sense single-stranded RNA virus encoding for six structural proteins (© Guy Ungerechts, NCT Heidelberg)

The hemagglutinin and the fusion protein are integrated as transmembrane glycoproteins into the phospholipid bilayer of the envelope, which is descendent from the host cell membrane. Hemagglutinin is responsible for MeV receptor binding and therefore initiation of infection, as the following receptors can be recognized by H protein: SLAM (signaling lymphocyte activation molecule)/CD150 is a glycoprotein expressed on B and T cells [63], dendritic cells (DC),

Langerhans cells (LC) and macrophages [64] and therefore determining the lymphotropism of MeV. In 2011, an epithelial cell adherens junction protein, Nectin-4, was identified as a MeV receptor [65, 66] as well.

Another MeV receptor, human membrane cofactor protein (CD46) is ubiquitously expressed on all human nucleated cells and involved in complement activation and regulation of immune response [67-70], but utilization as MeV receptor was found to be limited to vaccine strains of measles and not the wild-type viruses [71]. These findings are of clinical importance, as Edmonston strain measles vaccine viruses (MeV-Edm) are used as oncolytic viruses for cancer treatment (see section 1.3.3). Anderson and colleagues^[72] found CD46 expression levels to be crucial for successful occurrence of typical MeV-mediated cytopathic effect - portrayed by syncytia forming (i.e. cell-cell-fusion) - as MeV entry and also substantial oncolysis correlated positively with CD46 receptor densities on tumor cells. Additionally, CD46 expression levels in cancer cells are frequently found to be elevated as a tumor cell-mechanism to prevent complement-mediated oncolysis [73, 74] and, by implication, selectively targeting oncolytic measles vaccine viruses to this particular subset of neoplastic tissue.

After binding to target cells utilizing the H protein, MeV entrance into host cells is mediated by the fusion protein F and virus propagation in the cytoplasm of the host cell is dependent on a negative sense ribonucleo-protein complex (RNP), comprised of the RNA strand, the N structural protein, as well as the RNA dependent RNA polymerase (composed of the viral L and P protein) [75].

Besides, two non-structural proteins are encoded on the measles genome: V protein, which participates in the inhibition of several pro-inflammatory signaling cascades [75] and C protein, with various functions including suppression of viral transcription and replication [76] as well as controversial interactions in circumvention of host interferon-induction (discussed in [75]).

1.3.2 Suicide transgene expressing MeV-SCD

As mentioned above (see section 1.2.2), first-generation oncolytic vectors often lacked sufficient anti-tumor activity, but genetic engineering makes it possible to enhance efficacy by inserting transgenes into viral nucleic acid encoding e.g. for

transmembrane channels (that can later be used to deliver cytotoxic radioisotopes into tumor cells), immunostimulating factors (such as GM-CSF, see above) or prodrug converting enzymes.

In this thesis, we used a recombinant Edmonston strain derived measles vaccine virus encoding for a fusion protein (Super-Cytosine Deaminase, Super-CD or SCD) [78] of cytosine deaminase (CD; yeast origin) and uracil phosphoribosyl-transferase (UPRT; also yeast origin) [79] to boost catalytic enzyme activity of 5-FC (5-fluorocytosine) \rightarrow 5-FU (5-fluorouracil) conversion and subsequent steps in this prodrug toxification (see Figure 1.5).

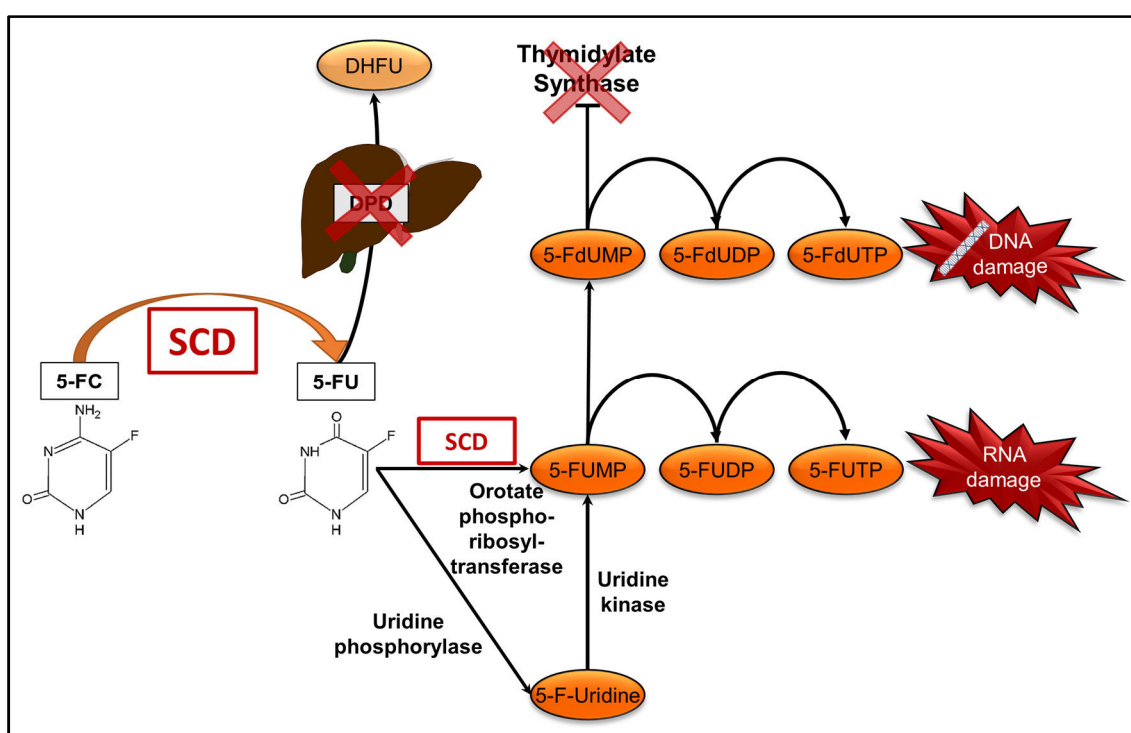


Figure 1.5: Mechanism of action of MeV-SCD prodrug convertase Super-Cytosine Deaminase (SCD): Prodrug 5-fluorocytosine (5-FC) is converted into chemotherapeutic 5-fluorouracil (5-FU) by cytosine deaminase part of SCD. 5-FU is further metabolized by orotate phospho-ribosyltransferase or alternatively by uracil phosphoribosyltransferase (UPRT) domain of SCD into 5-fluorouridine monophosphate (5-FUMP). 5-FUMP can further be metabolized to the corresponding triphosphate 5-fluorouridine triphosphate, which is falsely integrated into RNA as a substrate of RNA polymerase. Reduction of 5-FUMP results in 5-fluorodesoxyuridine monophosphate (5-FdUMP), which is an inhibitor of thymidylate synthase and can also be triphosphorylated to 5-desoxyfluorouridine triphosphate (5-dFUTP), which leads to DNA damage by incorporation. SCD activity is responsible for a reduction of 5-FU clearance by dihydropyrimidine dehydrogenase (DPD, localized in the liver) into dihydrofluorouracil (DHFU) with subsequent renal excretion after further metabolism. Figure modified from Longley et al.^[77].

Enzymatic conversion of 5-FC - a pyrimidine analogue that is clinically applied as an antimycotic drug [80] - into the well-established chemotherapeutic 5-FU is catalyzed by cytosine deaminase, which is part of the bifunctional enzyme-

complex SCD. UPRT participates in the conversion of 5-FU into 5-fluorouridine monophosphate (5-FUMP) [81].

Cytotoxic effects of 5-FU are mediated by (i) covalent inhibition of tumor cell thymidylate synthase leading to a lack of newly synthesized thymidine [82], (ii) direct damage to RNA as well as DNA through insertion of 5-FU as an antimetabolite (reviewed in [83]).

The introduction of the bifunctional enzyme complex SCD into tumor cells that are selectively infected with MeV-SCD allows the systemic administration of the prodrug 5-FC, as conversion into cytostatic 5-FU is restricted to SCD-expressing tumor cells. Therefore, manifold higher concentration of the chemotherapeutic 5-FU can be accomplished at the site of the tumor with a reduction of systemic toxicities to a minimum and as 5-FU is highly diffusible, primarily unharmed cancer cells after virus infection are also affected by 5-FU, which is known as a so-called “bystander effect” [84].

1.3.3 Measles vaccine viruses (MeV)-based oncolytic monotherapy in selected clinical trials

Measles vaccine virus (MeV) has been safely applied to millions of patients during vaccination programs as live-attenuated commercial vaccine since 1963 [85] and has ever since shown excellent safety profiles, which also applies for the clinical setting when used as anti-cancer agents. As outlined above (see section 1.2.4), analysis of application schemes for virus administration can help to identify limitations to MeV-based oncolytic mono-virotherapy (see also section 1.4). Here, “a comprehensive assessment of current application schemes could help to identify basic application approaches and assign these to successful regimens” [27] also for measles vaccine-based oncolytic virotherapy.

Thus, in this section, current state-of-the-art application schemes for MeV clinical trials are condensed and displayed in two easy-to-read figures:

“To date, two Edmonston strain-derived measles vaccine viruses (MeV-Edm) are intensively explored clinically, namely MeV-CEA and MeV-NIS. MeV-CEA encodes for carcinoembryonic antigen which can be employed as a marker gene

for viral gene expression *in vivo* [86]. MeV-NIS encodes for the human thyroidal sodium iodide symporter and can be used for both non-invasive imaging for viral gene expression e.g. by SPECT/CT and for radiovirotherapy e.g. with ionizing gamma-radiation-emitter ^{131}I radioiodine [87].

Repetitive application schemes for MeV:

First results of a MeV-CEA dose-escalating clinical trial on refractory ovarian cancer (NCT00408590) were published in 2010 [39]. Patients were treated with MeV-CEA through an intraperitoneal catheter every 4 weeks for up to 6 courses (application scheme depicted in Figure 1.6 (A)). Treatment was well tolerated, as no dose-limiting toxicities occurred. Anti-tumor activity led to stable disease in 14/21 patients with a median duration of 92.5 days. CEA marker-gene detection was reported in peritoneal fluid and serum favorably in patients receiving high dosages of the study virus. Encouraged by these results, MeV-NIS was also applied to women diagnosed with drug-resistant ovarian cancer in a subsequent part of the same phase I/II trial (NCT00408590). Again, MeV-NIS was administered into the peritoneal cavity every 4 weeks for up to 6 courses (see Figure 1.7 (A)) and results regarding safety and efficacy correlated well with the previous MeV-CEA trial but additional information was gained by radio imaging of viral gene expression [40].

Pointing out a high level of protocol adherence, another phase I trial on malignant pleural mesothelioma (NCT01503177) also applied MeV-NIS with 6 courses every 4 weeks into the pleural cavity (see Figure 1.7 (B)).

Notably, another innovative application scheme is included in the protocol of another MeV-NIS clinical trial on therapy-resistant ovarian cancer (NCT02068794): intraperitoneal application on the first course with MeV-NIS is followed by subsequent courses every 4 weeks for up to 6 courses with MeV-NIS infected mesenchymal stem cells (MSC). These cell-based virus delivery systems are administered intraperitoneally as well (see Figure 1.7 (C)). The use of virus-loaded cell carriers to evade premature sequestration of virotherapeutics by the host immune response (e.g. by preexisting anti-measles antibodies) after an initial uncoated loco-regional (i.e. intraperitoneal) measles infection has

already shown very promising results in a xenograft mouse model. Tumor-specific infiltration of parenchyma with subsequent virus delivery by measles virus-infected mesenchymal stem cells was found to prolong overall survival when compared to “naked” infectious virus particles in mice. Therefore, a strong preclinical rationale had been built for exploring this innovative application design in the clinical setting [88].

MeV single-shot application schemes:

Russell and colleagues^[41] from the Mayo Clinic have recently presented a case report (NCT00450814) describing a durable complete remission of a patient with therapy-refractory multiple myeloma after a single shot of intravenous MeV-NIS (see Figure 1.7 (D)). MeV-NIS expression allowed the investigators to monitor infection of disseminated tumor sites with subsequent vanishing of all detectable tumor masses. Another application of a single shot of MeV-NIS in the treatment of head and neck cancer is part of a phase I trial (NCT01846091) but here administered by intratumoral injection (see Figure 1.7 (E)). A trial with MeV-CEA on brain and central nervous system tumors (NCT00390299) is using an altered application scheme. A single-shot application into the resection cavity after brain surgery is compared to a double-hit course with one application pre-surgery (via catheter) and another post-surgical intervention into the resection cavity (application scheme also depicted in see Figure 1.6 (B)).

As outlined above, insights gained from the MeV-NIS trial on multiple myeloma serve as a prime example to substantiate the single-shot “hit hard and early” paradigm. Here, Russell and colleagues provided a proof-of-principle that a single shot of systemically administered MeV at the maximum achievable dosage could lead to a complete clinical response even at advanced stages of disease. Key factors for a successful implementation of the single-shot paradigm were proposed to be the high dosage of infectious particles used for patient treatment (= “hit hard”) and no detectable amount of preexisting anti-virus serum antibodies (= “hit early”; i.e., prior to induction of a virus-specific immune response).” [27]

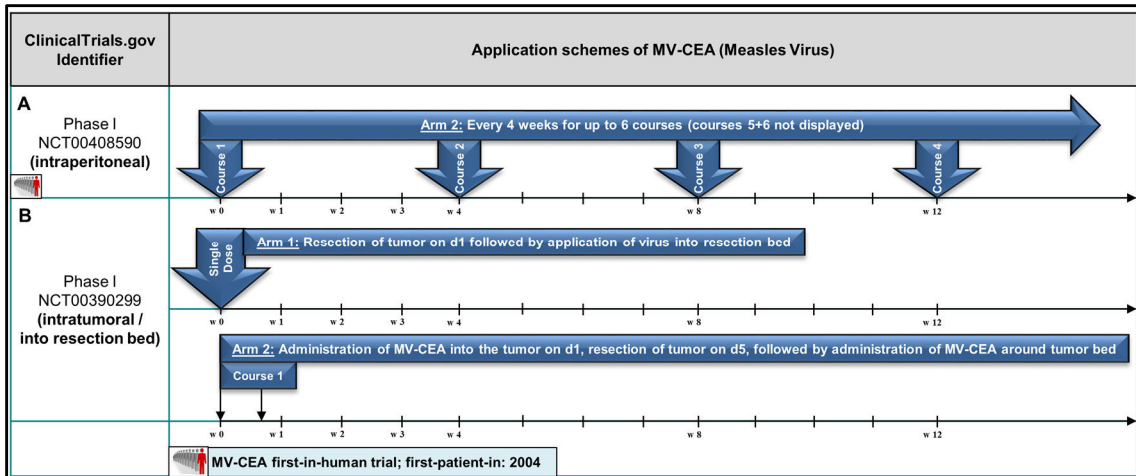


Figure 1.6: Selected application schemes of MeV-CEA: (B) results published by Galanis et al. [39]; (figure modified from published version [27])

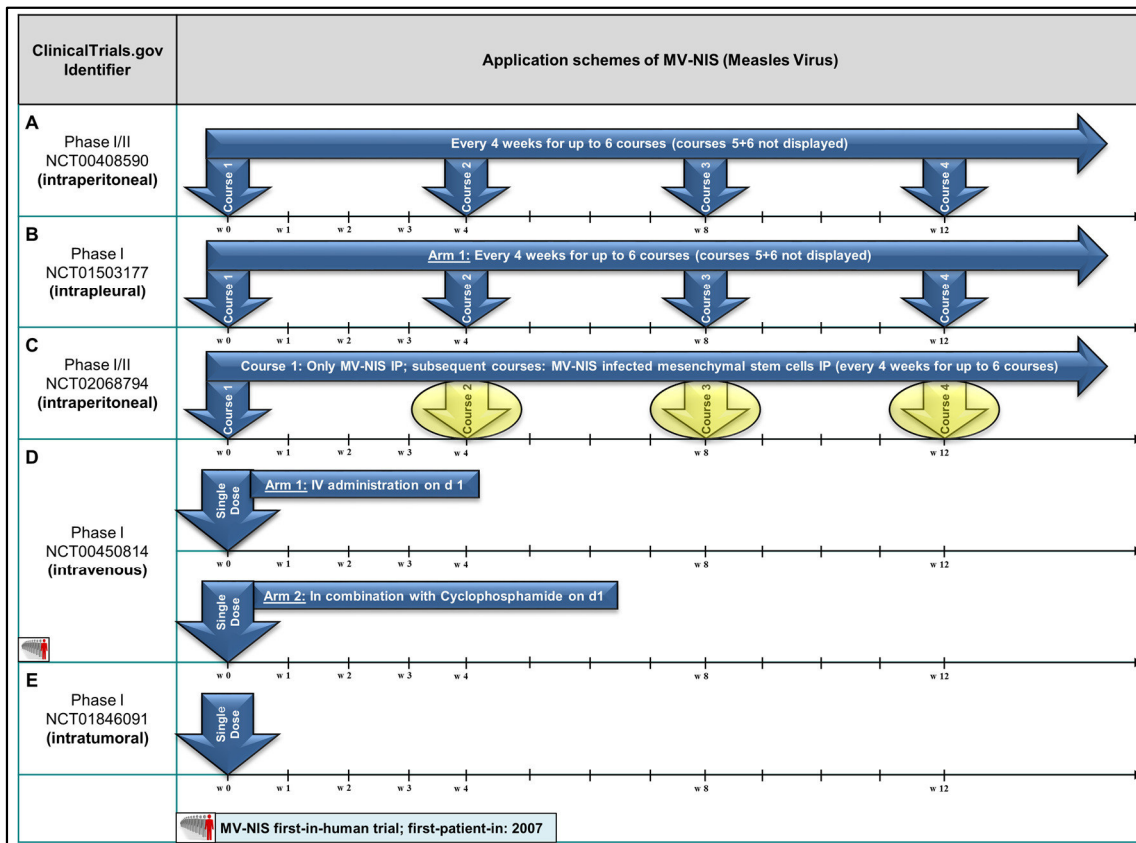


Figure 1.7: Selected application schemes of MeV-NIS: (A) Results published by Galanis et al. [40], (D) results published by Russell et al. [41]; (figure modified from published version [27])

1.4 Limitations to oncolytic virotherapy

Oncolytic virotherapy still struggles with various limitations, e.g. in case of measles virus, its premature neutralization by preexisting antibodies in the vaccinated population. This limits its clinical efficacy, as only few virotherapeutic particles are able to reach the respective tumor sites. Beyond that, phenomena of primary tumor cell resistances against MeV-based virotherapeutics also seem to constitute an important issue [89]. Recently, a screening of 54 cell lines derived from solid tumors revealed a high variation of susceptibility to measles virus-mediated oncolysis, revealing primary resistance phenomena to virotherapy in about 50% of all tested human tumor cell lines [90]. A further screening on a human sarcoma cell line panel revealed that differences of acquired defects in innate immunity signaling pathways are crucial for the efficiency of MeV-mediated oncolysis, as most resistant tumor cell lines were shown to exhibit at least partly intact IFN signaling pathways [79]. To further address those issues, combination strategies for oncolytic viruses are desperately needed, as it is more likely to exploit the full potential of virotherapy by affiliating the viral vectors with suitable combination partners.

In case of MeV-Edm-based virotherapy, there have been several approaches to challenge these limitations: employing the expression of the NIS transgene, pre-clinical studies of a radiovirotherapeutic approach showed enhanced anti-tumor effects when MeV-NIS was co-administered with ionizing gamma-radiation-emitter ^{131}I radioiodine [91] and MeV-CEA with conventional radiation even demonstrated synergistic benefits of this combinational approach [92].

The group of epigenetically operating histone deacetylase inhibitors (HDACi) distinguished itself to be of special interest for combination with OV's since they are believed to have a great potential to unmask cancer antigens as they destroy malignant cells and promote an inflammatory response [93] but are likewise able to prevent initial innate immunity signaling in infected tumor cells.

1.5 Innate immunity signaling following oncolytic virus infection

“In response to viral pathogens, mammalian cells have developed an arsenal of innate immunity factors to prevent viral infections, with a central role assigned to the interferon (IFN) system [94]. Virus derived pathogen-associated molecular patterns (PAMPs) are detected by e.g. cytoplasmic viral nucleic acid sensors such as RIG-I (retinoic acid-inducible gene 1) and MDA5 (melanoma-differentiation-associated protein 5) [95] or membrane associated Toll-like receptors (TLRs) [96], with subsequent activation of downstream NF- κ B signaling [97] or IRF-3/IRF-7 binding to the IFN promoter site [98], resulting in transcription and secretion of type I interferons. Autocrine and paracrine produced IFN binds to the membrane associated IFN-receptor with consecutive activation of the downstream JAK/STAT signaling pathway [99]. As a result, transcription of IFN stimulated genes (ISG) is induced, such as IFN-induced proteins with tetratricopeptide repeats (IFIT family), establishing an antiviral state within the infected cell as well as in non-infected bystanding cells [100]. Recently, it was shown that measles virus (MeV) vaccine strains such as the Edmonston strain of MeV, but not wild-type MeV, induce production of IFN- β , e.g. via IRF-3 activation [101, 102]. Since MeV-based virotherapeutics are generated on backbones of MeV vaccine strains [29, 79], MeV-induced production of IFN- β could have strong implications on rates of primary infection, replication and spread of MeV in tumor tissues, thereby constituting a severe limitation to MeV-based oncolytic virotherapy approaches.” [103]

1.6 Inhibitors of histone deacetylases (HDACi)

1.6.1 Principles of HDACi-based cancer therapy

The family of human histone deacetylases aggregates 18 protein complexes subdivided into four classes (class I, IIa/b, III, IV) in analogy to yeast HDACs with distinct enzymatic activity and localization within the cell [105]. Histone deacetylases are enzymes (together with e.g. histone acetyl transferases (HAT), DNA methyltransferases, etc.), involved in epigenetic regulation of gene expression, catalyzing posttranslational modification of histones (see Figure 1.8).

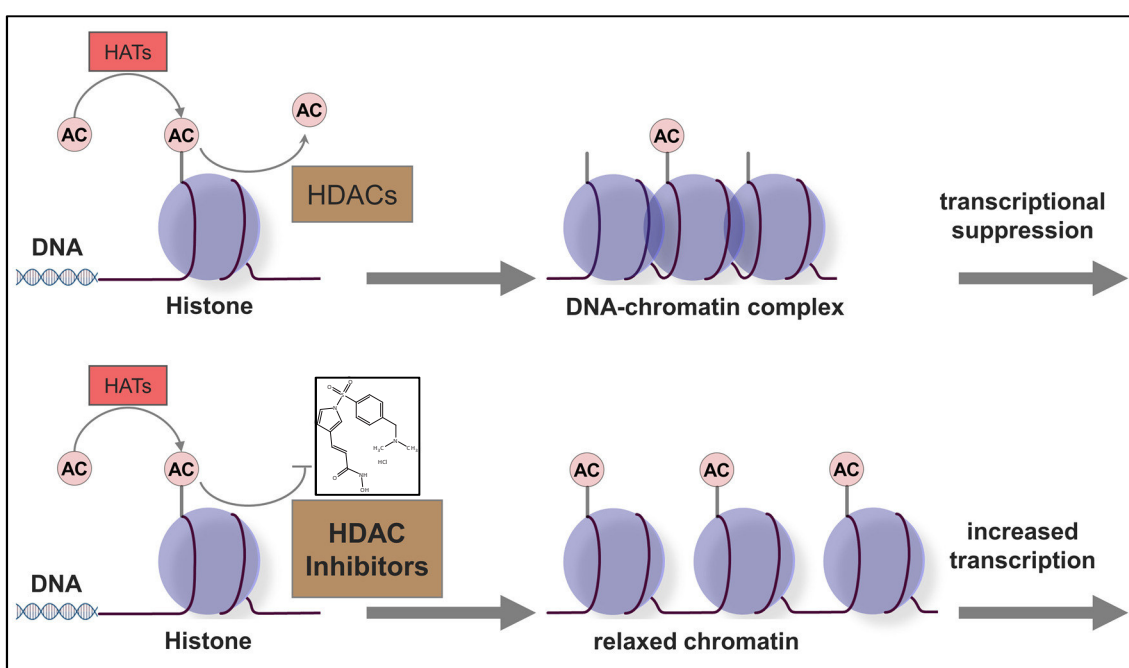


Figure 1.8: Principles of histone deacetylase inhibition.

Histone acetyl transferases (HAT) catalyze the transfer of an acetyl group (from acetyl-CoA) on lysine amino acids of histone proteins. Removing of these acetyl groups is catalyzed by histone deacetylase (HDAC) enzymes, leading to the formation of a tight DNA-chromatin complex and subsequent transcriptional suppression. Inhibition of HDACs results in less compact coiling of negatively charged phosphate backbone of DNA around histone proteins. This relaxed chromatin allows increased transcriptional activity of former silenced genes. Figure modified from Kazantsev et al.^[104].

In particular, HDAC catalyze removing of acyl groups on acetylated lysine residues of histones resulting in an electrophysiological condensation of histone proteins with DNA phosphate backbones and subsequent transcriptional suppression [106].

Among classical mechanisms of carcinogenesis involving malignant alterations in DNA sequences, epigenetic modifications - including acetylation and

methylation of histones - seem to be of particular importance during malignant transformation [107, 108].

The restoration of the non-transformed (i.e. the non-malignant/healthy) condition of these structurally intact (but disorganized through epigenetic regulation) genes has evolved as a potential target for HDACi cancer therapy, either by prohibiting an improper recruitment of HDACs to DNA promoter sites, by epigenetic modification of non-histone proteins, or by induction of pro-apoptotic genes that were otherwise aberrantly silenced in malignant cells [109, 110].

As a result, inhibition of histone deacetylases in cancers was found to result in cell cycle arrest or implementation of an intrinsic as well as extrinsic apoptotic program together with antiangiogenic and immunomodulatory effects [105, 110].

In 2006, the first histone deacetylase inhibiting compound vorinostat (SAHA) received FDA approval for treatment of cutaneous T-cell lymphoma (CTCL) and in 2009, the HDACi Romidepsin was approved for peripheral T-cell lymphoma [111, 112]. In contrast, epigenetic compounds have yet to demonstrate their potential to be efficient in the treatment of solid tumors as most HDACi clinical trials showed limitations in anti-tumor activity with at least to some extent concomitant toxicities [113]. As employment of epigenetic compounds as monotherapeutics is subject to particular controversy (e.g.: is pan-HDAC inhibition of therapeutic benefit compared to single class or single enzyme inhibiting compounds? [114]), these issues have to be further addressed before implementation into clinical routine. Combination of HDACi with other established cancer treatment regimen showed encouraging additive or even synergistic effects (e.g. [115, 116]). Proof of principle has been demonstrated for combination with other epigenetic compounds, such as DNA methyl transferases [117-119], microtubule interfering compounds, such as paclitaxel [120], proteasome inhibitors (such as bortezomib, marizomib, and carfilzomib) [121-123], conventional chemotherapeutic drugs (such as platinum based agents, 5-fluorouracil, gemcitabine, epirubicin) [124] and importantly conventional radiotherapy [125].

Therefore, inhibitors of histone deacetylases have emerged as ideal combination partners to overcome resistances, enhance therapeutic efficiency and on top of this minimize toxicities, as combinational approaches allow to reduce therapeutic dosages applied to cancer patients [110].

The special interest of histone deacetylase inhibition in combination with oncolytic virotherapy as an innovative treatment option for various malignancies is covered in section 1.7.

1.6.2 Resminostat, a novel histone deacetylase inhibitor

Involvement of epigenetic alterations are found for the origination and development of HCCs as well (reviewed in [126]). Preclinical and clinical studies have demonstrated inhibition of histone deacetylases by HDACi to be an efficient treatment option for this specific tumor entity [127-129].

“Resminostat constitutes an oral histone deacetylase inhibitor currently undergoing clinical evaluation in several phase I/II clinical trials in patients with advanced stage HCC (NCT00943449)” [103], patients exhibiting refractory Hodgkin’s lymphoma (NCT01037478), patients with advanced colorectal cancers (NCT01277406) and a small study on advanced solid tumors in a Japanese cohort [130].

The SHELTER (NCT00943449) study evaluated resminostat in combination with sorafenib compared to resminostat-monotherapy as second-line treatment option in patients with HCC progression under first-line sorafenib treatment. Here, a median overall survival of 8.1 months (resminostat + sorafenib) compared to 4.2 months in the resminostat monotherapy arm was achieved. This median overall survival (OS) in the combination arm means a benefit of nearly 3 months additional survival compared to an expected median OS of 5.2 months after tumor progression under sorafenib first-line therapy [131, 132]. Thus, resminostat showed – while being generally well tolerated – potential to re-sensitize therapy-refractory liver cancer to sorafenib treatment.

The SAPHIRE (NCT01037478) trial on relapsed/refractory Hodgkin’s lymphoma (HL) showed clinical efficacy of resminostat monotherapy for this malignancy as

19/34 patients (55.6%) obtained PET/CT accessed response or stabilization of disease [133].

In the SHORE (NCT01277406) trial on advanced colorectal cancer (CRC) resminostat was tested in combination with standard FOLFIRI therapy regimen and was overall found to be well tolerated and safe, as no dose limiting toxicities were observed [134].

Mechanistically, resminostat was found to inhibit class I and IIb HDACs (especially isoenzymes 1, 3, and 6) and therefore, by changing the acetylation status of both histones and other cellular proteins, altering the gene expression and transcriptional profile within tumor cells. “*In vitro* resminostat was shown to induce apoptosis in concentrations above 2.5 μ M, whereas lower concentrations resulted in a proliferation stop and cell cycle arrest [135].” [103]

Recently, zinc finger protein 64 (zfp64), a DNA binding transcription factor, was identified as a surrogate parameter for resminostat treatment, its expression being downregulated as early as 5 hours after treatment with resminostat [136]. Clinical evaluation hereby revealed that biomarker zfp64 could potentially predict resminostat responses in cancer patients as high zfp64 expression levels before treatment intervention correlated with achievement of a longer overall survival (OS) in Hodgkin’s lymphoma and hepatocellular carcinoma patients [131].

It is of special interest that resminostat proved its immunomodulating potency (see Figure 1.9) *in vitro* by enhancing the expression of several tumor associated antigens (TAA), by enhancing the expression of MHC I molecules and – in addition – by enhancing the expression of NKG2D ligands on tumor cell surfaces (including hepatoma cell line HepG2) and therefore boosting the recognition and subsequent NK cell-mediated killing of cancer cells. On top of this, resminostat treatment showed potential to re-establish antitumor immunosurveillance by reducing expression of both Indoleamine 2,3-dioxygenase 1 (IDO1) and Arginase1 [137] which are essential for repression of T-cell activation leading to peripheral tumor tolerance (reviewed in [138, 139]).

“This profile proposes resminostat as an interesting partner for novel epivirotherapeutic concepts in the combinatorial treatment of patients exhibiting advanced stages of HCC” [103]

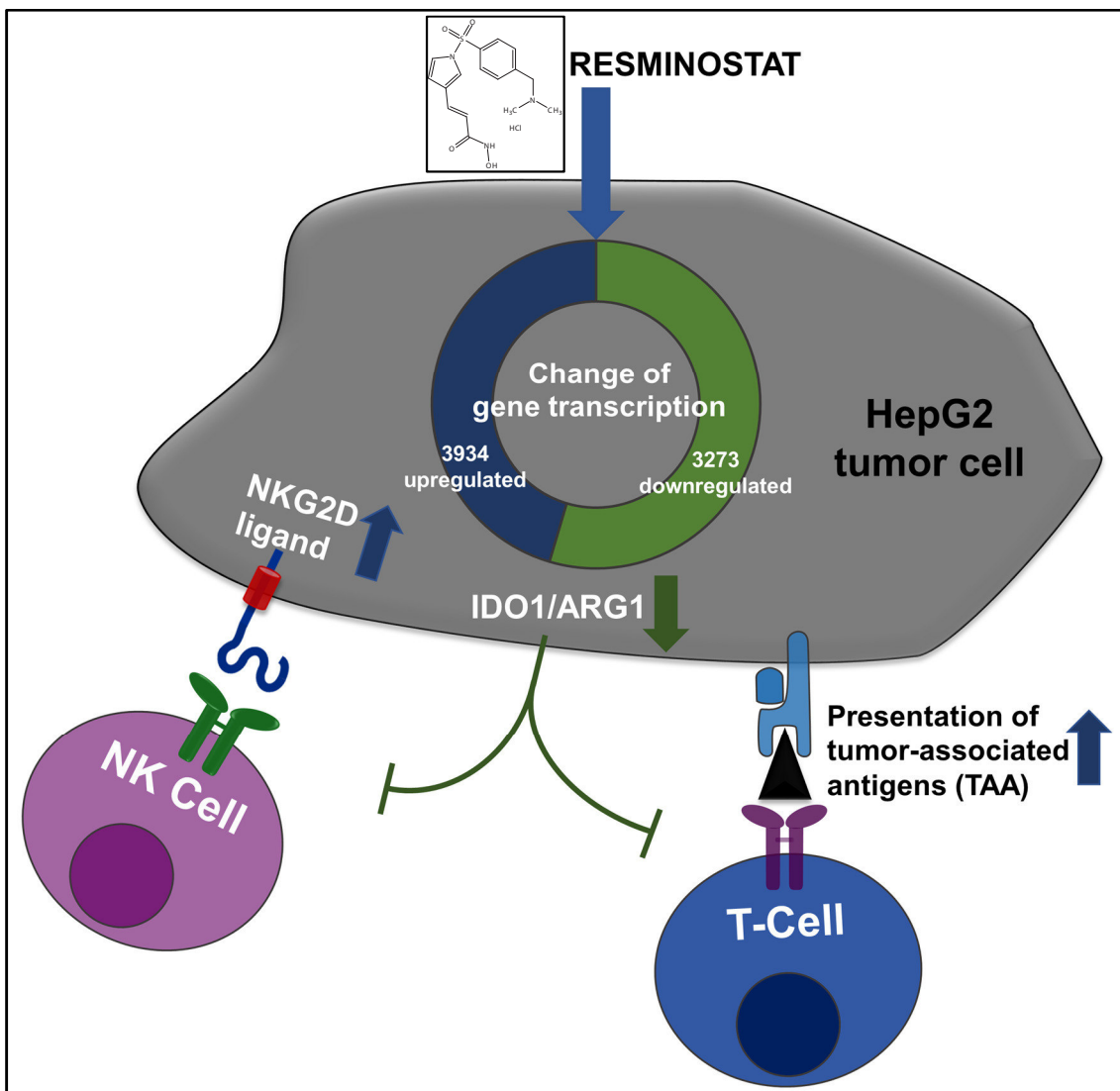


Figure 1.9: Immunomodulating effects of resminostat

Inhibition of different histone deacetylases by resminostat alters acetylation status of histones as well as other proteins resulting in altered transcriptional activity within tumor cells. Upregulation of NKG2D ligand expression on HepG2 cell surface leads to an enhanced recognition and subsequent elimination of tumor cells by natural killer cells (NK cells). On the other hand, resminostat treatment results in an enhanced expression of tumor-associated antigens (TAA), boosting a T-cell-mediated anti-tumor adaptive immune response. Downregulation of both Indoleamine 2,3-dioxygenase 1 (IDO1) and Arginase1 (ARG1) blocks unspecific tumor cell evasion of the patient's immune system. For further details, see text.

Figure modified from Hamm et al.^[137]

1.7 Epi-virotherapeutic combination therapies

As described above, successful oncolytic virotherapy (OV) depends to a great extent on tumor biology specifics. Therefore, combining OVs with immunomodulating compounds (such as HDACi) or radio-/chemotherapy promises to improve the prospect of successful virotherapeutic treatments [140, 141]. Successful combinations of HDACi and OVs have been reviewed by Nguyen et al.^[142], revealing distinct mechanisms of action, depending (i) on the specifics of viral vectors in use as well as (ii) on the individual HDACi used.

Recently, re-sensitization to vesicular stomatitis virus (VSV) induced oncolysis by HDAC inhibitors like entinostat (MS-275) and vorinostat (SAHA) has been demonstrated to result in a significant improvement of viral replication [143] in preclinical studies. Interestingly, entinostat combined with a virotherapeutic prime-boost using vectors of VSV and adenovirus origin, both expressing human dopachrome tautomerase (hDCT), were found to suppress primary immune responses, but to enhance secondary immune responses, resulting in a prolonged survival in a murine melanoma model [144]. In another experimental system, vaccinia virus replication and spread were found to be boosted by combination with the HDAC inhibitor trichostatin A (TSA) [145, 146]. A similar pattern was found for the combination of herpes simplex virus (HSV) and the HDAC inhibitor valproic acid (VPA) [147] revealing that VPA treatment impaired recruitment of immune cells as well as innate immunity signaling [89]. Replication of HSV was found to be intensified when employing a whole panel of different HDACi [148] and additional anti-angiogenic effects were identified for the combination of TSA plus HSV [149]. Another virotherapeutic vector, parvovirus H-1PV, led to additional functional insights on potential combinational mechanisms: addition of VPA was found to increase acetylation and thereby cytotoxicity of the NS1 protein of H-1PV [150]. HDAC inhibition in combination with adenovirus results in the upregulation of CAR, a membrane receptor for coxsackie and adenovirus subgroups [151]. However, opposite outcomes such as VPA-mediated inhibition of both adenovirus replication and spread have also been reported [152], indicating that every individual combination of HDAC inhibitor and oncolytic virus has to be investigated in detail.” [103]

1.8 Objective

Despite recent accomplishments in establishing oncolytic viruses as a new therapeutic option for cancer patients with advanced-stage disease, oncolytic virotherapy was found to face various limitations in clinical trials, which encompass not only poor delivery of virotherapeutics to tumor sites, but also primary and secondary resistances against those virotherapeutics resulting in rapid and uncontrolled tumor progression.

To address those limitations, epigenetic compounds, especially histone deacetylase inhibitors (HDACi), seem to be qualified for putative combination (i.e. epi-virotherapeutic) strategies in the field of oncolytic virotherapy.

Based on encouraging results in combining oncolytic viruses with histone deacetylase inhibitors, the aim of this dissertation was to establish a preclinical therapy regimen for the epi-virotherapeutic approach in the treatment of hepatocellular carcinoma (HCC), using the prototypic suicide gene-armed measles vaccine-based virotherapeutic MeV-SCD and the oral HDACi resminostat (Res) for *in vitro* studies on a panel of three well-established hepatoma cell lines (HepG2, Hep3B & PLC/PRF/5).

First, cytotoxic effects of both agents, resminostat & MeV-SCD, had to be tested on the hepatoma cell lines to determine single agent concentrations (for resminostat) and multiplicities of infection (MOIs, for MeV-SCD) to achieve a threshold of $\approx 75\%$ of remnant tumor cell mass, ensuring still sufficient amounts of viable tumor cells available for combinational testing scenarios.

As a next step, diverging application schemes had to be tested, varying the time schedule for both treatment modalities aiming to find out, whether pre- or post-treatment with the epigenetic compound is of positive influence for the therapeutic outcome. For the most efficient approach it had to be tested if combination of MeV + Res is accompanied by enhanced toxicity for non-malignant liver cells. In addition, anti-tumor effects of a triple therapy, superinducing prodrug 5-FC conversion by SCD expressing, MeV-SCD-infected tumor cells, had to be determined to exploit the full potential of the prodrug conversion enzyme encoding measles virus.

To further characterize mechanisms of action in the epi-virotherapy-based oncocytoxicity, cell cycle profiles were set out to evaluate differences in co-treated cells compared to the corresponding single-agent treatments.

Based on the results gained in the cytotoxicity assays, influences of resminostat HDAC inhibition on virus kinetics were investigated by working out viral growth curves and subsequent comparison between measles infection alone and in combination with resminostat. In a next step, alterations of measles primary infection rates under resminostat treatment needed to be determined as well as accompanying possible alterations in MeV entry-receptor (CD46) expression levels underlying an amended viral growth behavior.

To further reinforce the arguments for the epi-virotherapeutic approach in advanced HCC, another aim of this thesis was to demonstrate immunomodulatory properties of resminostat relating to an enhanced efficacy of measles-based virotherapy. This was set out to further simulate the *in vivo* situation, as an intact innate immunity signaling is crucial to oncolytic virotherapy.

2 Materials and Methods

2.1 Safety

The laboratory at Otfried-Müller-Str. 27, 72076 Tübingen, Germany, is constructed according to the “Act on the Prevention and Control of Infectious Diseases in Man” (Infektionsschutzgesetz, IfSG), of July 20, 2000, which is in conformity with the “directive 2000/54/EC” of the European Parliament and of the Council of September 18, 2000 “on the protection of workers from risks related to exposure to biological agents at work” for laboratories with Biosafety Level 2.

Therefore, it was necessary that all experiments including work with potentially contagious or hazardous biological and non-biological agents were performed under a HERAsafe laminar flow laboratory hood (*Heraeus*; Hanau, Germany). Surfaces and materials were disinfected using 70% isopropanol (*SAV Liquid Production*; Flintsbach a. Inn, Germany) or Descosept (*Dr. Schuhmacher GmbH*; Melsungen, Germany) and irradiated with ultraviolet light. Both solid as well as liquid waste were autoclaved at 2 bar pressure and 121 °C for 20 minutes (Autoclave 3850 EL, *Systemec*; Linden, Germany).

2.2 Cell biology methods

2.2.1 Cell lines

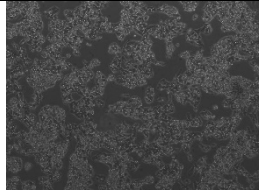
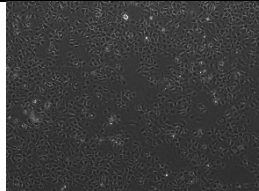
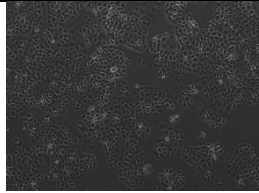
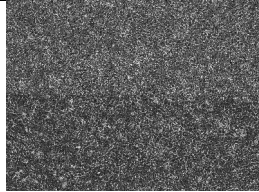
Name of the cell line	Origin	Source (Catalogue No)	Morphology
HepG2	Human hepatocyte carcinoma, 15 year-old-male	DSMZ (Catalogue No ACC 180)	
Hep3B	Human hepatocyte carcinoma, 8 year-old-male	DSMZ (Catalogue No ACC 93)	
PLC/PRF/5	Human hepatoma, 24-year-old male	ECACC (Catalogue No 85061113)	
VERO-B4	Monkey: African green monkey (<i>Chlorocebus aethiops</i> (<i>Cercopithecus aethiops</i>))	DSMZ (Catalogue No ACC 33)	

Table 2.1: Commercial cell lines used for the studies in this thesis:

Data available online for ECACC (= European Collection of Cell Cultures) <https://www.phe-culturecollections.org.uk/> (retrieved: 23.08.2014) and DSMZ (= Leibniz-Institut DSMZ-Deutsche Sammlung von Mikroorganismen und Zellkulturen GmbH): <http://www.dsmz.de/catalogues.html> (retrieved 23.08.2014). Microscopic picture of VERO-B4 cells provided by Dr. Susanne Berchtold, UKT.

2.2.2 General cell culture

The cell lines listed in Table 2.1 were cultured in tissue culture flasks with filter caps (either 75 cm² or 150 cm², *Greiner Bio One*; Frickenhausen, Germany) and stored in an incubator at 37 °C in a humidified atmosphere enriched with 5% CO₂. Hep3B and PLC/PRF/5 cells were cultured in Dulbecco's Modified Eagle's Medium (DMEM, *Sigma Aldrich*; Munich, Germany) plus 10% Fetal Bovine Serum (FBS, *biowest*; *Nuailié, France*). HepG2 cells were cultured using a minimum glucose DMEM (*Sigma Aldrich*) plus 10% FBS and additional L-glutamine [10 ml/l]. Vero cells were cultured with DMEM plus 10% FBS.

“Stimulation with human Interferon- β (IFN- β ; *Pepru-Tech*, Rocky Hill, NJ, USA) was achieved by adding 1,000 U/ml IFN- β to the culture medium.” [103]

Cells in culture flasks were microscopically examined on a daily basis with a CK40 contrast light microscope (*Olympus*, Shinjuku, Tokyo, Japan). Once confluence in the cell layer was reached, cells were washed once with sterile phosphate buffered saline (PBS, *Sigma Aldrich*) and subsequently detached with Trypsin/EDTA solution (*Biochrom*, Berlin, Germany or *Sigma Aldrich*). After an incubation of 2-5 minutes at 37 °C the cells were brought into solution with the corresponding FBS-supplemented medium and either split and discarded or seeded in cell culture multiwell plates (6 well-plates, *Corning*, Tewksbury, MA, USA; 24 well-plates, *TPP*; Trasadingen, Switzerland; 96 well-plates, *TPP & Corning*).

2.2.3 Cryoconservation of cultured cells

All cell lines could be long-term stored in liquid nitrogen (LN₂) at -196 °C or a freezer at -145 °C in a cryoconservation tube (1ml, *Corning*). Therefore, a cell suspension (prepared as described above) in a 50 ml conical-bottom tube (*Falcon/BD Bioscience/Becton Dickinson*, Franklin Lakes, NJ, USA) was centrifuged at 1300 rotations per minute (rpm) for 5 minutes, supernatant fluid was discarded and the cell pellet was resuspended in a cryoconservation medium (containing 90% DMEM-medium supplemented with 20% FBS and 10% Dimethylsulfoxid [DMSO, *Appli Chem*; Darmstadt, Germany]) and filled into the cryo tubes.

2.2.4 Thawing of cell lines

When a high number of passages was reached, which limited the “doubling potential” of our cultivated cells *in vitro* in accordance with the so called “Hayflick limit” [153] it was necessary to reculture the frozen cells. Therefore, frozen cells were thawed at 37 °C, suspended in 8 ml of warm DMEM supplemented with the appropriate amount of FBS and transferred into a 15-ml conical tube (*BD Bioscience*) and centrifuged with 1200 rpm at room temperature. The supernatant was discarded and the cell pellet was resuspended in 10 ml of fresh medium and transferred in a 75 cm² tissue culture flask.

2.2.5 Cell counting using a Neubauer haemocytometer

Determination of a diluted number of cells was accomplished using an improved Neubauer haemocytometer (see Figure 2.1) as described by Bastidas [154] (*Celeromics*; Grenoble, France): after getting the cells in suspension, the counting chamber was prepared by engaging the moistened covering glass with the central area of the Neubauer chamber. Then a 10µl sample of a cell suspension diluted with Trypan Blue (*Biochrom*) - which allows the differentiation between vital cells and dead ones - was pipetted close to the edge of the covering glass. After the sample had been soaked in by capillary action between covering glass and counting chamber, the chamber was examined under a CK40 light microscope (*Olympus*). The chamber's counting grid is represented in Figure 2.2 and is divided into small and large squares. The vital cells, which are not stained by Trypan Blue – since an intact cell membrane results in color retention of the dye – remain colorless in light microscopy. The four large squares were counted. As the distance between the covering glass and the bottom of the chamber is 0.1 mm, a 0.1 mm x 0.1 mm large square contains a volume of 0.1 µl.

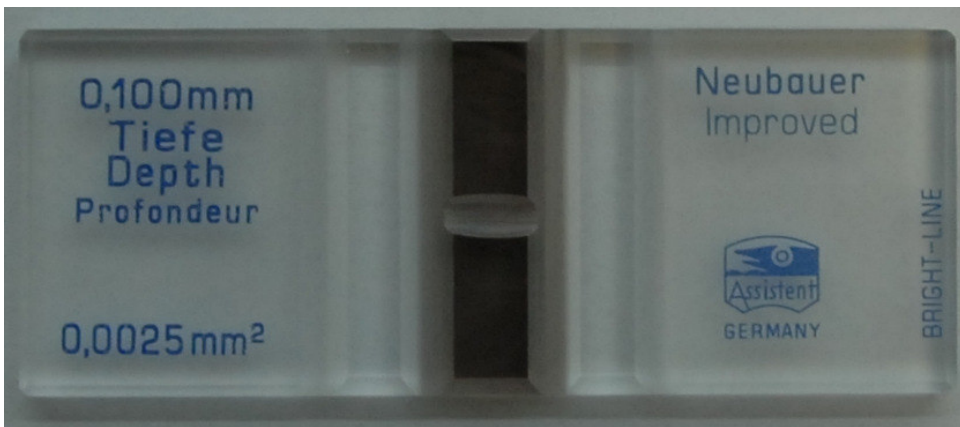


Figure 2.1: Representative Neubauer haemocytometer used for cell counting.

Hence, the formula of concentration calculation is:

$$\text{Concentration [cells/ml]} = \frac{\text{Number of cells} \times 10.000 \times \text{Dilution}}{\text{Number of counted squares}}$$

Equation 1: Determination of cell count using a Neubauer counting chamber

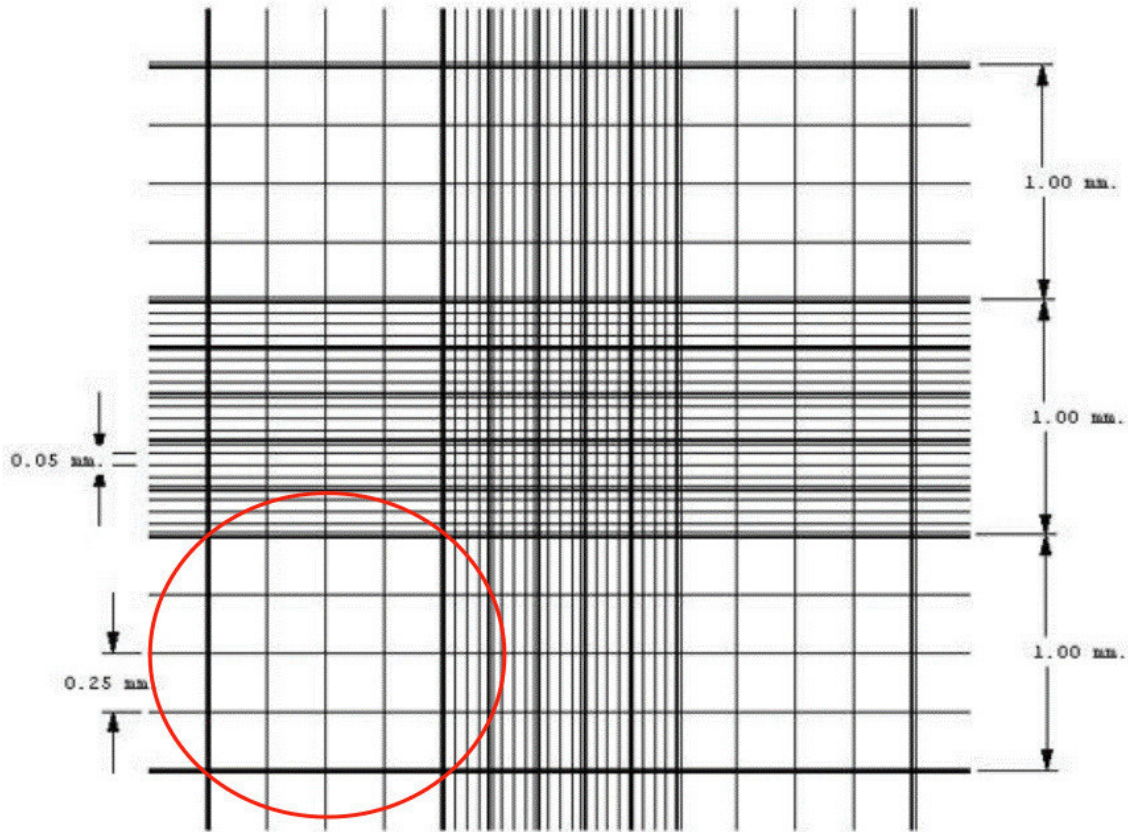


Figure 2.2: Improved Neubauer chamber grid detail:

Modified after manufacturer's user's guide www.celeromics.com/en/resources/docs/Articles/Cell-counting-Neubauer-chamber.php (retrieved on 23.08.2014). Usage as described in the text. Red circle marks a large square.

2.2.6 Infection with MeV-SCD/MeV-GFP and/or treatment with resminostat

24 h before any treatment, a defined number of cells was seeded into cell culture multiwell plates. Cells were washed once with sterile PBS (37 °C) and infected with different multiplicities of infection of viral vectors diluted in reduced serum medium Opti-MEM (*gibco*, Grand Island, NY, USA). Three hours post infection (hpi), the supernatant was removed and replaced with growth medium or medium containing resminostat, which was generously provided by 4SC AG, Planegg-Martinsried. Infection with measles vaccine virus MeV-SCD/MeV-GFP or treatment with the Histone-Deacetylase-Inhibitor (HDACi) resminostat was performed at variable orders and time-sequences, seeking for the most effective application setting. Further details will be described in section 3.2.

2.3 Virological methods

2.3.1 Titration of measles vaccine virus

“Construction of recombinant measles vectors MeV-GFP (measles vector encoding for green-fluorescent protein as a marker gene integrated into the viral genome) and MeV-SCD (encoding for suicide gene *Super-cytosine deaminase*, *SCD* [78]) has been described elsewhere [79].” [103]

Production and propagation of the measles virus vectors were performed in our group, and therefore, it was necessary to determine the concentration of virus in different frozen stocks of virus solutions. Viral titers were defined using the TCID₅₀ (tissue culture infective dose 50) endpoint titration according to Spearman [155] and Kärber [156] and results were converted into plaque-forming units/ml (pfu/ml).

24 h before infection with the virus containing sample, VERO cells were plated in a 96-well plate (*Corning*, 1×10^4 cells per well), diluted in 200 μ l DMEM plus 5% FBS. The day of infection, a dilution row was prepared on a single row of twelve wells on a 96-well plate: first, the twelve wells were filled with 270 μ l DMEM plus 5% FBS per well. 30 μ l of the original virus sample were pipetted into the first well and thoroughly mixed six times (resulting in a 1:10 dilution). The pipette tip was discharged and with a new tip, 30 μ l of the 1:10 diluted viral sample were pipetted into the following well. This procedure was performed on all twelve wells, resulting in a dilution range from 10^{-1} to 10^{-12} . Subsequently, the virus dilutions were transferred to the VERO cell plate, each dilution factor with a volume of 30 μ l into all eight wells of a column (see Figure 2.3).

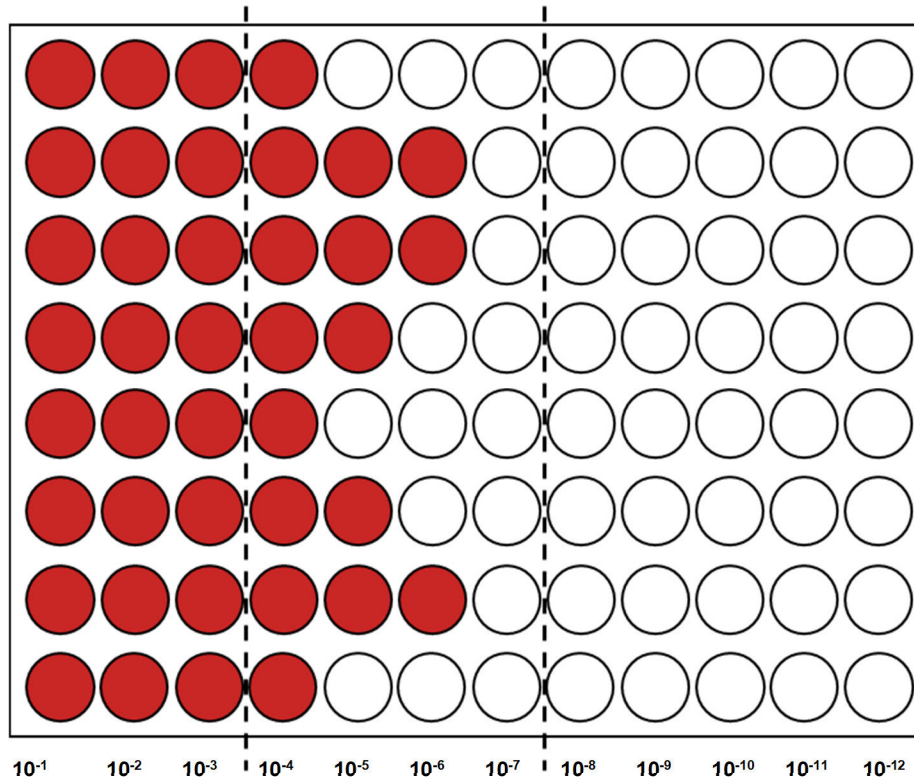


Figure 2.3: Scheme of MeV titration on VERO cells:
 VERO cells seeded 24 hpi in a 96 well plate were infected with MeV-SCD with indicated dilution factors. As an example MeV-positive wells are colored in red, the first four columns were considered “all positive”. Staining with anti-NP-antibodies was executed in the area of the plate between the dotted lines.

After incubation at 37 °C for 96 hpi, the VERO plate was examined under the light microscope and viral plaques, caused by cytopathic syncytia formation due to measles infection, were evaluated. Using this technique, all wells showing signs of viral infection were considered as “positive”. Immunofluorescence staining (only necessary for MeV-SCD) was executed for the last serial dilution with all “positive” wells, plus the following three dilution steps. Prior to staining, the entire plate was washed with 100 µl PBS per well (self-prepared: NaCl 137 mM (8 g) + KCl 2.7 mM (0.2 g) + Na₂HPO₄ 10 mM (1.44 g) + KH₂PO₄ 1.8 mM (0.24 g) + H₂O_{dd} filled up to 1 l) and then fixated with 50 µl of 4% paraformaldehyde (*Otto Fischar GmbH*) for 10 minutes and subsequently washed two times with PBS. The plates could then be stored at 4 °C for a few days.

After blocking the unspecific protein-binding sides with 100 µl/well 1% FBS in TBS-T (TBS-Tween (0.02%): 5 ml Tween-20 + 500 ml 10 x TBS + H₂O_{dd} filled up to 5 l) and simultaneously permeabilizing the cell membrane of the fixed cells with Tween-20, which is included in the TBS-T buffer for intracellular antibody binding,

the blocking solution was replaced after 30 minutes with 50 μ l of the primary antibody “MeV N-Protein NP clone 120 Mouse IgG2” (ECACC), diluted 1:1000 in TBS-T. After another 30 minutes and three washing steps with TBS-T (100 μ l per well), the secondary antibody “Alexa Fluor® 546 Goat Anti Mouse IgG (H+L), A11003” (Invitrogen, Carlsbad, CA, USA), diluted 1:1000 in TBS-T, was applied and incubated a last time for 30 minutes in the dark. After the final washing steps (three times with TBS-T) and addition of 100 μ l PBS/well, the plate was analyzed via fluorescence microscopy using a fluorescence microscope IX50 (Olympus), which is able to visualize the fluorescence dye of the “Alexa Fluor 546®” secondary-antibody (excitation: 557 nm, emission: 572 nm). Wells were considered as “positive” when more than one fluorescent particle was present in one well (single fluorescent signals were considered as non-replication-competent viral particles, which were excluded for determination of the viral titer). The calculation of the amount of infectious particles in the undiluted sample was calculated with the following formula:

$$x [pfu/ml] = a * 10^{(y-0.5+1.5)}$$

Equation 2: Calculation of viral titers using the TCID₅₀ method with included conversion into pfu/ml units.

With: $a = 0.7$ which is the conversion factor of the original TCID₅₀-method to the less abstract unit plaque forming units (pfu)

and $y =$ sum of the fractions of positive wells per dilution factor, e.g. for Figure 2.3 8/8 positive for the first 4 dilution factors (plus 8/8 for the undiluted) plus 5/8 for dilution factor 10^{-5} and 3/8 for dilution factor 10^{-6}

2.3.2 Viral growth curves

To compare the kinetics of viral growth in our hepatoma cell lines after infection with MeV-SCD alone or in combination with resminostat, virus titration of samples taken at five different time points over a period of 96 h was performed.

Therefore, HepG2, Hep3B and PLC/PRF/5 cells were plated in a 24-well plate 24 h before infection. The hepatoma cells were infected with adjusted MOIs (see Table 2.2), as preliminary experiments revealed varying susceptibility of different cell lines to viral oncolysis. Three hours post infection, after washing the plate

three times with PBS, the inoculum was substituted with DMEM or DMEM-containing resminostat (1 μ M). The first set of samples was collected immediately by pooling the supernatants of four wells of the same treatment into a 2-ml reaction tube (*Eppendorf*, Hamburg, Germany), then adding 0.5 ml OptiMEM per well and scraping the attached cells into the medium with a pipette tip. The cell suspensions of the two different treatment modalities were likewise filled into 2 ml reaction tubes. The samples were frozen at -80 °C until further usage. This procedure was repeated every 24 h until 96 hpi.

Cell line	Number of cells per well	MOI (MeV-SCD)	C _(resminostat) : [3 hpi]
HepG2	4 x 10 ⁴ /well	0.15	1 μ M
Hep3B	3 x 10 ⁴ /well	0.01	1 μ M
PLC/PRF/5	2 x 10 ⁴ /well	0.075	1 μ M

Table 2.2: Plating/treatment conditions for sample collection in the viral growth curves experiments. Adjusted number of cells per well and adjusted MOIs and were empirically determined by viability assays (as described in section 2.5). MOI: multiplicity of infection; c: concentration; hpi: hours post infection

After all samples had been collected, the day before titration, Vero cells were plated as described in section 2.3.1. The following day, the samples were thawed in a water bath (*Köttermann*, Uetze/Hänigsen, Germany) at 37 °C for only a few minutes, thoroughly vortexed and centrifuged at 3.000 rpm for 2 minutes. Dilution of the samples was performed according to a similar protocol as described above, but differed because serial dilution was carried out in a column of eight wells on a 96-well plate and more importantly, the first well was filled with 300 μ l of undiluted centrifuged supernatant, owing to the experience that the viral titer in the samples taken from the non-optimal growth system (in this case the hepatoma cell lines) was lower than those of the pure virus stocks. The serial dilution of eight factors was then transferred using a multichannel pipette (*Eppendorf*), applying a volume of 50 μ l per well to the VERO cells. This process was repeated for three further wells.

The read-out of the infected VERO cell plates was carried out exactly as described above in section 2.3.1.

2.3.3 Fluorescence microscopy on MeV-GFP infected cells

To visualize viral spread in the hepatoma cells, cells were seeded in 6-well culture plates the day before infection. Inoculation with MeV-GFP was performed with standardized multiplicities of infection [133] of 0.1 (pfu/cell) and 1 (pfu/cell) for all cell lines. Substitution of the virus containing OptiMEM with DMEM plus resminostat was implemented three hours post infection. Every 24 h for up to four days, comprehensive fluorescence microscopy was realized, using an IX50 (*Olympus*) microscope with a permanently connected F-view camera system (*Soft Imaging System GmbH*, Münster, Germany). *Analysis 3.1* software (*Soft Imaging System GmbH*) was used for post-processing phase contrast pictures (taken with 50 ms exposure time) as well as for fluorescence pictures (taken with 3000 ms exposure time). Both images were finally overlaid with the photoshop software GIMP 2 (free download available at <http://www.gimp.org/>).

Cell line	Number of cells per well	MOI (GFP)	C _(resminostat) [3 hpi]
HepG2	4 x 10 ⁵ /well	0.1 & 1	1 µM
Hep3B	2.5 x 10 ⁵ /well	0.1 & 1	1 µM
PLC/PRF/5	1.5 x 10 ⁵ /well	0.1 & 1	1 µM

Table 2.3: Conditions for fluorescence microscopy of MeV-GFP experiments
 MOI: multiplicity of infection; c: concentration; hpi: hours post infection

2.4 Flow Cytometry

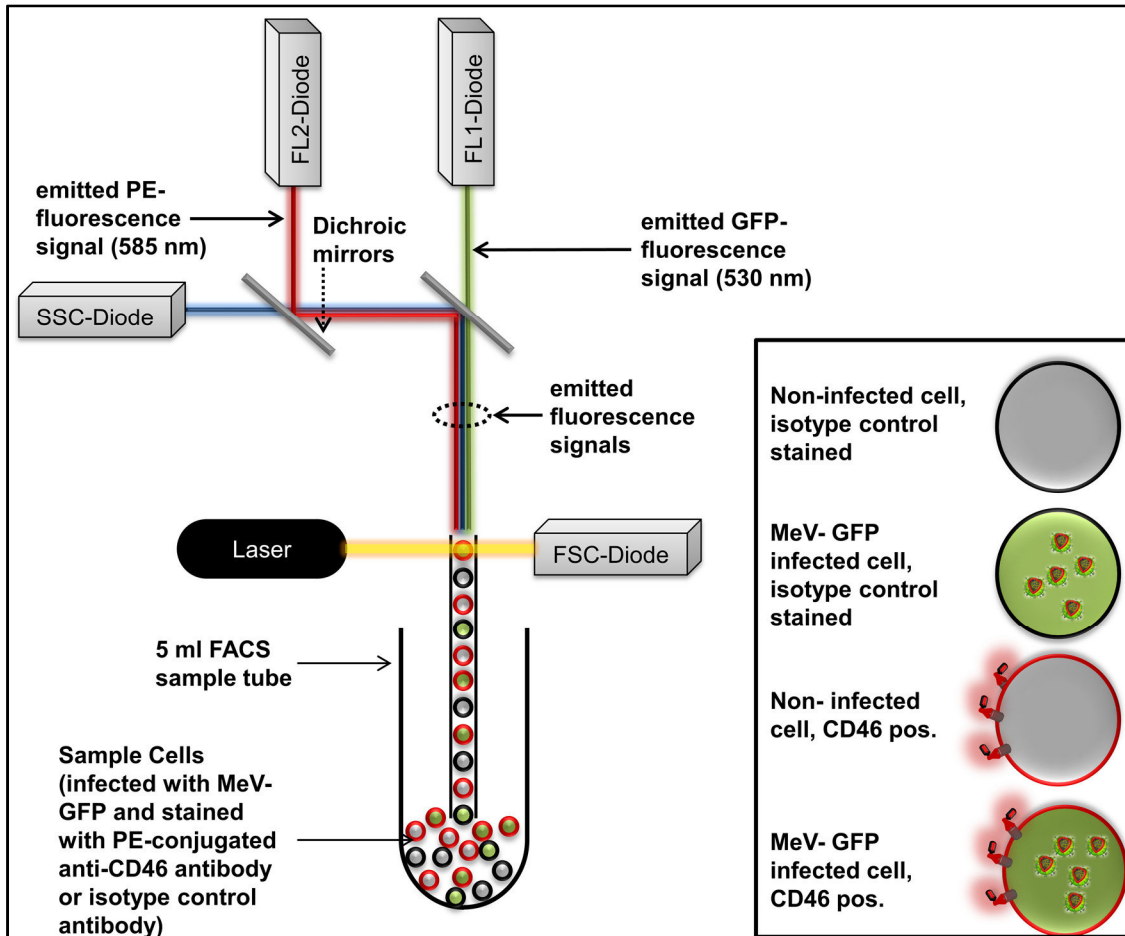


Figure 2.4: Schematic construction of a flow cytometer as used for analysing MeV-GFP infection rates, CD46-expression on hepatoma cells and analysis of cell cycle phases:

The sample cells pass a laser beam, which is scattered by the passing cell. The FSC-Diode detects the scattered light that correlates with the size of the cell. Emitted fluorescence signals from stimulated fluorescent molecules (i.e. GFP or PE) are filtered by dichroic mirrors and detected by additional diodes. GFP = green-fluorescent-protein, PE = phycoerythrin; CD46= Cluster of differentiation, FSC= forward-scatter, FL1/FL2= name of channel, SSC= side-scatter. For further details see text. Figure based on http://www.semrock.com/Data/Sites/1/semrockimages/drawings/flow-cytometry_500.jpg (accessed: 07.09.2014) and http://www.tiho-hannover.de/uploads/pics/Flowzytografik_10.jpg (accessed 07.09.2014).

2.4.1 Analysis of altered primary infection rates by fluorescence-activated cell sorting (FACS) using MeV-GFP

“Human hepatoma cells ($1.5 - 4 \times 10^5$ /well) were cultured in 6-well plates and then infected with a measles vaccine virus encoding a GFP marker gene (MeV-GFP) at MOI 1 and treated with resminostat at $1 \mu\text{M}$. At 24 hpi, hepatoma cells were washed once with 2 ml PBS/well and detached with 0.5 ml *Accutase* (PAA Laboratories, Cölbe, Germany). Subsequently, *Accutase* was inactivated with 2 ml FACS-buffer (PBS plus 10% FBS). Tumor cells were washed with PBS. After

centrifugation (302 x g, 5 min), the cell pellet was resuspended in FACS buffer. Cells were fixed by adding paraformaldehyde (*Fischer*) to a final concentration of 1.3%. Differences in rates of primary infection were analyzed on the *FACSCalibur* cytometer (*Becton Dickinson*, Franklin Lakes, NJ) and digitally processed with the *CellQuest* software (*Becton Dickinson*).” [103]

2.4.2 Quantitative analysis of CD46 receptor expression using flow cytometry

To further investigate the molecular mechanisms that underlie the combined treatment of the marker-gene expressing measles vaccine virus MeV-GFP and the HDACi, alterations of CD46-receptor expression in the hepatoma panel were investigated by fluorescence-activated cell sorting (FACS). To quantify the expression of the cellular receptor for measles virus binding (CD46) on cancer cells by flow cytometry, CD46 was labelled with an anti-CD46-antibody (*eBioscience*) that is conjugated with the fluorescent dye phycoerythrin (PE).

Within the flow cytometer, cells in solution pass, one by one, through a laser beam. A Forward Scatter (FSC-) diode detects the diffraction of emitted light and calculates the diameter of the passing cell, whereas different emitted fluorescent signals (which occur after stimulation with the laser beam) are detected by additional fluorescent channel diodes. Filters ahead of these diodes allow only one particular wavelength of light to pass (e.g. virus encoded eGFP emission wavelength: 509 nm), enabling the flow cytometer to detect different fluorescent signals within/on the cell currently rushing past (see Figure 2.4). In our case, the flow cytometer allowed us to calculate mean fluorescence indices for anti-CD46-surface-protein-stained cells under the influence of MeV-GFP and/or resminostat (co-)treatment. Isotype control staining is necessary to calculate the amount of non-specific background signals of the conjugated antibody.

Cell line	Number of cells per well	MOI (GFP)	C _(resminostat)
HepG2	4 x 10 ⁵ /well	1	1 μM
Hep3B	4 x 10 ⁵ /well	1	1 μM
PLC/PRF/5	1.5 x 10 ⁵ /well	1	1 μM

Table 2.4: Cell culture conditions in CD46-expression experiments.
 MOI: multiplicity of infection; c: concentration

The preparation of samples was performed as follows and is a modified protocol of Kolev and Kemper [157]: cells were seeded in 6-well plates and treated under the conditions listed in Table 2.4. Two wells of the same condition were pooled to ensure a suitable number of cells. At 24 hpi, cells were washed once with 2 ml of PBS per well and removed from the culture vessel by adding 1 ml of *Accutase* for 3-5 minutes, which was inactivated by 2 ml of FACS buffer per well. Transfer into a 15 ml conical tube was followed by 5 min of centrifugation at 1200 rpm. After counting the cells in a disposable Neubauer counting chamber (C-Chip, *Biochrom*), 5 x 10⁵ cells for the CD46 staining and the same count for an isotype control sample were transferred into 5-ml round-bottom tubes, washed with 3 ml of PBS, resuspended in 50 μl FACS buffer and 10 μl of *Gamunex* (=human IgG immunoglobulin; *Grifols*, Barcelona, Spain), which blocks unspecific F_c receptor binding sites, were added to the solution. 5 min of incubation on ice was terminated by adding 2.5 μl of PE-conjugated anti-human CD46-antibody (*eBioscience*) or 2.5 μl of PE-conjugated mouse IgG1κ as the isotype control (*eBioscience*) with a subsequent incubation for 30 minutes at 4 °C in the dark. After a washing step with 3 ml of PBS, centrifuging as described before and resuspending the cell pellet in 200-500 μl FACS buffer, flow cytometry could be performed using the *FACSCalibur* flow cytometer. *CellQuest* software was used during measurement and for post-processing digital data.

2.4.3 “Analysis of cell cycle profiles by flow cytometry

For this assay, human hepatoma cells (2 - 4 x 10⁴/well) were again cultured in 24-well plates and infected with MeV-SCD the next day at indicated MOIs in Opti-

MEM. Three hours post infection, medium was changed to DMEM or DMEM containing 1 μ M resminostat. After an incubation period of 96 h, cells were stained using the Nicoletti staining protocol [158]: both cell culture medium as well as PBS, which was used to wash the plates, were collected together with the cells, being detached by using trypsin. Cells were centrifuged at 300 x g. The cell pellet was resuspended in a hypotonic propidium iodide buffer (1 mg/ml sodium citrate; 0.003 ml/l Triton X-100; 0.02 mg/ml Ribonuclease A; 0.1 mg/ml propidium iodide, filled up with double distilled water) and cells were incubated for 30 min in the dark. As the buffer solubilizes plasma membranes and RNase digests intracellular RNA, propidium iodide as an intercalating nucleic acid binding fluorescent dye interacts exclusively with intracellular DNA in a proportional manner. As the intracellular DNA content is dependent on the stages of the cell cycle, cellular DNA content indicates in which phase of the cell cycle the trespassing cell currently is (e.g. hypoploid signals are detected in apoptotic cells). Fluorescence signals were detected on a FACSCalibur flow cytometer (*Becton Dickinson*) and data analysis was performed using *FLOWJO* flow cytometric analysis program (*FLOWJO LLC*; Ashland, OR, USA).“ [103]

2.5 Cell Mass and Viability Assays

2.5.1 Sulforhodamine B (SRB) cytotoxicity assay

As a routine screening method for cytotoxicity of the compounds under investigation, we used the Sulforhodamine B (SRB) cytotoxicity assay, which was first described by Skehan and colleagues [159]. The SRB dye binds to basic amino acid residues of protein chains under acid conditions and can be brought into solution under basic conditions. The amount of the released dye follows a linear correlation to the number of remaining cells and can be measured in a photometer [160].

As the SRB cytotoxicity assay is an endpoint measurement, cells were cultured and treated as described before (see section 2.2.6) in 24-well plates and after the appropriate incubation time, plates were washed once with 0.5 ml ice-cold PBS and fixed with 250 μ l 10% trichloroacetic acid (TCA) per well. The plates were then stored at 4 °C for 30 minutes and thereafter, the TCA was removed and the

plates were washed four times with tap water. Subsequently, the plates were dried at 40 °C for at least 24 h. The protocol then demanded the addition of 250 µl SRB staining solution (*Sigma Aldrich*, 0.4% w/v in 1% acetic acid) per well, which was removed after 10 minutes of gently shaking by washing the plate four times with 1% acetic acid to remove unbound staining solution. Following at least 6 hours of drying, the cell-bound dye was dissolved with 0.5 ml-2 ml of 10 mM TRIS pH 10.5 (*Sigma Aldrich*) per well. After a 10 minutes incubation period with careful shaking, the samples were transferred into a transparent flat bottom 96-well plate as duplicates with a volume of 80 µl each. For determination of optical density (OD), the microtiter plate reader Tecan Genios Plus (*Tecan*, Maennedorf, Switzerland) was used with an excitation filter of 550 nm and the data was processed by the *XFluor 4* (*Tecan*) software.

2.5.2 CellTiter-Blue® Cell Viability Assay

To confirm our cytotoxicity data gained from the SRB assay, we chose the more functional CellTiter-Blue® Cell Viability Assay, as this assay indicates the metabolic capacity of the treated cells, which is considered to be a direct marker of cell viability. The CellTiter-Blue® assay is based on the measurement of the potential of cells to reduce the active compound *resazurin* (7-Hydroxy-3H-phenoxazin-3-one 10-oxide) which is dark blue and non-fluorescent. Reduction of the dye to the pink and fluorescent *resofurin* by the cellular redox system is proportional to the number of viable cells and can be measured by a fluorometer or photospectrometer [161].

Treatment conditions were the same as for the SRB assay (see section 2.5.1) and the assay was used as an endpoint measurement after the scheduled incubation time. As treatment was carried out in 24-well plates, the manufacturer's protocol had to be slightly adapted. "To ensure equal amounts of culture medium per well, the supernatants of all wells of the same condition were pooled in a 2-ml reaction tube and 200 µl were readed per well. The admixture of 40 µl CellTiter-Blue® reagent (*Promega*, Madison, WI) per well started the incubation time that had to be empirically determined and took 1 h for HepG2 cells. Read-out was performed on the microtiter plate reader Tecan Genios Plus

(Tecan) with an excitation filter of 584 nm and run under the XFluor software.” [103]

2.6 Molecular Biology Methods

2.6.1 Immunoblotting

2.6.1.1 Preparation of cell lysates

“Human hepatoma cells were seeded in 6-well plates ($1.5 - 4 \times 10^5$ /well) and the next day stimulated with 1,000 U/ml IFN- β and/or treated with 5 μ M resminostat. Another 24 hours later, cells were washed with PBS and transferred into lysis buffer (50 mM Tris, 150 mM NaCl, 1% IGEPAL CA-630 [Sigma-Aldrich]). A total of three freeze-thaw cycles was followed by centrifugation to remove cell debris” [103], supernatants were transferred into new 1.5 ml reaction tubes and stored at -20 °C until further usage (see section 2.6.1.2 and section 2.6.1.3).

2.6.1.2 Bradford protein dye assay for measuring protein concentrations

To determine the concentration of total protein in the cell lysates, a quantification assay first described by M. Bradford [162] was performed, which is based on the shift in absorption maximum of the Coomassie Brilliant Blue G-250 dye after binding to the protein in solution. Binding to arginine-rich and aromatic sides of the proteins [163] causes a color change from red/brown to blue. This change in color is concentration-dependent and can be extrapolated by reference to a standard curve.

We used the BIO-RAD protein assay kit (*Bio-Rad Laboratories GmbH*, Hercules, CA, USA) to determine the amount of protein in our lysates.

A calibration curve was established by a serial dilution of a bovine serum albumin (BSA) protein standard (*Roth*; stock solution: 10 mg/ml) ranging from 0.5, 0.25, 0.1, 0.05 to 0 mg BSA/ml in H₂O_{dd}. 10 μ l of the BSA serial dilution as well as 10 μ l of the 1:20 diluted samples were pipetted as duplicates in a 96-well flat bottom microtiter plate and 200 μ l of the 1:5 diluted (in H₂O_{dd}) Bradford dye (*Bio-Rad Laboratories GmbH*) was supplemented.

Absorbance at 595 nm was measured in a 96-well microplate ELISA reader *Genios Plus* (Tecan) run by the *magellan* software and calculation of protein concentration based on the Lambert-Beer's law by referring to the standard curve.

2.6.1.3 Sodium dodecyl sulfate polyacrylamide gel electrophoresis (SDS-PAGE)

20 ml resolving gel (8% acrylamide)	
H ₂ O _{dd}	9.3 ml
30% acrylamide mix (<i>Carl Roth</i>)	5.3 ml
1.5 M Tris (pH 8.8)	5.0 ml
10% SDS (= sodium dodecyl sulfate)	0.2 ml
10% APS (= ammonium persulfate)	0.2 ml
TEMED (= tetramethylethylenediamine)	0.016 ml

Table 2.5: Ingredients of the resolving gel used for SDS-PAGE:
To start the polymerization process of the acrylamide APS and TEMED were added last.

8 ml stacking gel (5% acrylamide)	
H ₂ O _{dd}	5.5 ml
30% acrylamide mix (<i>Carl Roth</i>)	1.3 ml
1 M Tris (pH 6.8)	1.0 ml
10% SDS (= sodium dodecyl sulfate)	0.08 ml
10% APS (= ammonium persulfate)	0.08 ml
TEMED (= tetramethylethylenediamine)	0.008 ml

Table 2.6: Ingredients of the 5% stacking gel used for SDS-PAGE:
To start the polymerization process of the acrylamide APS and TEMED were added last. For detailed production information see text.

The emended method used in this thesis for separating proteins according to their molecular weight was first described by U. Laemmli in 1970 [164]. This assay uses a denaturation step as well as β -mercaptoethanol, which is an ingredient of

the loading buffer, to detach tertiary structure elements in proteins resulting in a linearized amino acid chain. Sodium dodecyl sulfate (SDS) is an anionic detergent that binds protein in a size-dependent way, negatively charging the proteins proportional to their mass [165].

To produce two 1.5-mm polyacrylamide gels consisting of a stacking gel (5% acrylamide) fraction and a resolving gel (8% acrylamide) fraction, 20 ml of the resolving gel solution (Table 2.5) were filled between two glass plates, covered with 70% isopropanol and left until polymerization was completed (about 30 minutes). After discarding the isopropanol and washing the gel surface with H₂O_{dd}, the stacking gel solution (Table 2.6) was filled on top of the resolving gel and a ten-fingered comb was inserted. After 15 minutes of polymerization, removing the comb left pockets in the stacking gel, which could be used for protein insertion.

Subsequently, the gels were assembled in an electrophoresis chamber which was filled with a 1:5 H₂O_{dd} diluted 5x running buffer (15.1 g/l Trizma Base, 72 g/l Glycine, 5 g/l SDS, filled up to one liter with H₂O_{dd}).

To 40-50 µg of a protein sample a fifth of the sample volume 6x loading buffer (37.5 ml TRIS 1 M pH= 6.8; 30 ml Glycerol, 12.3 g SDS, 60 mg bromphenole blue filled up to 100 ml with H₂O_{dd} plus additional 60 µl β-mercaptoethanol) was added and the mixture was boiled up to 95 °C for 5 minutes and centrifuged afterwards.

The first pocket of the gel was filled with 5 µl of a prestained PageRuler Plus protein ladder (*Thermo Scientific*, Waltham, MA, USA), whereas the protein samples were pipetted in the remaining pockets. Vertical electrophoresis was executed at a constant voltage of 70 V until all samples reached the resolving gel and then carried out with a constant amperage of 40 mA for one to two hours.

2.6.1.4 Western Blotting

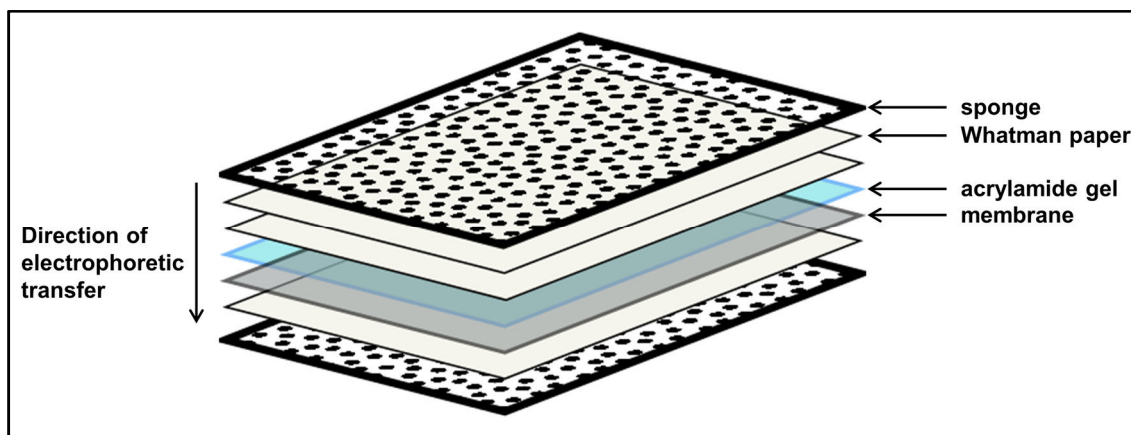


Figure 2.5: Correct arrangement of accessories and supplies in a Western Blot "sandwich":

All parts were clamped in the blotting system, keeping the gel in close contact with the membrane, ensuring that no air bubbles were trapped between the different components.

The separated proteins were electrophoretically transferred from the gel onto a polyvinylidene difluoride (=PVDF) membrane, where the proteins bind due to hydrophobic or polar interferences [165].

For electrophoretic blotting a blotting system of *BioRad* was used which made the correct arrangement of accessories and supplies (see Figure 2.5) necessary. Before stacking, the PVDF membrane was activated in methanol, washed once with H_2O_{dd} and then soaked together with the other materials in transfer buffer (48 mM TRIS; 39 mM glycine; 20% methanol, filled up with H_2O_{dd}).

The "sandwich" was installed into the blotting chamber, which was then filled with blotting buffer and cooled with an ice pack. Electrophoretic transfer was performed for 1 h at 300 mA.

After the transfer, the membrane was fixed in methanol and then stained with Ponceau S solution (0.1% Ponceau S [*Sigma Aldrich*] in 5% acetic acid,) to ensure successful protein transfer onto the membrane. At this point, marker bands were traced and the membrane was cut into two pieces at a predefined marker band of the rainbow colored protein ladder (e.g. at the red marker band which represented a molecular weight of 70 kDa). The membrane was rinsed with H_2O_{dd} to remove Ponceau S dye and then incubated for 1 h in 5% milk powder (*Roth*, blotting grade & low fat) dissolved in TRIS-buffered saline including 0.02% Tween 20 (= TBS-T: 150 mM NaCl, 13 mM TRIS, 0.02% Tween 20) to block

unspecific binding sites. Incubation over night at 4 °C with primary antibodies (for details see Table 2.7) was followed by three washing steps for 15 minutes with TBS-T and addition of the secondary antibody for 1 h at room temperature while shaking. To remove unbound antibodies, the membranes were washed once again for 3 x 10 minutes with TBS-T. Visualization of protein bands was performed with an enhanced chemiluminescence (= ECL) Western Blotting Detection Reagents kit (*GE Healthcare Ltd*, Buckinghamshire, UK) that uses the horseradish peroxidase (HRP)-coupled secondary antibody to blacken a high performance chemiluminescence film Amersham Hyperfilm™ ECL (*GE Healthcare Ltd*). A Fuji developer (*Fuji Photo Film Ltd*) was used to develop the films.

Molecular target	Description, species	Dilution	Brand
Primary antibodies			
anti-IFIT1	GTX103452; polyclonal, rabbit	1:1000 in TBS-T with 5% powdered milk	<i>GeneTex</i>
anti-Phospho-Stat1	58D61; polyclonal, rabbit	1:1000 in TBS-T with 5% BSA	<i>Cell signaling Technologies</i>
anti-Stat 1	sc-591; polyclonal, rabbit	1:500 in TBS-T with 5% powdered milk	<i>Santa Cruz Biotech</i>
β-Actin	A4700; monoclonal, mouse	1:5000, TBS-T with 5% powdered milk	<i>Sigma Aldrich</i>
Secondary antibodies			
anti-Rabbit IgG	HRP-coupled, goat	1: 8000 in TBS-T with 5% powdered milk	<i>Bio-Rad</i>
anti-Mouse IgG	HRP-coupled, goat	1: 8000 in TBS-T with 5% powdered milk	<i>Bio-Rad</i>

Table 2.7: List of antibodies used for Western Blotting:

TBS-T = TRIS-buffered saline including 0.02% Tween 20, HRP = horseradish peroxidase.

To add a second set of primary antibodies (e.g. for housekeeping genes as a loading control) the membranes could be stripped with 50 mM sodium hydroxide (NaOH) for 10 minutes after washing with H₂O_{dd}. Blocking with powdered milk,

the addition of the antibodies and following steps were then executed as described above.

2.6.2 “Real-time-quantitative Polymerase Chain Reaction (qPCR)

RNA was isolated using the NucleoSpin® RNA kit (*Macherey-Nagel*, Düren, Germany) according to the manufacturer’s instructions. 500 ng of each RNA sample were mixed with 2 µl M-MLV RT buffer (*Promega*, Madison, WI, USA), 1 µl RNase-inhibitor RNasin Plus (*Promega*), 1 µl oligo-dT-Primer (*TIB MolBio*, Berlin, Germany), 0.5 µl dNTP mix (Roti-Mix PCR3, *Carl Roth*) and added up to a total volume of 9.6 µl in RNase-free water. Samples were then incubated at 70°C for 2 min. After adding 0.4 µl reverse-transcriptase M-MLV RT H(-) Point Mutant (*Promega*), samples were incubated at 42 °C for 60 min.

The cDNA samples were diluted (1/20) with tRNA-H₂O; primers were used in a concentration of 500 nM. PCR was carried out in an iCycler (*BioRad*) with iQ5 Multicolor Real-time Detection System (*BioRad*), using the following setup: 10 µl iQSYBR Green PCR Master Mix (*Promega*), 0.1 µl of each primer (100 µM stock), 7.8 µl H₂O and 2 µl cDNA (diluted 1/20). The following primer pairs were used: zfp64 (splicing variants 1,3,4) forward: ACCTGCCACGGAAAGTAAT; zfp64 (splicing variants 1,3,4) reverse: TATGGGGTTTGTCTCCCGTG; RPS18 (housekeeping gene) forward: GAGGATGAGGTGGAACGTGT; RPS18 reverse: TCTTCAGTCGCTCCAGGTCT. PCR was carried out with the following thermal profile: 3 min at 95 °C with subsequently 40 cycles for 15 sec at 95 °C, 20 sec at 60 °C, and 15 sec at 62 °C. Heating up for 1 min at 95 °C was followed by 1 min at 65 °C and 81 cycles at 65 °C cooling down to 20 °C. Target gene expression was evaluated via the 2^{-ΔCt} method and normalized to the housekeeping gene *RPS18* and subsequently graphed relative to the respective MOCK sample for each time point and expressed as "relative gene expression". [103]

3 Results

3.1 Preliminary experiments

3.1.1 Cytotoxic effect of MeV-SCD monotherapy

"Combinations of oncolytic viruses with various epigenetic compounds have been shown to result in the enhancement of their therapeutic efficacy, encouraging further investigation of novel combinatorial epi-virotherapeutic settings. In this context, we have tested the anti-tumoral potency of either resminostat, a novel oral histone deacetylase inhibitor (HDACi), or MeV-SCD, a prototypic suicide gene-armed measles vaccine virotherapeutic, in a commonly used panel of human hepatoma cell lines (HepG2, Hep3B, PLC/PRF/5).

For this purpose, human hepatoma cells were infected in a first step with different multiplicities of infection (MOIs), ranging for HepG2 cells from MOI 0.01 to 1, for Hep3B cells from MOI 0.001 to 0.1, and for PLC/PRF/5 cells from MOI 0.001 to 1 (Figure 3.1 (B)). Then, at 96 hours post infection (hpi), the remaining hepatoma cell masses were quantified by a sulforhodamine B (SRB) viability assay (Figure 3.1 (A)). As a result, susceptibilities of these hepatoma cell lines to MeV-SCD mediated oncolysis were found to vary within a large range (Figure 3.1 (B)). Thus, in subsequent experiments we used different (adjusted) MOIs for hepatoma cell lines HepG2 (MOI 0.1), Hep3B (MOI 0.01), and PLC/PRF/5 (MOI 0.075). On this basis, remnant tumor cell masses of $\approx 75\%$ (Figure 3.1 (B), dotted lines) were ensured for monotherapy with MeV-SCD. This $\approx 75\%$ threshold was highly instrumental in providing still sufficient amounts of viable hepatoma cells to be killed in later tested scenarios, in which we applied the epi-virotherapeutic combination of MeV-SCD plus resminostat (MeV + Res)." [103]

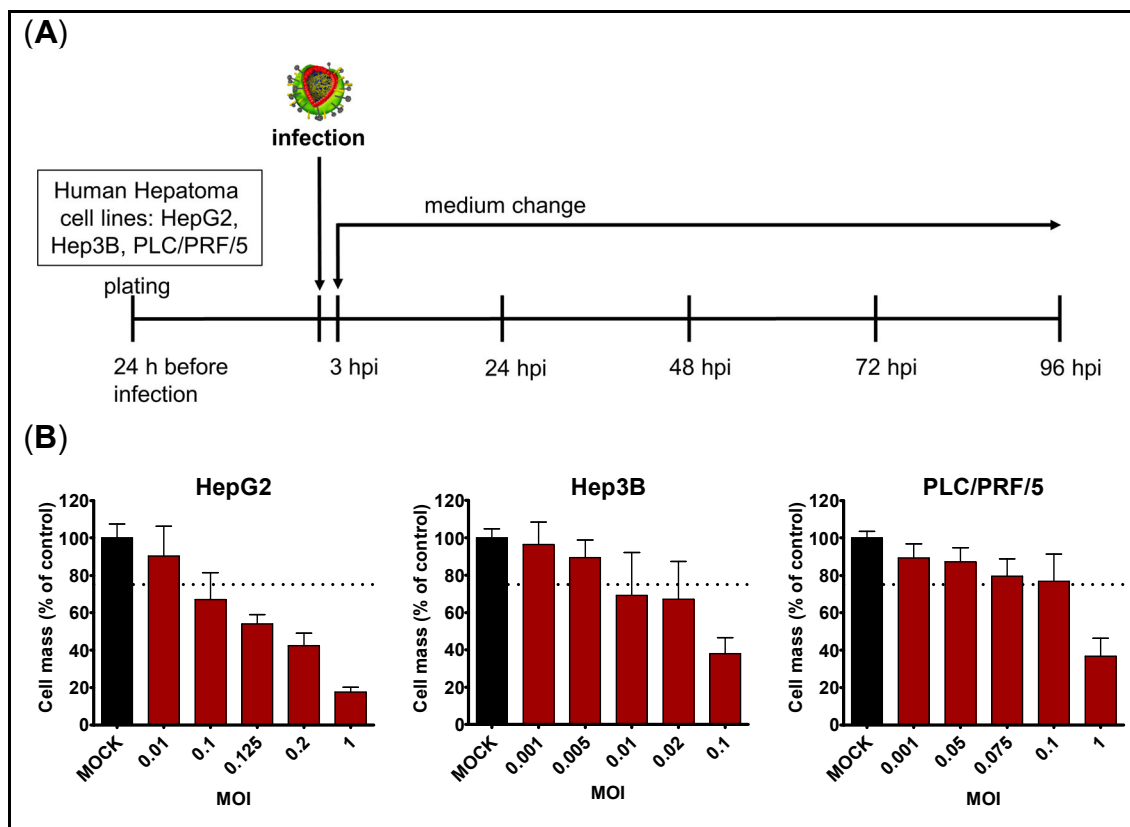


Figure 3.1: Remaining tumor cell masses after single (monotherapeutic) treatment with MeV-SCD: (A): timeline for MeV-SCD single-agent treatment. (B, published in [103]) Human hepatoma cell lines HepG2, Hep3B, and PLC/PRF/5 were infected with the prototypic suicide gene-armed measles vaccine-based virotherapeutic MeV-SCD at the indicated multiplicities of infection (MOIs). 96 hours post infection (hpi), the remaining hepatoma cell masses were determined by a sulforhodamine B (SRB) viability assay. Displayed are means and standard deviations (SD) of three independent experiments each carried out in quadruplicate. Dotted lines indicate the 75% threshold of remnant tumor cell masses at 96 hours post therapeutic intervention. MOCK: untreated control.

3.1.2 Anti-tumor activities of resminostat on human hepatoma cell lines

“In a second step, we also investigated the monotherapeutic cytotoxic potential of resminostat on human hepatoma cell lines. For this purpose, HepG2, Hep3B, and PLC/PRF/5 cells were incubated either for 24, 48, 72 or 96 hours (see timeline in Figure 3.2 (A)) with increasing concentrations of resminostat (ranging from 0.5 to 10 μ M; see Figure 3.2 (B)). As a result, resminostat was found to reduce hepatoma cell masses being residual at 96 hours in a time- and dose-dependent manner (see Figure 3.2 (B)) Again, we set out to attain a residual hepatoma cell mass of \approx 75% also in the monotherapeutic use of resminostat” [103] (see Figure 3.2 (B), dotted lines), and agreed for subsequent combinational settings to focus on the time point 96 h post intervention, mainly owned to experiences in corresponding virus treatment. This could be easily achieved by

applying a uniform resminostat concentration of 1 μM for all three hepatoma cell lines used.” [103]

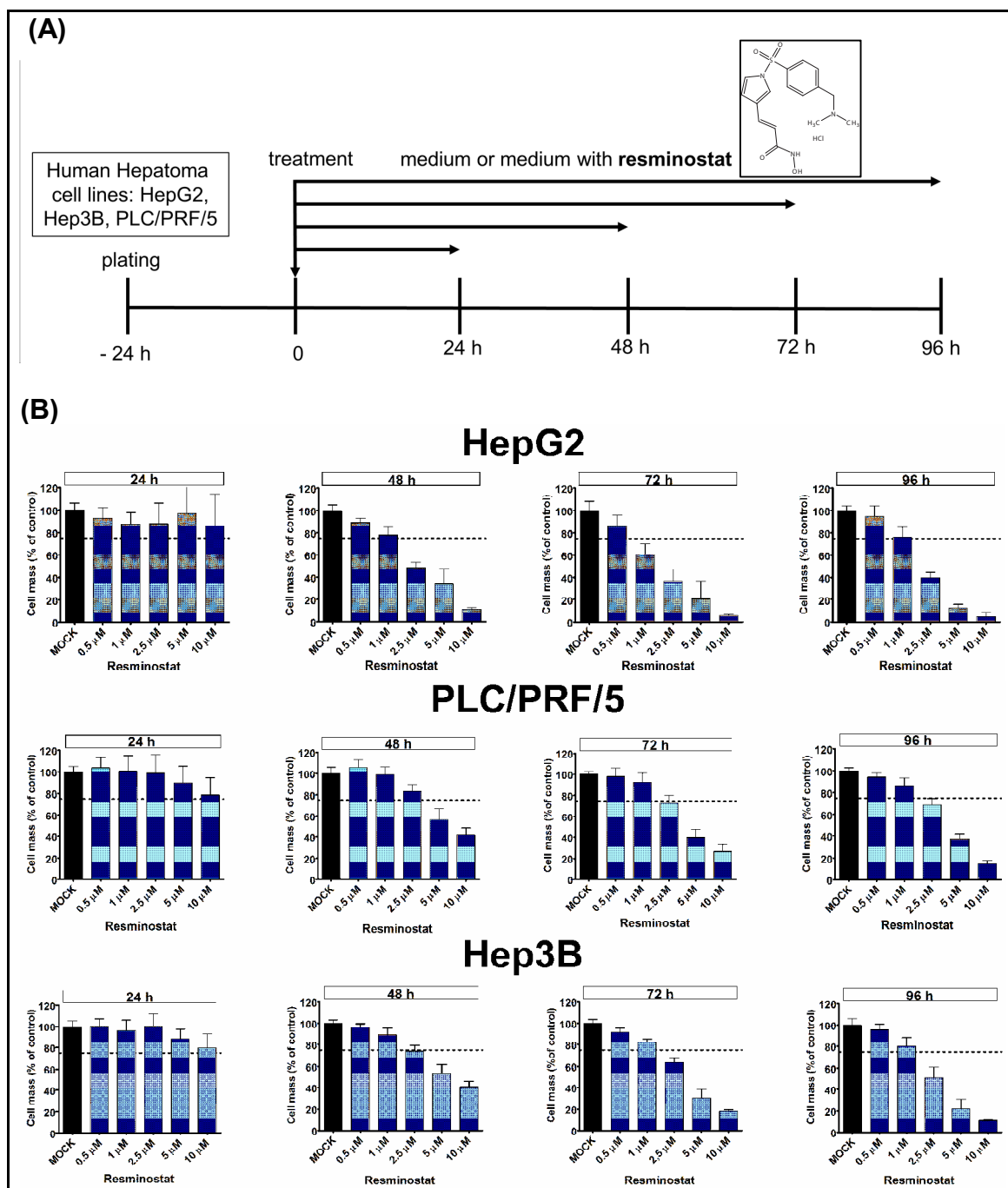


Figure 3.2 Cytotoxic effect of resminostat as a monotherapeutic agent in hepatoma cell lines Human hepatoma cell lines HepG2, Hep3B, and PLC/PRF/5 were treated with increasing concentrations of resminostat as indicated. Sulforhodamine B endpoint measurement was performed 24 h, 48 h, 72 h & 96 h later (see timeline in (A)). Values in (B) show means of at least three independent experiments performed in quadruplicates. Error bars: SD, Dotted lines indicate the 75% threshold of remnant tumor cell masses at indicated hours post resminostat treatment. Figures for 96 h values (columns on the far right) published in [103].

3.2 Resminostat + MeV-SCD-based combination treatment settings

3.2.1 Boosted cytotoxic/oncolytic effect of the epi-virotherapeutic combination treatment

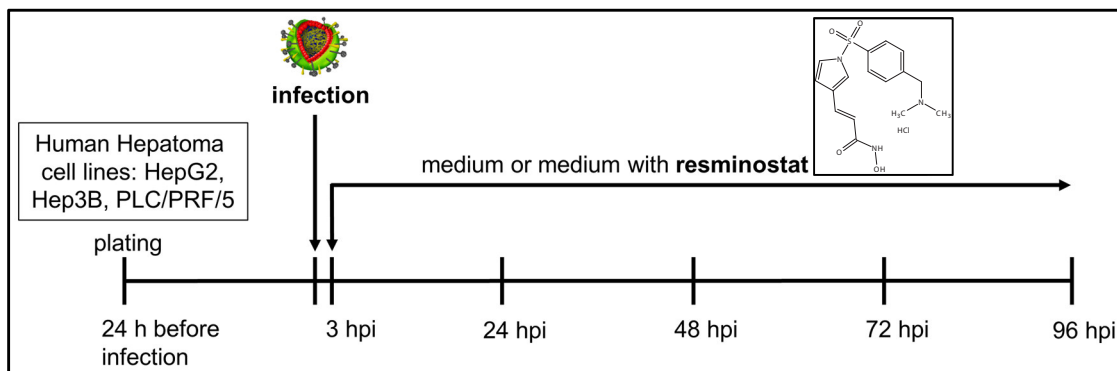


Figure 3.3: Application scheme for MeV-SCD and resminostat co-treatment in hepatoma cells

“In a next step, we investigated the specific combinatorial epi-virotherapeutic potential of HDAC inhibition plus virus-mediated oncolysis (MeV + Res). For this purpose, hepatoma cells HepG2, Hep3B, and PLC/PRF/5 were first infected with MeV-SCD (using threshold-adjusted MOIs as described above). At 3 hpi, resminostat was added (see timeline in Figure 3.3) also in a threshold-adjusted manner (1 μ M). As a result, boosted combined cytotoxic/oncolytic effects were observed in all three human hepatoma cell lines, HepG2, Hep3B & PLC/PRF/5, when compared with any of the two corresponding single agent / monotherapeutic treatment regimens, leading to a significant reduction of tumor cell masses as being quantified by SRB (Figure 3.4 (A), column on the left) and CellTiter-Blue (Figure 3.4 (B), column on the right) viability assays (purple bars (*combi*) versus blue/red bars (*mono*)). In detail, for HepG2 cells we found a reduction of hepatoma cell masses (i.e. SRB assay) for the combinatorial setting down to 37.6% compared to 84.7% (resminostat alone) and 65.2% (MeV-SCD single agent treatment). In Hep3B cells, hepatoma cell masses were reduced to 59.1% (*combi*) whereas reduction to only 81.4% (resminostat) or 76.8% (MeV-SCD) could be achieved in monotherapeutic approaches. PLC/PRF/5 hepatoma cells reached a 48.1% residual tumor cell mass (*combi*) compared to 77.8% (resminostat) and 69.4% (MeV-SCD) in monotherapeutic approaches.

Interestingly, these findings could not be confirmed in primary human hepatocytes (PHH), where addition of resminostat to MeV infected primary cells did not further reduce PHH cell masses (Figure 3.4, panel on the bottom).” [103]

Comparison of cell viability, determined by the CellTiter-Blue assay (see Figure 3.4 (B)), showed a decreased cancer cell viability for HepG2 cells in the combinational setting to 49.2% compared to resminostat (80.4%) and MeV-SCD (62.5%) single-agent treatment. In Hep3B cells, viability was found to be further reduced to a mean of 61.0%, compared to 78.1% (Res) and 74.4% (MeV-SCD) in the corresponding monotherapies. In this assay, viability of tumor cells was found for the cell line PLC/PRF/5 to be diminished to a minimum of 69.5% in the MeV + Res setting which is also a further reduction compared to 77.6% (Res) and 81.4% (MeV) respectively. In non-malignant PHH cells, no significant reduction was found in co-treated cells, compared to solely MeV-SCD infected samples.

“Although addition of resminostat to MeV-infected cells did not further reduce PHH cell viability (Figure 3.4 (A) and (B) panels on the bottom) compared to the corresponding monotherapies, combination treatment (MeV + Res; (Figure 3.4 (A), lower right panel, lane 4) did significantly affect PHH viability compared to the untreated control (Figure 3.4 (A) and (B), panel on the bottom, lane 1). This effect seems to be largely dependent on MeV-infection (Figure 3.4 (A) and (B), panel on the bottom, lane 3) as resminostat treatment alone had been found to have no impact on PHH viability (Figure 3.4 (A) and (B), panel on the bottom, lane 2).

[...] Thus, a proof-of-principle has been provided for the profound anti-tumoral effects of a novel combination therapy based on the oral HDAC inhibitor resminostat (Res) combined with oncolytic measles vaccine virus MeV-SCD (MeV). Since this specific epi-virotherapeutic combination (Res + MeV) potentially could define a new therapeutic option for HCC patients, we further investigated molecular mechanisms possibly underlying the observed boosted anti-tumoral effect in detail.” [103]

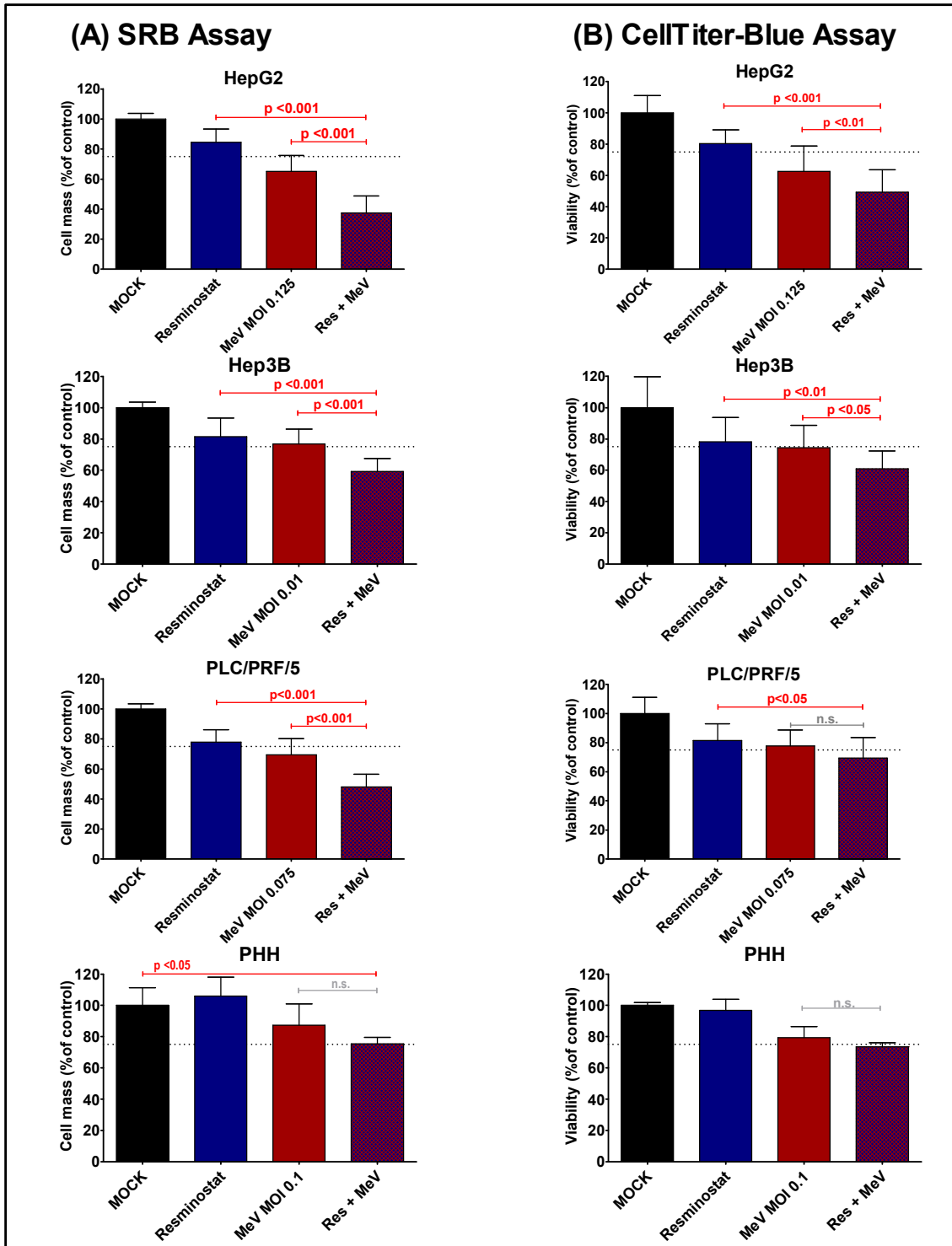


Figure 3.4: Boosted cytotoxic effects obtained by epi-virotherapeutic co-treatment with MeV-SCD and resminostat

Human hepatoma cell lines HepG2, Hep3B, and PLC/PRF/5 and non-malignant primary human hepatocytes (PHH; lower panel) were infected with MeV-SCD (at adjusted MOIs) and co-treated with resminostat (1 μ M) at 3 hpi. Endpoint measurements were performed at 96 hpi using the SRB viability assay (left panel: (A), published in [103]) and CellTiter Blue Viability assay (right panel (B)). Displayed are means and standard deviations (SD) of at least three independent experiments for hepatoma cells and one experiment for PHH cells, each carried out in quadruplicates; p-values of one-way ANOVA with a Tukey post-test. Res: resminostat. MeV: suicide gene-armed measles vaccine-based virotherapeutic MeV-SCD. MOI: multiplicity of infection. hpi: hours post infection.

3.2.2 Other application settings in MeV-SCD/resminostat co-treatment

3.2.2.1 Pre-treatment with resminostat 48 hours before infection

To test whether chronology of resminostat co-application is of influence for treatment outcome (determined by residual tumor cell masses after epi-viro-therapeutic intervention), we pre-treated the human hepatoma cell line panel with resminostat at varying concentrations for 48 hours (see timeline in Figure 3.5 (A)). Our idea was to induce a vulnerable state within the cells for subsequent boosted MeV-SCD infection by blocking residual innate immunity pathways. We found no significant benefit for the pre-treatment combinational setting (Figure 3.5 (B), purple bars) compared to the corresponding single-agent treatment regimens (Figure 3.5 (B), blue/red bars) and also compared to the application scheme described in section 3.2.1 (Figure 3.3).

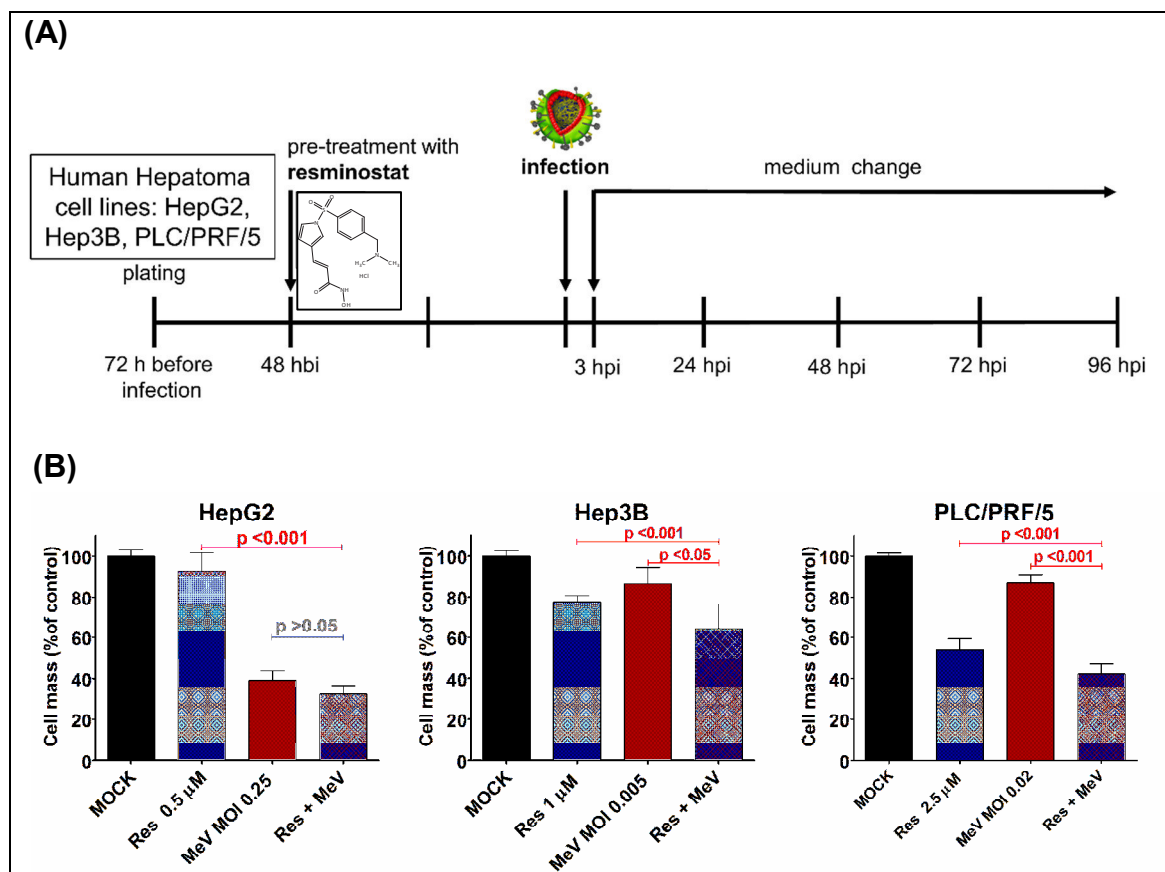


Figure 3.5: Combination setting of Res + MeV co-treatment (resminostat pre-treatment 48 hbi): (A) Application scheme for this setting: Human hepatoma cell lines were treated with resminostat as indicated and 48 h after pre-treatment, infection with prototypic measles vaccine vector MeV-SCD was performed. 3 hpi (MOI as indicated), a simple medium change was executed. (B) 96 hpi, residual cell masses were determined by SRB viability assay. Displayed are means of two independent experiments each carried out in quadruplicates + SD; hbi: hours before infection, hpi: hours post infection, MOI: multiplicity of infection. p-values of one-way ANOVA with a Tukey post-test.

Therefore, we ceased trying to continue further improvement of this specific chronological application setting, although to this point, optimized concentrations of resminostat as well as ideal MOIs for the combination setting (determined by the instrumentally installed $\approx 75\%$ threshold for single-agent treatment) were yet to be found.

3.2.2.2 Pre-treatment with resminostat 6 hours before infection and until 96 hpi

In this prime-boost approach on epi-virotherapeutic treatment of primary liver cancer derived tumor cells, hepatoma cells were pre-treated with the HDAC inhibitor resminostat (1 μM) for 6 hours before infection took place. Resminostat was re-added (1 μM) again at 3 hours post infection (hpi) until endpoint measurement was performed 96 hpi (see timeline in Figure 3.6 (A)). We observed by tendency an enhanced cytotoxic/oncolytic effect in the combinational setting (Figure 3.6 (B), purple bars), which was found not to be statistically significant compared to both corresponding single-agent treatments (Figure 3.6 (B), blue/red bars). Although overall cumulative time of resminostat exposure was prolonged relative to section 3.2.1, no benefit compared to the treatment setting described above could be found, indicating that in general pre-treatment with resminostat in this specific cell line panel (in which none of the cell lines showed primary resistance phenomena towards MeV-SCD treatment) does not augment the benefits of the epi-virotherapeutic tumor therapy.

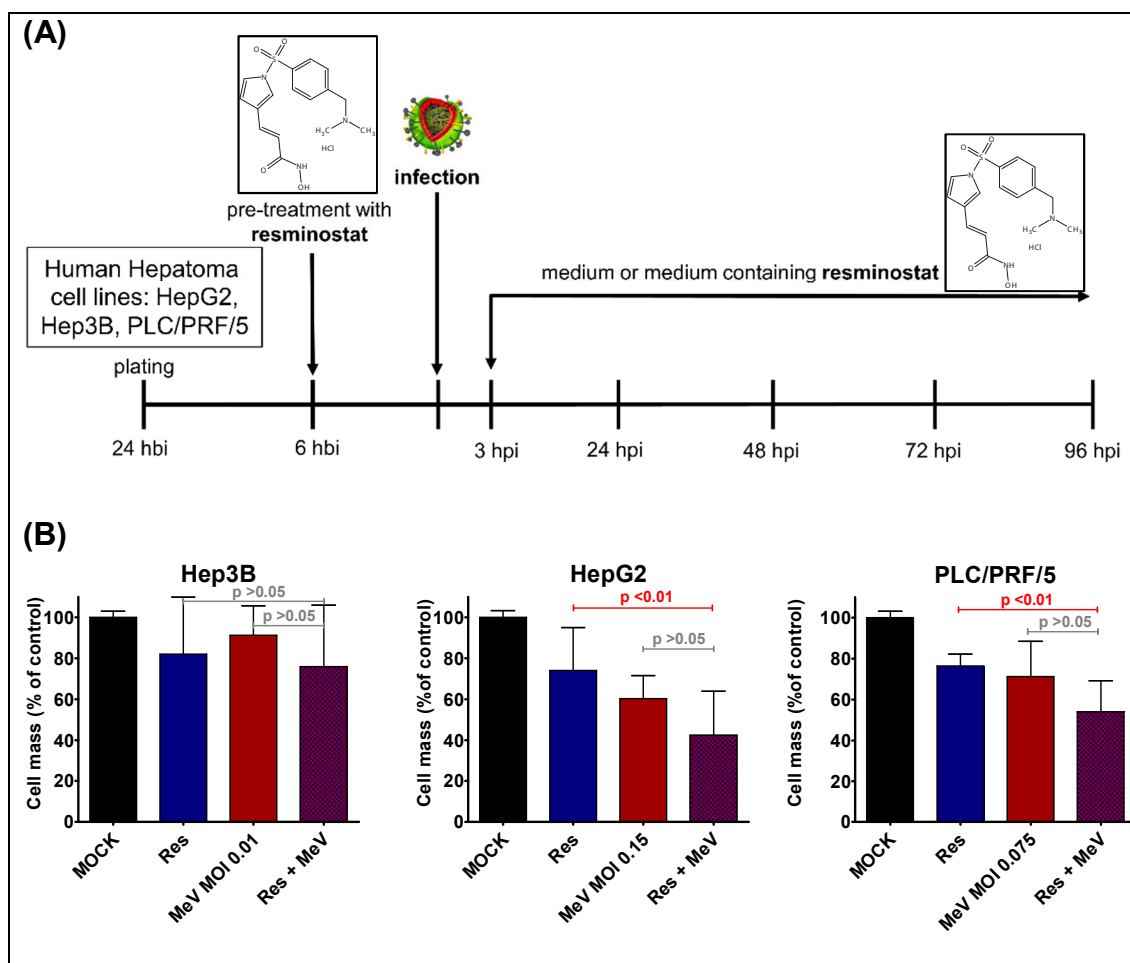


Figure 3.6: Prime-boost approach for epi-virotherapeutic treatment:

(A) HepG2, Hep3B and PLC/PRF/5 cell lines were treated with resminostat (invariably 1 μ M) 6 hours before infection (hbi) with armed measles virus MeV-SCD (at adjusted MOIs) and again 3 hpi as medium was changed. (B) Residual cell masses were determined 96 hpi using SRB endpoint measurement. Displayed are means of two independent experiments each carried out in quadruplicates + SD; p-values of one-way ANOVA with a Tukey post-test.

3.2.3 Triple-therapy: Addition of prodrug 5-FC to the MeV/Res combination setting

To exploit the full potential of our suicide gene-encoding oncolytic measles vaccine virus, MeV-SCD, we addressed the favorable opportunity to further reduce hepatoma cell masses by employing the expression of the Super-cytosine deaminase (SCD) in infected tumor cells. Therefore, as an amplification of the boosted cytotoxic/oncolytic effect observed in the resminostat/MeV-SCD combination setting in section 3.2.1, we extended the protocol by adding the prodrug 5-FC to MeV + resminostat co-treated cells 3 hours post infection (see

3 Results

timeline in Figure 3.7 (A)). The successful conversion of 5-FC into the chemotherapeutic antimetabolite 5-fluorouracil (5-FU) has already been demonstrated by Lampe and colleagues [166] for HepG2 and Hep3B cells. The results of enhanced triple-therapy regimen are represented in Figure 3.7 (B):

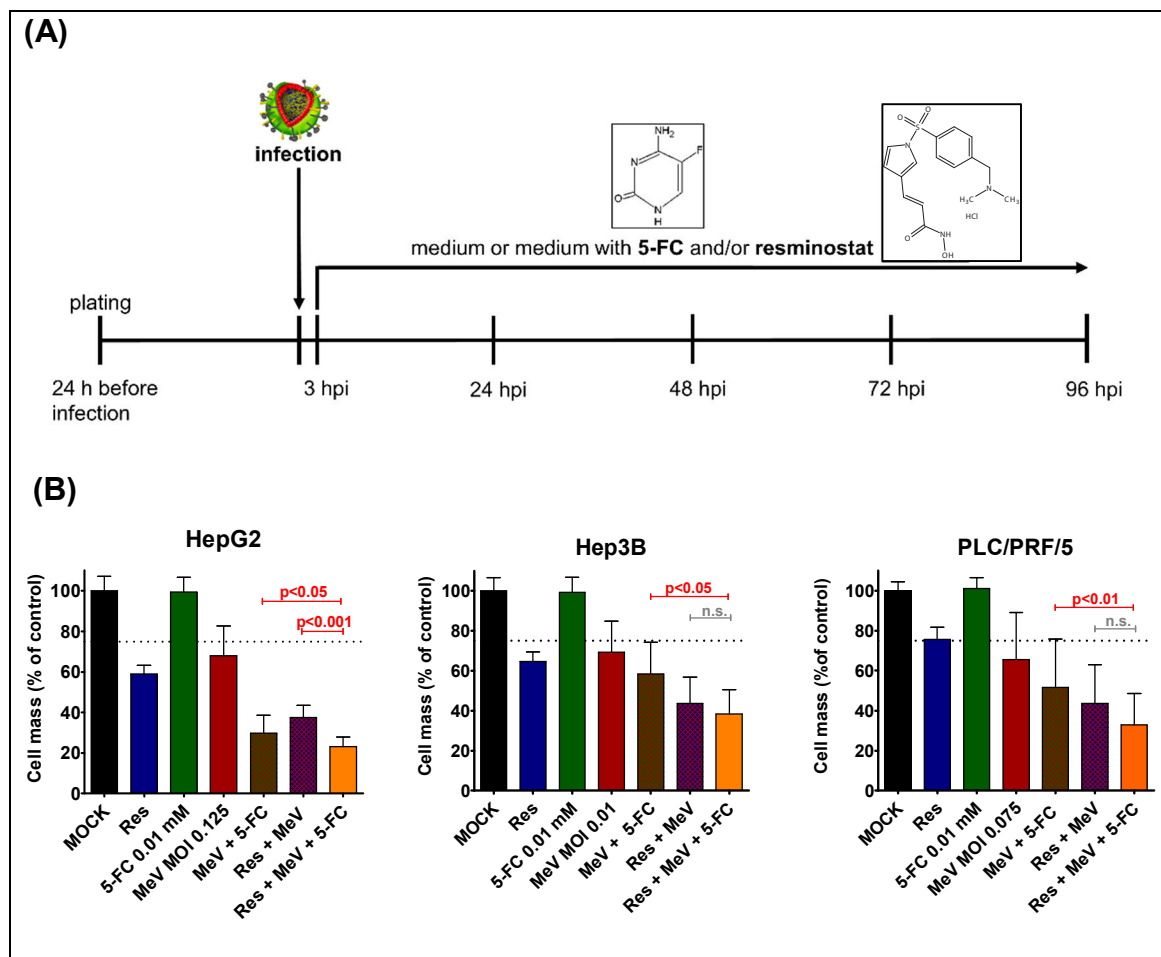


Figure 3.7: Triple-therapy: Addition of prodrug 5-FC to the MeV/Res combination setting: (A) Human hepatoma cell panel was infected with the oncolytic measles vaccine vector MeV-SCD (MOI as indicated) and co-treated with 1 μ M resminostat and/or prodrug 5-FC at 0.01 mM 3 hours post-infection. (B) 96 hpi sulforhodamine B viability assay was performed to measure remaining tumor cell masses. Displayed are means + SD of three independent experiments performed as quadruplicate. Res: resminostat. MeV: suicide gene-armed measles vaccine-based virotherapeutic MeV-SCD. MOI: multiplicity of infection. hpi: hours post infection; p-values of one-way ANOVA with a Tukey post-test.

As expected, addition of the antifungal prodrug 5-fluorocytosine (uniformly 0.01 mM) did not impair hepatoma cell growth (Figure 3.7 (B), green bars) *in vitro* and applied virus titer (at adjusted MOIs, Figure 3.7 (B), red bars) and concentration of resminostat (consequently 1 μ M, Figure 3.7 (B), blue bars) were instrumentalized to achieve a residual cell mass of \approx 75%. Addition of 5-FC to MeV-SCD-infected cells at 0.01 mM further reduced the percentage of viable

hepatoma cells (Figure 3.7 (B), green/red check pattern bars), indicating a successful conversion of 5-FC into cytotoxic 5-fluorouracil (5-FU). Importantly, the triple therapy setting, Res + MeV-SCD + 5-FC, (Figure 3.7 (B), yellow bars) was by tendency found to even further reduce remaining cell masses compared to either combination setting (MeV + Res [Figure 3.7, purple bars] as well as MeV + 5-FC).

3.3 Influences of resminostat on biological activity/growth characteristics of measles vaccine virus

3.3.1 Examination of measles virus growth kinetics under the co-treatment with resminostat

After an enhanced cytotoxic/oncolytic effect was observed for the combination setting (see section 3.2.1), kinetics of virus infection and spread under the influence of resminostat were visualized by fluorescence monitoring utilizing the green-fluorescent protein (GFP)-encoding measles vaccine vector MeV-GFP.

Therefore, the HepG2, Hep3B and PLC/PRF/5 cells were infected at an unvarying MOI of 0.1 with marker gene-encoding MeV-GFP or left untreated. 3 hpi, resminostat was added or not. The resulting fluorescence pictures are displayed in Figure 3.8: in HepG2 (Figure 3.8, (A)) uninfected cells (MOCK), as expected, showed no fluorescence signal, and fluorescence microscopy of solely MeV-GFP-infected and resminostat co-treated cells showed no evidence of altered fluorescence signals, at later time points between the combinational setting and the MeV-mono-infection. Analogous observations could be made in Hep3B cells (Figure 3.8, (B)) and PLC/PRF/5 clones (Figure 3.8, (C)), but here typical MeV-mediated cytopathic/oncolytic effect due to syncytia-formation and subsequent lateral spread of infectious particles could be documented (e.g. at 72 hpi for MeV-GFP and MeV-GFP + resminostat).

Quantification of primary infection rates of MeV-GFP (see section 3.3.2) as well as replication and spread (see section 3.3.4) are demonstrated below.

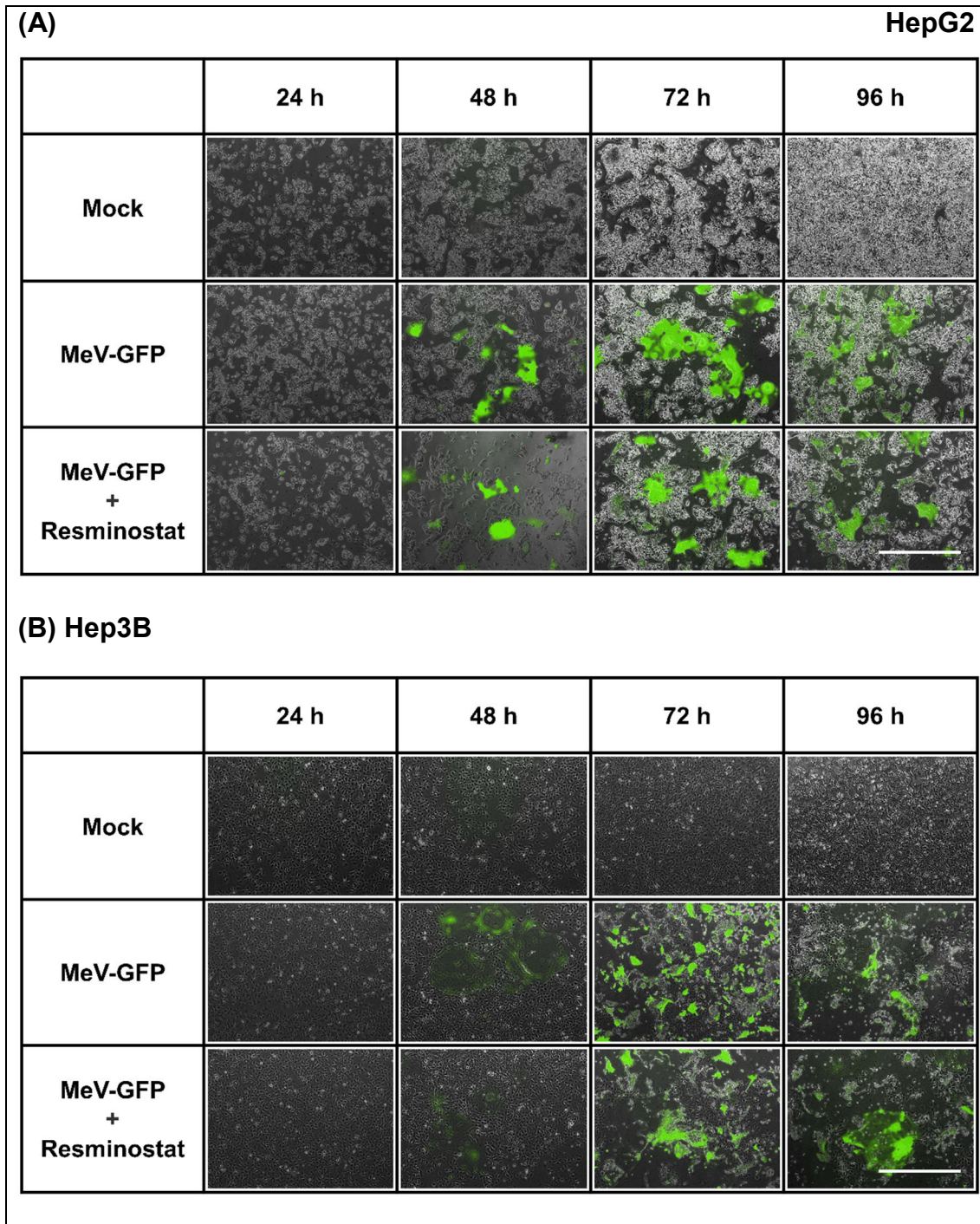


Figure 3.8: Influence of resminostat co-treatment on MeV-GFP infection in hepatoma cells: HepG2, Hep3B and PLC/PRF/5 cells were mock infected (upper row), infected with MeV-GFP at MOI = 0.1 (middle row) or co-treated with resminostat (lower row). Phase contrast and fluorescence pictures were taken at indicated time points. Infected cells show expression of green-fluorescent protein (GFP). The white scale bar on the lower right represents 1000 μm . Figure continued on next page.

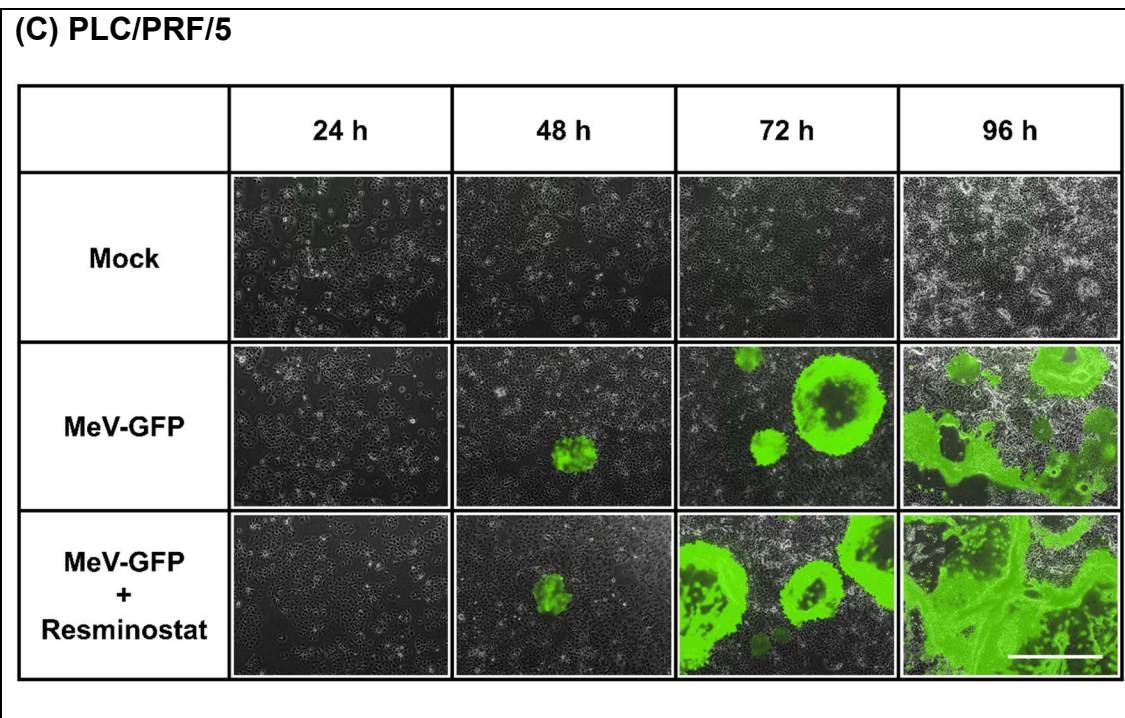


Figure 3.8: Continued

3.3.2 “Resminostat-mediated enhancement of primary infection rates in hepatoma cell lines

To further investigate the underlying molecular mechanisms of the epi-virotherapeutic boosted anti-hepatoma effect, primary infection rates were determined using flow cytometry. For this purpose, HepG2, Hep3B, and PLC/PRF/5 cells were first infected with a derivative measles vaccine virus encoding the green-fluorescent marker protein (MeV-GFP) at a non-adjusted MOI of 1, and then co-treated with resminostat (1 μ M). As a result, the percentage of infected hepatoma cells being determined at 24 hpi (a time point at which replication of MeV has not yet resulted in release of progeny virus particles and secondary infections of target cells) was found to be enhanced in all three human hepatoma cell lines in the combination groups (MeV + Res; Figure 3.9, purple bars) compared to the solely MeV-GFP infected groups (Figure 3.9, red bars). In detail, addition of resminostat elevated the percentage of MeV-GFP-infected HepG2 cells at 24 hpi from 13.2% to 21.9%, in Hep3B cells from 32.5% to 45.0%, both in a statistically significant manner; only in PLC/PRF/5 cells addition of resminostat was found to result in a minor rise of MeV-GFP-infected cells from 9.2% to 11.1%, which was statistically insignificant.

Interestingly, we found that all primary infection rates correlated quite well with the susceptibility of the hepatoma cell lines to MeV mediated oncolysis (Figure 3.1). Notably Hep3B cells, exhibiting the most distinct MeV-mediated oncolytic effect already at quite low MOIs (i.e., MOI 0.01), showed the highest primary infection rate, indicating that the efficiency of hepatoma cell infection within the first 24 hours is crucial to oncolytic tumor cell destruction. In this context, it is of interest that resminostat was found to be able to induce a boost of primary infection, at least partially contributing to a boosted oncolytic effect being determined by the endpoint measurement of tumor cell viability (i.e. at 96 hpi).”

[103]

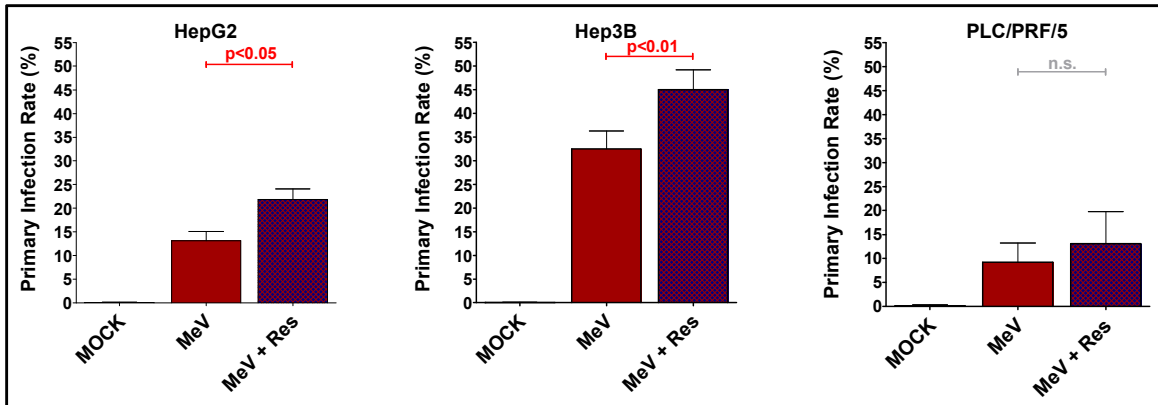


Figure 3.9: Resminostat enhances rates of primary infection of human hepatoma cells by Measles vaccine virotherapeutics.

Human hepatoma cell lines HepG2, Hep3B, and PLC/PRF/5 were infected with MeV-GFP at a standardized MOI of 1 and co-treated with resminostat (1 μ M) from 3 hpi on. At 24 hpi, quantitative differences in primary infection rates (defined as the percentage of infected cells [%]) were determined by flow cytometry. Displayed are means and standard deviations (SD) of three independent experiments. *p*-values of one-way ANOVA with a Tukey post-test; MeV: virotherapeutic vector MeV-GFP encoding the GFP marker gene. MOI: multiplicity of infection. Res: resminostat. MOCK: untreated control. hpi: hours post infection. Figure published in [103].

3.3.3 Enhanced primary infection rates are independent of measles receptor (CD46) expression levels

To analyze possible involvement of alterations in measles virus entry receptor (CD46) expression levels possibly underlying the observed enhanced primary infection rate of MeV-GFP in resminostat co-treated cells, mean fluorescence intensities as an index for CD46-receptor expression levels on human hepatoma cells were determined by flow cytometry (Figure 3.10). Untreated (MOCK-infected) cells were used as a baseline expression level for CD46 and defined as 100% (Figure 3.10, black bars). As a result, neither resminostat treatment (Figure 3.10, blue bars), MeV-GFP infection (Figure 3.10, red bars), nor combinational treatment (Res + MeV, Figure 3.10, purple bars) was found to have a statistically significant effect on CD46-expression, although means of fluorescence intensity were generally found to be decreased in treated cells with no differentiation between virus infection and HDAC-inhibition (exception: in HepG2 cells, MeV-GFP-treatment increased MFI in this specific case). Therefore, no correlation was found between an enhanced MeV-GFP primary infection rate under resminostat-treatment and CD46-surface-receptor expression levels in our hepatoma panel and thus underlying mechanisms yet remain concealed.

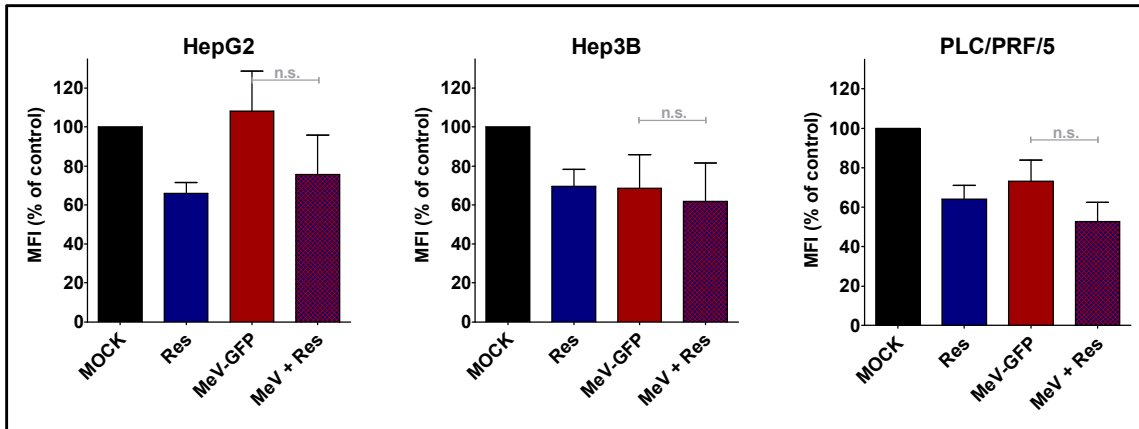


Figure 3.10: Alterations of CD46 expression levels on MeV-GFP and/or resminostat-treated human hepatoma cells:

Human hepatoma cells were infected with MeV-GFP at MOI 1 and treated with resminostat 1 μ M. 24 hpi, phycoerythrin (PE) conjugated anti-CD46 antibodies or isotype control was used for staining of HepG2, Hep3B and PLC/PRF/5 cell lines and expression levels were determined by flow cytometry. Mean Fluorescence Intensity (MFI) was calculated as ratio of the arithmetic means of CD46-stained / isotype control-stained cells. Displayed are Means and SEM of three independent experiments. Statistical analysis carried out with a one-way ANOVA and a Tukey post-test; n.s.: not significant

3.3.4 “Addition of resminostat does not impair MeV replication and spread

To gain further insight into the kinetics of MeV-SCD replication and spread under the influence of resminostat, we worked out viral growth curves in absence/presence of resminostat (Figure 3.11). For this purpose, hepatoma cells were infected with MeV-SCD at adjusted MOIs as being defined before (HepG2: 0.1; Hep3B: 0.01; PLC/PRF/5: 0.075). At 3 hpi, resminostat (1 μ M) was added and MeV replication was quantified at 3, 24, 48, 72, and 96 hpi. As a result, we did not find any impairment of MeV-SCD replication and spread in HepG2 and PLC/PRF/5 hepatoma cell cultures (Figure 3.11, panels at the top and at the bottom). Interestingly, in Hep3B cells (Figure 3.11, panels in the middle) we found a slight, statistically insignificant enhancement of MeV progeny virus production in the presence of resminostat (both for cell associated as well as for MeV particles released into cell culture supernatants).

Therefore, boosted anti-tumoral effects of the epi-virotherapeutic combination treatment (MeV + Res) seem to be largely independent of a putative resminostat-enhanced viral replication and spread.” [103]

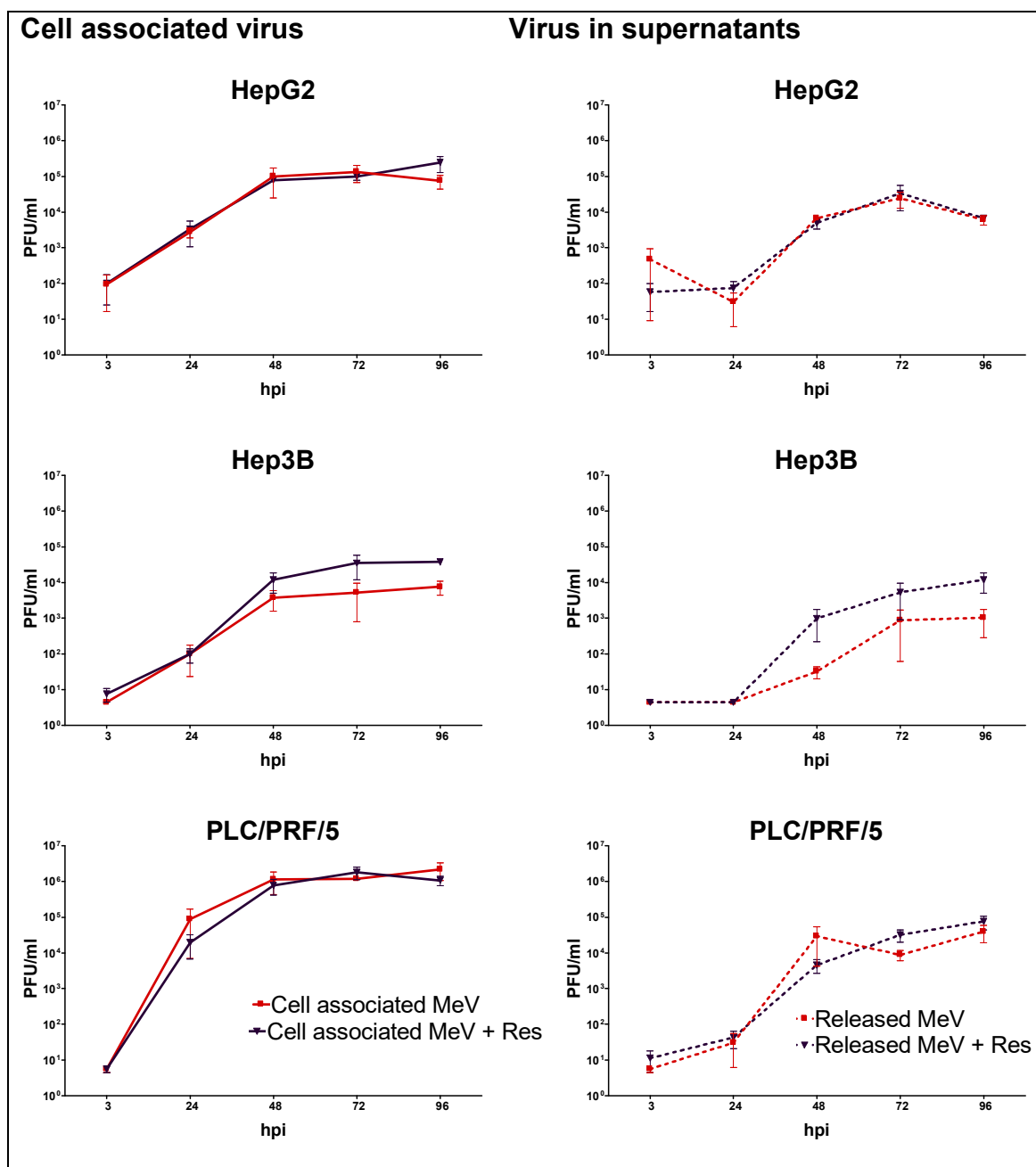


Figure 3.11: Resminostat does not impair replication of MeV-SCD and subsequent spread of progeny viral particles

At 3, 24, 48, 72, and 96 hpi, cell lysates (comprising cell associated MeV particles; panels on the left) and supernatants (comprising MeV particles being released into cell culture medium; right column) were sampled either from solely MeV-SCD infected human hepatoma cells (HepG2, Hep3B, PLC/PRF/5; employing adjusted MOIs) or obtained after epi-virotherapeutic co-treatment with resminostat applied at a concentration of 1 μ M (MeV + Res). Vero cells were used for virus titrations and results were converted into PFU/ml. Results of solely MeV-infected cells (red lines) are displayed along with results of MeV + Res co-treated cells (purple lines). Solid lines are representative for the quantification of cell-associated viral particles (left column), whereas dotted lines are used to highlight viral particles being released into hepatoma cell supernatants (column on the right). Means and standard errors of the mean (SEM) are shown for three independent experiments. PFU: plaque forming units. hpi: hours post infection.

Figure modified from version published in [103].

3.4 “Resminostat-induced downregulation of zfp64 in MeV infected hepatoma cells

To provide proof for an unimpaired activity of resminostat in the course of MeV-based infections of human hepatoma cells, we determined zinc finger protein 64 (zfp64) expression levels, which functions as a well-established surrogate parameter for the pharmacological activity of resminostat, in absence/presence of MeV-SCD. As shown before [136], when resminostat (1 μM) was applied alone (i.e. in absence of MeV-SCD) it was found to inhibit zfp64 mRNA production quite effectively in all three human hepatoma cell lines at early time points, i.e. at 5 hours after addition of resminostat (Figure 3.12, blue bars). Interestingly, when resminostat (1 μM) was added subsequent to infections with MeV-SCD (employing adjusted MOIs), lower zfp64 mRNA expression levels were observed when being compared to untreated controls (Figure 3.12, purple bars). In contrast, monotherapeutic applications of MeV-SCD (Figure 3.12, red bars) were found to enhance zfp64 expression levels in HepG2 cells and no alteration in zfp64 expression was found in PLC/PRF/5 cells. Thus, resminostat-induced downregulation of zfp64 expression was found to take place also in the course of MeV-based infections of human hepatoma cells, indicating an unimpaired effect of resminostat in this specific epi-virotherapeutic context.” [103]

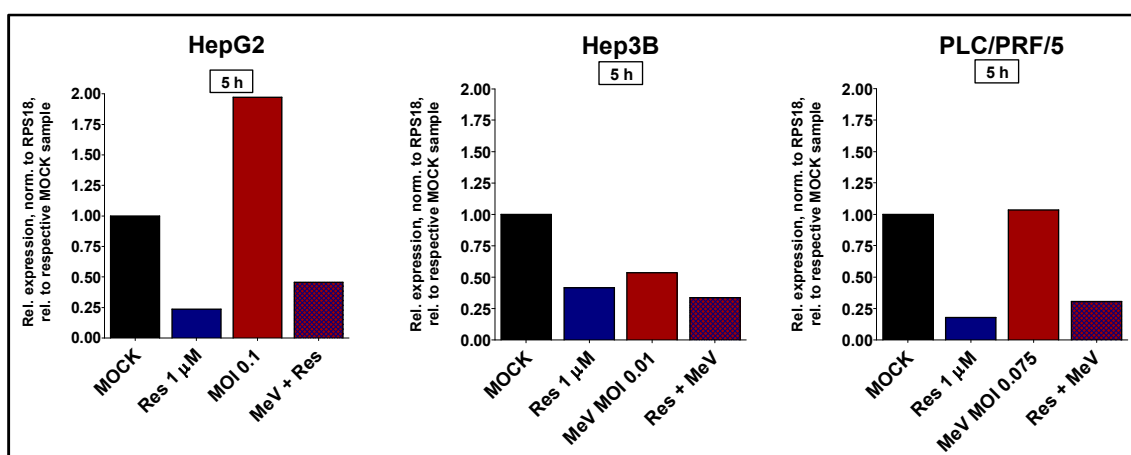


Figure 3.12: Expression levels of zfp64 (pharmacodynamic biomarker for resminostat activity) in human hepatoma cell lines after epi-virotherapeutic (Res + MeV) treatment: HepG2, Hep3B, and PLC/PRF/5 cells were infected with MeV-SCD at indicated MOIs and co-treatment with resminostat (1 μM) took place from 3 hpi on. RNA was isolated after 5 hours of incubation with resminostat. Then, zfp64 expression levels were determined using RT-qPCR. Values were normalized to the house-keeping gene RPS18 (Ribosomal-protein S18) and relative expression is displayed compared to corresponding control samples (MOCK). Data of one experiment are shown. Figure published in [103].

3.5 “Epi-virotherapeutic treatment (MeV + Res) enlarges apoptosis of hepatoma cells

To gain additional insight into boosted anti-tumoral effects of this specific epi-virotherapeutic (MeV + Res) treatment, we also analyzed cell cycle profiles of our human hepatoma cell panel. Again, HepG2, Hep3B, and PLC/PRF/5 cells were infected with MeV-SCD or mock infected and resminostat was added at 3 hpi or not. At 96 hpi, intracellular DNA was stained with propidium iodide and the percentage of hepatoma cells within each phase of the cell cycle was determined via flow cytometry (see Figure 3.13 (B)). Single-agent treatment with resminostat (Res; 1 μ M) led to a slight enhancement of the sub2N fraction of hepatoma cells with hypoploid DNA content, indicating intracellular DNA fragmentation as a consequence of an ongoing apoptotic program (HepG2 (control / Res): 11.6% / 20.8%; Hep3B: 13.6% / 25.2%; PLC/PRF/5: 6.1% / 11.9%). In contrast, infections with MeV-SCD (MeV) again being performed at adjusted MOIs (HepG2: 0.1; Hep3B: 0.01; PLC/PRF/5: 0.075) were found to augment the sub2N fraction (HepG2: 42.6%; Hep3B: 17.9%; PLC/PRF/5: 45.0%). Most interestingly, combinational epi-virotherapeutic treatment (MeV + Res) was found to further increase the rates of apoptotic cells (HepG2: 70.6%; Hep3B: 39.7%; PLC/PRF/5: 62.7%). Thus, the epi-virotherapeutic combination therapy showed a substantial induction of apoptosis in all human hepatoma cell lines investigated, leaving only few tumor cells capable to proliferate.” [103]

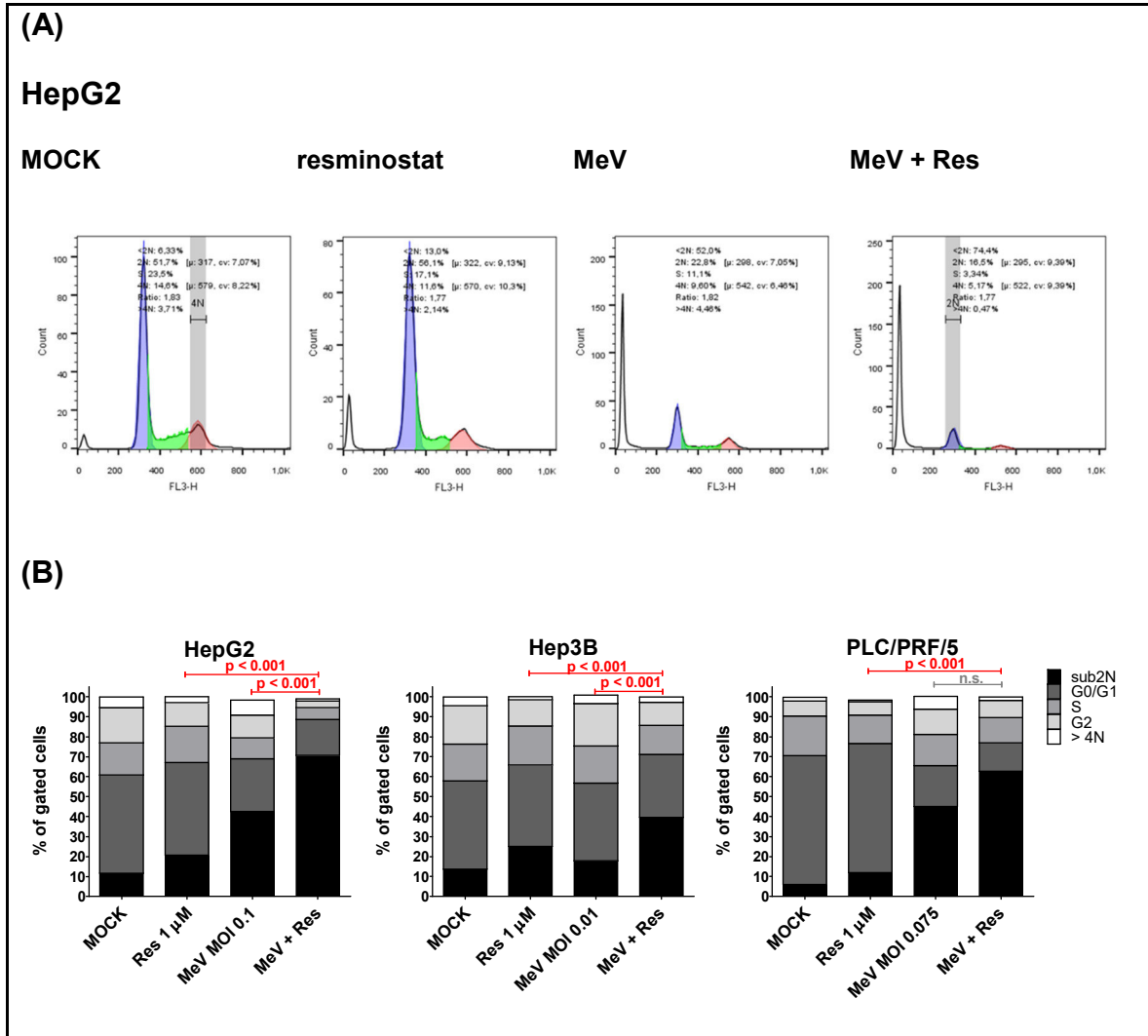


Figure 3.13: Cell cycle profiles of human hepatoma cells undergoing epi-virotherapeutic co-treatment with MeV-SCD and resminostat:

Human hepatoma cell lines HepG2, Hep3B, and PLC/PRF/5 were infected with MeV-SCD (MeV) or mock infected (MOCK) and resminostat (Res) was added at 3 hpi or not. Intracellular DNA was stained with propidium iodide (PI) at 96 hpi and measured by flow cytometry. (A) Exemplary raw data results for HepG2: area under the curve of different cell cycle phases are colorized. (B) Combinatorial treatment (MeV + Res) was found to enhance the population of hypoploid/apoptotic cells (black vertical bars: sub2N) compared to corresponding single-agent treatments (MeV or Res) while concurrently diminishing fractions of proliferating cells (represented in cell cycle phases S and G2). Means of three independent experiments carried out in duplicates or triplicates are shown; p -values of one-way ANOVA with a Tukey post-test. (B) modified from version published in [103].

3.6 “Resminostat impedes IFIT-1 expression after exogenous IFN- β stimulation

To investigate putative immunomodulating effects of resminostat on the interferon (IFN) pathway being important for the innate immune defense against infections with virotherapeutics, modulations of IFIT-1 expression and Stat1 phosphorylation were analyzed by immunoblotting. Notably, human hepatoma cell lines HepG2, Hep3B, and PLC/PRF/5 were found to be unable to produce detectable amounts of endogenous IFN- β neither at base-line (MOCK) nor after infection with MeV-SCD when using adjusted (low) MOIs (data not shown).” [103] Consequently, no detectable expression of IFN-stimulated genes, such as IFIT-1 was discovered in MeV-infected cells at low MOIs (data not shown). This can be considered as an indication for defects in innate immunity-dependent recognition of virus-associated pathogen-associated molecular patterns (PAMPs) in every single of our hepatoma cell lines. Thus, a possible explanation for our earlier observations in our preliminary experiments was found, where no resistance towards measles-based oncolysis was noted, neither in HepG2, Hep3B nor PLC/PRF/5 cell lines, implying severe acquired defects in defense reactions during malignant transformation towards intruding viruses for these particular cell lines.

“Therefore, we had to pre-stimulate hepatoma cells with exogenous human IFN- β (1,000 U/ml) for 24 hours, which then led to a significant induction of IFIT-1 expression and expression of Stat1 and its phosphorylation (P-Stat1) in all three hepatoma cell lines (Figure 3.14; lane 2 in all panels). In unstimulated/untreated controls, we found no baseline expression of IFIT-1 and no detectable amounts of P-Stat1 (Figure 3.14; lane 1 in all panels). As expected, treatment with resminostat (5 μ M) alone did not induce IFIT-1 expression nor phosphorylation of Stat1 (Figure 3.14; lane 3 in all panels). However, when adding resminostat (5 μ M) coincident on IFN- β stimulated (1,000 U/ml) hepatoma cells, a profound suppression of IFIT-1 expression was observed in HepG2, Hep3B, and PLC/PRF/5 hepatoma cells, but no alteration in the phosphorylation status of Stat1 (Figure 3.14; lane 4 in all panels). Thus, all three human hepatoma cell lines were unable to induce a profound antiviral state, showing the potential of

resminostat as an immunomodulating compound to favor an enhanced virus mediated oncolysis in combination therapies with oncolytic measles vaccine viruses.” [103]

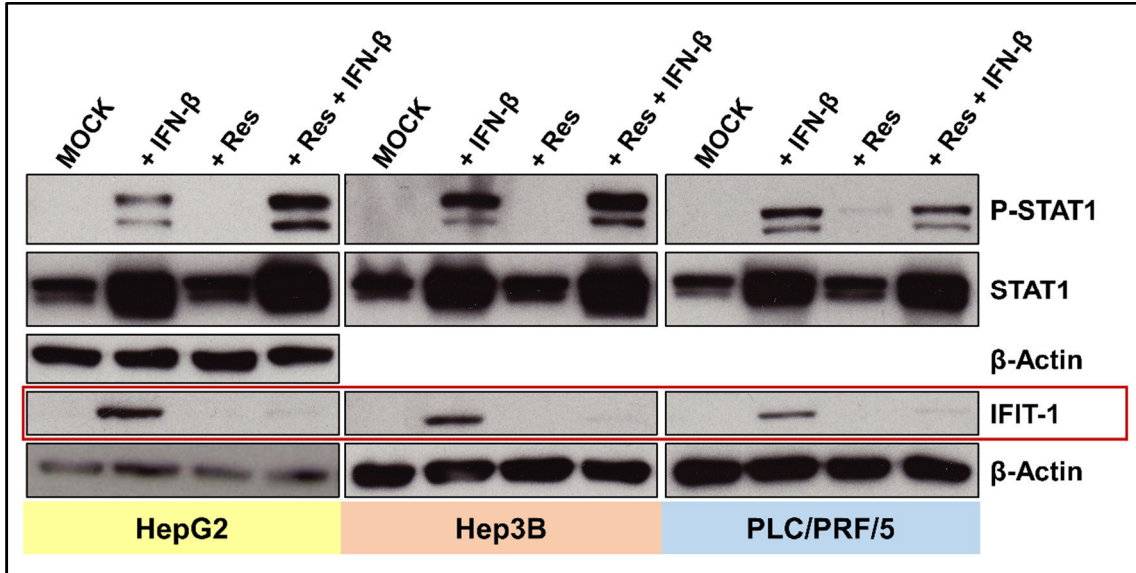


Figure 3.14 *IFN-β induced expression of IFIT-1 is suppressed by resminostat, whereas phosphorylation of Stat1 is not:* HepG2, Hep3B, and PLC/PRF/5 cells were first stimulated with IFN-β for 24 hours or left unstimulated and then treated with resminostat (5 μM) or left untreated. IFIT-1 expression as well as phosphorylation and expression of Stat1 were analyzed by immunoblotting. β-Actin was used as a loading control. Shown are representative blots of three independent experiments. Figure published in [103]

4 Discussion

“Despite recent improvements in the treatment of advanced stage hepatocellular carcinoma (HCC), clinical outcome for patients in late stages of this cancer entity is still poor and therefore further improvements of therapy modalities are urgently required.” [103]

4.1 Boosted cytotoxic effects in the epi-virotherapeutic approach

“Here, we investigated the potential benefit of a new epi-virotherapeutic approach, combining a novel histone-deacetylase inhibitor (resminostat [135]) with a state-of-the-art oncolytic measles vaccine virus (MeV-SCD [166]) in a panel of three human hepatoma cell lines. We found all hepatoma cell lines to be primarily susceptible to infection with MeV-SCD (defined by a remnant tumor cell mass of < 50% at 96 hpi at MOI 1 [90]), but susceptibility to virus infection was found to vary by a factor of 10 between the different hepatoma cell lines. Treatment with resminostat alone (monotherapeutic approach) resulted in a coincided dose-dependent reduction of tumor cell masses in all three hepatoma cell lines. However, coadministration of resminostat and MeV-SCD (Res + MeV) resulted in a potentiated oncolysis/cytotoxic effect warranting further investigations on this combinational therapy regimen. In contrast, in non-malignant primary human hepatocytes (PHHs) no enhancement of cell mass reduction was found when comparing the epi-virotherapeutic approach (Res + MeV) to any of the monotherapeutic modalities, suggesting the combinational approach to be safe for hepatocytes and possibly also for other non-transformed cells. However, when comparing mock-treatment of PHH cells with the combinational (Res + MeV) treatment setting of PHH cells, a reduced PHH viability was found (Figure 3.4, lower panel). Of note, such MeV-SCD-triggered effects on in vitro cultured non-malignant primary human hepatocytes (PHHs) has already been found before (our unpublished data). Of note and in contrast to these in vitro findings, in vivo experiments in nude mice [166, 167], in transgenic mice as well as in macaques [168] were overall well tolerated without revealing any safety concerns (e.g., no rise in liver enzymes). Beyond that, results of

published clinical trials using measles vaccine viruses (e.g.[39-41]) exhibited excellent safety profiles not indicating induction of any organ problems such as liver failure.” [103]

“We previously have demonstrated that resistance phenomena to MeV-SCD-based oncolysis could be overcome by increasing the MOI of MeV-SCD or by employing the suicide gene function of MeV-encoded Super-cytosine deaminase (SCD), which results in converting the non-toxic antifungal prodrug 5-FC to the well-known cytotoxic drug 5-FU [79, 90, 166, 169].“ [103] Beyond that, we were able to show that exploitation of MeV-SCD-encoded prodrug conversion system (SCD) by addition of 5-FC to the Res + MeV co-treated cells - representing a triple therapy - was able to further enhance anti-tumor efficacy. These findings can be used to provide another therapeutic tool to further upgrade epi-virotherapy (which was accompanied by enhanced primary infection rates) as this triple-hit strategy can result in increased release of potentially antigenic tumor epitopes by tumor cell rupture.

Nevertheless, as suicide gene function is dependent on preceding infection of tumor tissue, “increasing the dosage of administered viral vectors in patients is yet limited due to constraints in the respective manufacturing processes. And as those oncocytotoxic agents face various biological barriers (consisting e.g. of the host immune system as well as the tumor microenvironment), it is essential to enhance OV potency by prudent combination strategies.” [103]

4.2 HDACi + OV treatment: is apoptosis the answer?

“In our epi-virotherapeutic combination setting, enhanced hepatoma cell mass reduction was associated with a boosted rate of cells with hypoploid intracellular DNA content indicating an ongoing apoptotic program. Previous work by others has confirmed this mechanism of action when combining HDACi with OVs. The combination of e.g. either entinostat (MS-275) or vorinostat (SAHA) together with a VSV-based virotherapeutic vector was found to enhance intrinsic apoptotic pathways, a pattern which could also be observed in a combination study employing the HDACi valproic acid (VPA) together with the virotherapeutic parvovirus vector H-1PV [150]. In contrast, combination of trichostatin A and

HSV-1 mainly induced proliferation/cell cycle arrest by induction of p21 [170]. Other HDACi / OV combination studies found an enhanced therapeutic effect by induction of oxidative stress [150], whereas combination of vorinostat with VSV resulted in an induction of autophagy via modulation of NF- κ B signaling [171]. Finally, addition of TSA to oncolytic treatment with HSV resulted in anti-angiogenic effects indicated by a reduction in secretion of VEGF [149].” [103]

Therefore, the precise mechanism of action for combining oncolytic viruses with inhibitors of histone deacetylases needs to be fully elucidated, as tumor cell killing by oncolytic viruses is not entirely describable by classical concepts of apoptosis [29]. This is owned to the experience that intruding virus pathogens often take over host cell transcription and translation equipment, thus limiting the initiation of classical pro-apoptotic pathways [172]. Yet combination studies on HDACi with several anti-cancer agents revealed a synergistic induction of apoptosis as the predominant mechanism of activity, as re-sensitization to apoptotic stimuli and concomitant activation of apoptotic pathways were identified in many cases [105].

4.3 Influences on virus biology by epigenetic manipulation

4.3.1 MeV-SCD replication and spread is hardly affected by resminostat

“Enhanced oncocytotoxic effects of epi-virotherapeutic treatment modalities have frequently been associated with a facilitation of virus replication and spread [146, 150, 170], which seems to be dependent on dosing schedules. Thus, HSV replication could be enhanced by HDACi pretreatment but not by simultaneous co-treatment [147]. Nevertheless, no influence was found neither on primary infection rates nor on virus replication and spread in a setting of TSA plus HSV-1 (G47 Δ) [149] in different human proliferating endothelial cells and cancer cell lines. When testing a larger panel of HDAC inhibitors, some, but not all HDACi were found to increase replication of a HSV-1 based virotherapeutic in breast cancer cells [148]. [...] Here, we report that co-treatment with resminostat, a novel oral histone deacetylase inhibitor, did not negatively influence MeV-SCD replication and spread but was found to increase rates of primary infection of human hepatoma cells. Hereby, the moderate effects on enhanced virus entry did not translate into increased viral titers in the replication assays. Furthermore,

MeV RNA synthesis and assembly require a plethora of host factors, e.g. heat-shock-protein 72 (HSP), casein kinase II, peroxiredoxin 1 (PRDX1), several unidentified kinases and structural cytoskeletal proteins such as actin [173]. These elements could all be possible intersections with the pleiotropic activities of HDACi compounds such as resminostat but have not been further elucidated so far. Accordingly, further work has to bring light into these interplays for the respective combination of MeV-SCD with resminostat in hepatoma cells and preferably also in other tumor cell entities. Additionally, we did not observe any enhanced or decreased oncolytic effect when varying the timing of resminostat application (adding resminostat before or after infections with MeV-SCD). Accordingly, we were able to reason that resminostat treatment hardly interacts with the process of measles vaccine virus replication, at least in cancer cells lacking a sufficient antiviral program.

Variations in MeV-induced cell cytotoxicity among different cancer entities / cell lines seem to be dependent on a multitude of (independent) factors, including virus-specific as well as tumor cell-specific biologies, which have lately been characterized by Noll et al. [90] for our study virus MeV-SCD on the NCI-60 tumor cell panel. In this work, primary resistance phenomena were observed for about 40% of the tested tumor cell lines; but not all resistant tumor cell lines were able to induce an antiviral state via the IFN-signaling pathway, clearly indicating the existence of further determinants being involved in the variation of tumor cell line-specific MeV-mediated cytotoxicities. In this context, it is of interest that Lampe et al.^[166] identified MeV-SCD-mediated oncolysis not to be solely dependent on functionally intact apoptotic pathways, a finding which underlines the diversity of the complex virus-tumor-cell-interactions leading to cancer-cell destruction. In another work, Berchtold et al.^[79] found high expression levels of the measles entry receptor CD46 on tumor cell surfaces well correlating with high primary infection rates of our MeV virotherapeutics. However, this feature was not found to apply to our combinational therapy regimen (Res + MeV): hepatoma cell-specific expression levels of CD46 were not found to be enhanced by resminostat co-treatment. Another point that one has to consider is the diverse genetic equipment distinguishing even our small panel of hepatoma cells (e.g. p53

expression is not altered in HepG2 cells; no expression of p53 can be detected for Hep3B cells, and PLC/PRF/5 cells exhibit reduced p53 levels [174]), leading to distinct rates of apoptosis or altered regulation of cellular protein biosynthesis following virus infection.” [103]

Observations by Workenhe et al.^[175] on two herpes-based vectors with different replication properties indicate that “initial stages of immunogenic virus replication are more important than persistence of a replicating virus within the tumor”^[175], thus supporting our findings that an enhanced primary infection rate with marginal effects on subsequent replication and spread can favor an increased antitumor immunity.

4.3.2 Resminostat does not alter measles entry receptor CD46 expression levels

“Additional combination approaches applying adenoviral virotherapeutics revealed further mechanistic insights into the complex interactions of OV_s with HDAC_i, as adenovirus receptor CAR was found to be upregulated in presence of HDAC_i resulting in enhanced primary infection rates. Interestingly, ongoing HDAC inhibition then resulted in antagonistic interactions and was found to diminish adenovirus replication and spread [152, 176].” [103] In our own experiments, hepatoma cells showed rarely any alterations in CD46 MeV entry receptor expression levels, if at all, a slight downregulation following both monotherapies as well as in the combinational approach was noticed. This observation was described earlier (e.g. [177, 178]), as MeV-Edm strain vaccine viruses were found to be involved in post-infection down-regulation of CD46 but not SLAM/CD150 MeV receptor. “Recapitulating those findings, influences on OV replication and spread by coadministration of HDAC inhibitors seem to be multifactorial and no general rules can be applied, as outcomes seem to be greatly dependent on the specifics of the oncolytic vector system under evaluation and appertaining replication machineries as well as the particular HDAC inhibitor under investigation.” [103]

4.4 Resminostat functions as an immunomodulator in hepatoma cells

4.4.1 Interference with the host cell interferon system

“Among the multitude of genetic and epigenetic alterations which tumor cells acquire in the process of carcinogenesis, leading to independence of apoptotic signals, unrestricted proliferation and concealment of tumor cells from immune responses, some are responsible for a disruption of tumor pathways required for sufficient innate immunity signaling, making them preferred targets for oncolytic viruses. Accumulation of defects in interferons and interferon stimulated genes are vital for tumor evolution, as these pathways encompass involvement in programmed cell death [179], inhibition of angiogenesis [180] and immunostimulatory effects (e.g. tumor cell antigen expression) [181].

In the context of human hepatoma cell infections we found that MeV, when used at low MOIs, was not able to induce any detectable amounts of IFN- β , an inflammatory cytokine with a central role in the cellular antiviral repertoire [182], indicating defects in pathogen recognition. A screening on the NCI-60 tumor cell panel revealed that about 75% of tumor cell lines were found to have defective IFN-responses [142, 183]. However, the same does not necessarily apply to primary tumor cells [142] and in-patient situations, in which primary resistance phenomena towards oncolytic virotherapy are observed.

Measles vaccine virus strains (such as the Edmonston strain used in this work), but not wild-type measles virus, induce production of type I IFN in monocyte-derived dendritic cells and peripheral blood lymphocytes [101, 102]. Therefore, it is likely that monocyte-derived dendritic cells being part of the tumor micro-environment are responsible for a sturdy production of type I IFN, inducing (via paracrine secretion processes) an antiviral response in tumor cells lacking virus recognition. On the other hand, inhibition of different components of the IFN response has previously been shown to increase virus replication as well as virus yield in tumor cell cultures [184]. Therefore, combination strategies of OV and IFN-blocking agents potentially could help to overcome such limitations for the in-patient situation.

To address this heterogeneity in tumor cell susceptibility towards oncolytic virotherapy, HDAC inhibitors can be employed to repress innate immunity signaling with restriction to malignant cells [93]. Interestingly, HDACi were found to have the potency to undermine antiviral immunity resulting in enhanced OV replication [142]. Mechanistically, inhibition of HDAC activity by TSA was found to inhibit IFN- β production and silencing of HDAC6 was correlated with an increased replication of VSV [185]. Beyond those findings, HDAC inhibition with TSA/VPA resulted in an impairment of ISG expression after exogenous stimulation with IFN- β without altering activation of Stat proteins and ISGF3 formation [186]. In detail, HDAC1 was found to associate with Stat1 and Stat2 and inhibition by HDACi leads to a diminished transcription in response to IFN- α [187]. To summarize those observations, treatment with HDAC inhibitors has been found to inhibit both IFN secretion and transcriptional activity of several interferon stimulated genes. In line with these discoveries, we here investigated the potential of resminostat as a potent inhibitor of class I & IIb HDAC (including HDAC1 and HDAC6) to inhibit induction of ISG. We showed that resminostat suppressed expression of IFIT-1 in HepG2, Hep3B, and PLC/PRF/5 cells after exogenous IFN- β stimulation, possibly preventing the induction of an antiviral state within hepatoma cells, thereby constituting a possible positive modulator for oncolytic virotherapy in tumor cells exhibiting a residually intact antiviral IFN response (a summary of possible resminostat interaction with innate immunity signaling is presented in Figure 4.1). Because of the deficient IFN-response found in our hepatoma panel, the enhanced cytotoxic effects of the epi-virotherapeutic combination approach can therefore not be attributed to the IFN-response (immuno-)modulating effects of resminostat. These are proposed additional benefits expected for the *in vivo* application of Res + MeV and have to be tested next in an immunocompetent animal model system.

The IFIT family of antiviral proteins is found to be induced downstream of IFN-stimulation following virus infection [100] with distinct activities against viral functions: e.g. general inhibition of translation initiation is achieved by interaction of IFIT proteins with eIF3 [98]. Furthermore, IFIT-1 (also known as ISG56) was

found to directly bind triphosphorylated RNA, which often occurs in the cytosol during life cycles of RNA viruses [188].” [103]

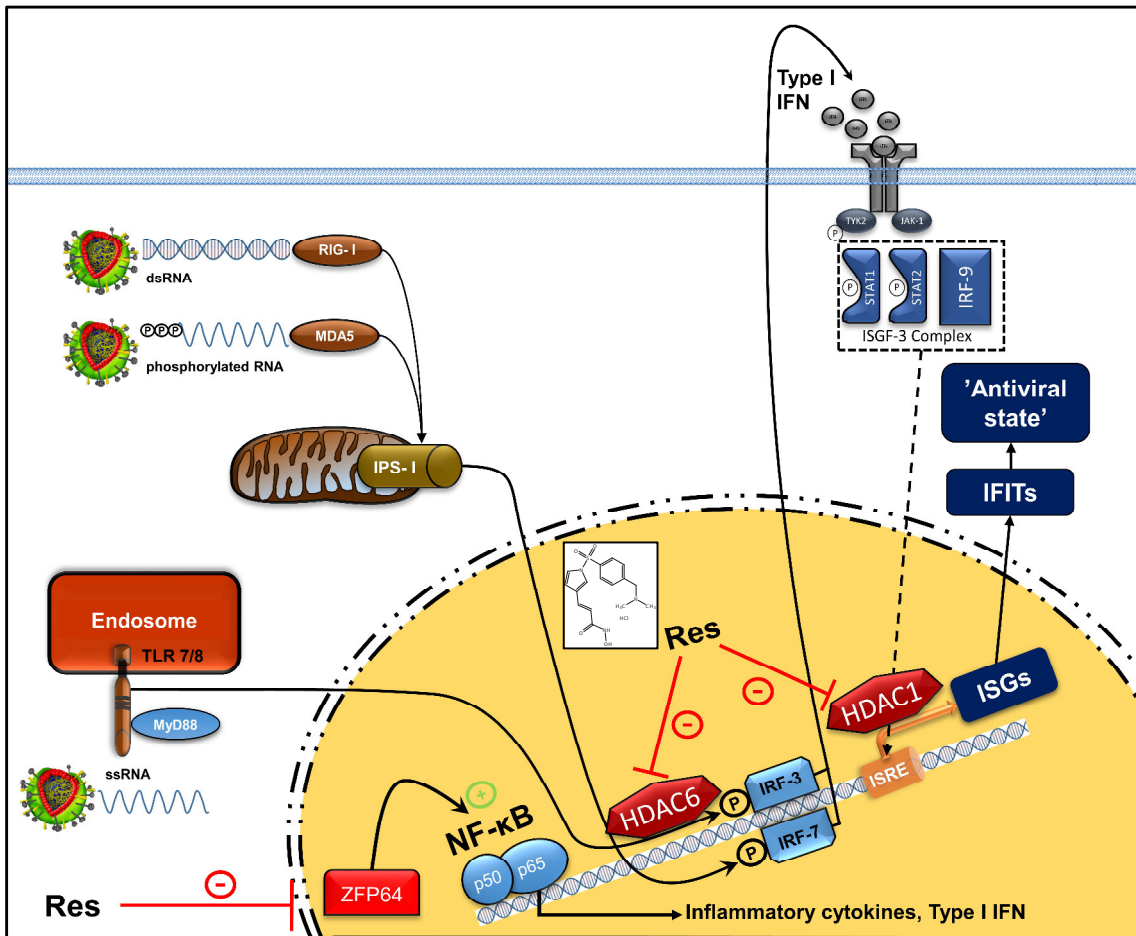


Figure 4.1: Possible influences of resminostat on interferon (IFN) signaling:
 Virus derived pathogen-associated molecular patterns (PAMPs), such as ssRNA, dsRNA or triphosphorylated RNA are recognized e.g. by cytosolic receptors, such as RIG-I/MDA5 or TLRs, followed by signaling cascades resulting in NF-κB or IRF-3/IRF-7 activation and translocation to type I IFN promoter sites. Subsequently, newly synthesized inflammatory cytokines (such as type I IFN) bind to membranous IFN-receptors, leading to phosphorylation of Stat1 & Stat2, which form a heterotrimeric ISGF-3 complex together with IRF-9. ISGF-3 complex binding to the IFN-stimulated response element (ISRE) promoter sites triggers ISG (interferon-stimulated genes) production, such as IFIT (interferon-induced protein with tetratricopeptide repeats)-family proteins, which are responsible for induction of an antiviral state within the infected cell. HDACs are involved in IFN production and induction of ISGs. Resminostat is an inhibitor of HDAC1 & HDAC6 and is responsible for down-regulation of ZFP64, a positive regulator of NF-κB signaling. dsRNA: double stranded RNA; ssRNA: single-stranded RNA; RIG-I: retinoic acid-inducible gene 1; MDA5: melanoma-differentiation-associated protein 5; IPS-1: IFN-β promoter stimulator 1; TLR: Toll-like receptor; MyD88: myeloid differentiation primary response gene 88; HDAC: histone deacetylase; IRF: IFN regulatory factors; IFN: interferon; Stat: signal transducers and activators of transcription; ISGF: IFN-stimulated gene factor; ISRE: IFN-stimulated response element; ISG: IFN-stimulated gene; IFIT: IFN-induced proteins with tetratricopeptide repeats; NF-κB: nuclear factor kappa-light-chain-enhancer of activated B cells.
 Figure published in [103]

Additionally, type I Interferons were classified as so-called “danger-associated molecular patterns (DAMPs)” [21] that are induced by cellular distress, followed by activation of dendritic cells (DCs) with subsequent activation of antigen-

specific T cells, which is defined as a so-called “immunogenic cell death” [21]. Resistance to adenovirus-based virotherapy was at least partly attributed to interferon-signaling by the tumor stroma/microenvironment (not the tumor cells themselves), resulting in recurrence of cancer disease in a complex mouse model [189]. Wojton et al.^[190] suggested the usage of HDACi to dampen innate interferon signaling to circumvent resistance barriers mediated by the tumor microenvironment.

Accordingly, transient inhibition of the type I interferon response by HDACi resminostat might favor MeV infection within the tumor niche and succeeding boosted immunogenic cell death.

4.4.2 Additional immunomodulating functions by down-regulation of zfp64

“NF-κB-signaling is also central for the activation of innate antiviral programs [191]. After cytosolic activation upon phosphorylation NF-κB induces inflammatory cytokines such as type I IFN [94]. Interestingly, zinc finger protein 64 (zfp64) expression was found to be downregulated following resminostat treatment *in vitro* and *in vivo* [136]. We here found no negative impact upon zfp64 mRNA levels when performing hepatoma cell infections with MeV-SCD, indicating that resminostat mediated effects are not impaired in the Res + MeV combination treatment setting. Of note, zfp64 has previously been found to be a positive modulator of NF-κB mediated signaling following TLR activated inflammatory response in macrophages and zfp64 knockdown was associated with the inhibition of TLR triggered production of IFN-β, TNF-α, and IL-6 [192]. Therefore, resminostat-mediated immunomodulation can be linked to these NF-κB dependent innate immunity signaling pathways throughout zfp64 down-regulation as well (see also Figure 4.1).” [103]

4.5 Future directions of immunovirotherapy

Preclinical data rather overestimated the cytolytic effects of virotherapy in immunocompromised xenograft (mouse) models [21] and early successful case reports were attributed to induction of a general immunosuppression in those rare

case reports especially in patients with hematological malignancies that favored a systemic virus dissemination [193].

Direct oncolysis as well as virus replication and spread are often found to be limited by host innate (e.g. rapid neutralization by natural IgM and complement factors [58]) and adaptive immune response [194, 195]. Immune reaction in the context of oncolytic virotherapy, however, can be considered either friend or foe: induction of immunogenic cancer cell death (i.e. immunogenic apoptosis/necrosis/pyroptosis and autophagy) by oncolytic viruses is associated with exposure of formerly dampened tumor associated antigens, damage associated molecular patterns (DAMPs) [196] and pathogen-associated molecular patterns (PAMPs) of virus origin. In turn, these immunogenic signals are recognized by antigen presenting cells (such as dendritic cells, DC) and are potent elicitors for an adaptive (T cell-mediated) antitumor immune response [197].

As a consequence, the field of experts largely seems to agree that success of oncolytic virotherapy is dependent on both cytoreductive activity through direct tumor lysis and concomitant stimulation of a boosted adaptive immune response for long lasting disease control. To maximize this effect, viruses being in late-stage clinical trials have shown to be of favorable efficiency when combining a direct oncolysis-dependent anti-tumor vaccinating effect with expression of immunostimulatory cargo, such as GM-CSF [21] (also tested for measles viruses by Grote et al.^[198]). Finding a compromise balanced on a razor's edge to maximize positive immune response effects, oncolytic viruses can be combined with other treatment modalities, such as radiation or classical chemotherapy.

For example, in preclinical studies MeV-NIS has been successfully combined with immunosuppressive alkylans such as cyclophosphamide [199] and pretreatment with cyclophosphamide - being instrumental to delay a sufficient anti-viral response - was found to enhance virus replication at early time points of the treatment but did not delay MeV-NIS clearance at later time points. Based on these findings, a phase I/II clinical trial on patients with refractory multiple myeloma was launched (NCT00450814) and a following Phase II efficacy study as well (NCT02192775). Here, a transient immunosuppression leads to a

beneficial outcome without augmentation of treatment-associated toxicities, showing the general applicability of these approaches. Evidence gained to date leads to the conclusion that the immune modulation by HDACi is restricted to transformed cells without increased susceptibility of healthy tissue to viral infection [142]. Of course, these safety issues have to be addressed when designing a first epi-virotherapeutic clinical trial by systematic repetitive sampling and biopsy analyses.

Another promising immunovirotherapeutic approach was identified, as innovative combination with systemic immunotherapies (e.g. immune checkpoint inhibitors like CTLA-4 and PD-1 antibodies) seems to be able to result in the induction of favorable inflammatory immune infiltrations even to metastatic tumor sites [200]. Releasing the brake of the antitumor T-cell response by checkpoint blockade was recently demonstrated by Engeland et al.^[201], as the group generated measles vaccine vectors encoding for CTLA-4 and PD-L1 antibodies. Testing these vectors in a fully immunocompetent mouse model revealed (i) enhanced therapeutic efficiency of the combined treatment of measles infection and local expression of therapeutic antibodies as well as (ii) favorable immunological profiles, as total amounts of T cells were increased while regulatory T cells were found to be reduced within the tumors. These results encourage the further usage of this immunovirotherapeutic approach and underline the importance of a balanced interplay between direct oncolysis on the one hand and beneficial immunomanipulation on the other hand.

“The intention of combining an oncolytic virus with an HDAC inhibitor is to generate a balanced treatment modality between temporary immunomodulation, favoring OV replication in cancer cells, and a maximum boosted host anti-tumor adaptive immune response through release of specific tumor antigens following measles infection.” [103]

As HDAC inhibitors deregulate the epigenetic code of tumor cells on various levels, a multitude of possible effects on viral oncolysis can be assumed. Additionally, HDACi and OV combinations were found to synergistically inhibit

tumor blood flow by repression of pro-angiogenic mediators leading to so-called vascular shutdown and regression of tumor sites [143, 149].

4.6 Perspectives

The aim of this thesis was to establish a preclinical therapy regimen for the epi-virotherapeutic treatment of hepatocellular carcinoma (HCC) using the oncolytic measles vaccine vector MeV-SCD and the epigenetically active compound resminostat.

“When testing a panel of human hepatoma cell lines, we found (i) a significantly improved rate of primary infections when using oncolytic MeV under concurrent treatment with resminostat, (ii) a boosted cytotoxic effect of the epi-virotherapeutic combination (Res + MeV) with enhanced induction of apoptosis, and, quite importantly, (iii) an absence of any resminostat-induced impairment of MeV replication and spread. Beyond that, we were also able to show (iv) that resminostat, after hepatoma cell stimulation with exogenous human interferon- β , is able to prevent the induction of interferon-stimulated genes, such as IFIT-1. This finding outlines the possible impact of resminostat on cellular innate immunity, being instrumental in overcoming resistances to MeV-mediated viral oncolysis” [103] and therefore provides a strong rationale to establish this epi-virotherapeutic approach as a multi-faceted treatment modality against cancer.

“Our data lead to the conclusion that combination therapies of the novel oral HDAC inhibitor resminostat with the oncolytic measles vaccine virus MeV-SCD bear a great potential for patients with advanced hepatocellular carcinomas, especially as both agents are currently under clinical investigation, which could allow a fast translation of our results “from bench to bedside”. The full benefit of the combination therapy of both compounds for those HCC patients may be even considerably larger, as resminostat *per se* could function as an immunomodulating compound. This could potentially suppress cellular innate antiviral responses in hepatoma cells being refractory to virotherapy, leading to higher concentrations of viral vectors at the respective tumor sites.” [103]

These effects could potentially be accompanied by resminostat immune priming attributes, consisting of accelerated NK cell recruitment, enhanced TAA

expression and presentation by cancer cells, as well as releasing the brakes on T-cell-mediated anti-tumor immune response [137].

“Based on these promising results, the next logical step is to test this approach in an immunocompetent murine model and to design a first epi-virotherapeutic clinical trial employing resminostat together with MeV-SCD in patients exhibiting advanced stages of HCC.” [103]

The design of a future clinical trial should thereby be based on systematic pre-clinical evaluation of varied dosing intervals in a multiple-hit (virotherapy-)setting compared to a single-shot MeV administration and -varying overlapping dosing intervals of resminostat co-treatment. This could reveal an even more potent application scheme in this epi-virotherapeutic context, especially when carried out in an immunocompetent model system to reveal immunological interactions and therefore unveil the proposed full therapeutic benefit of the combination of MeV and resminostat.

5 Summary

Hepatocellular carcinoma (HCC) is one of the leading causes of cancer-related deaths worldwide and therapy options for advanced stages of disease are, despite recent advantages, considered relatively poor.

Oncolytic viruses represent a novel therapy option for cancer treatment, as they were found to infect malignant tissue with subsequent substantial anti-tumor activity while toxicities for patients were generally found to be modest. Nevertheless, clinical testing of measles vaccine virus (MeV) as oncolytic vector platform revealed several limitations, such as inherent resistance phenomena as well as a lack of therapeutic efficiency. Therefore, prudent combination strategies are required to address those issues.

Inhibitors of human histone deacetylases (HDACi) are investigated as a therapeutic option for various cancer entities with capability to induce cancer cell death as well as inhibition of tumor proliferation with concomitant additive immunomodulating potency. Interestingly, HDACi were found to dampen innate immunity signaling after infection with oncolytic vectors in tumor cells and are therefore considered as commendable combination partners for oncolytic virotherapy.

Aim of this thesis was to investigate the potential of the epi-virotherapeutic combination using the prototypic suicide gene-armed measles vaccine-based virotherapeutic MeV-SCD and the oral HDACi resminostat for *in vitro* studies on a panel of three well-established hepatoma cell lines. To identify underlying mechanisms, alterations in virus biology parameters, as well as influences on tumor cell immune signaling and cell death were investigated.

We found an enhanced cytotoxic/oncolytic effect for the epi-virotherapeutic co-treatment (Res + MeV) compared to any of the two monotherapeutic modalities in human hepatoma cells, but not in non-malignant primary human hepatocytes (PHH), accompanied by an accumulation of tumor cells undergoing apoptosis. Rates of primary infection of hepatoma cells by MeV could be enhanced in the presence of resminostat, while no inhibitory effects of resminostat on subsequent MeV replication and spread were observed. On a molecular level, resminostat

was found to be a potent inhibitor of IFN- β -induced upregulation of IFIT-1 (interferon-induced protein with tetratricopeptide repeats), distinguishing itself as a transient immunomodulator being instrumental in promoting oncolytic virotherapy.

As both MeV and resminostat are currently under evaluation in several clinical trials, this epi-virotherapeutic combination therapy could be translated rapidly into clinical practice as an effective strategy against advanced stage liver carcinoma.

6 Zusammenfassung

Das Hepatozelluläre Karzinom (HCC) gehört zu einer der häufigsten Krebstodesursachen weltweit und Behandlungsmöglichkeiten für fortgeschrittene HCC-Tumorstadien sind, trotz gewisser Fortschritte in den letzten Jahren, immer noch eingeschränkt.

Der Einsatz onkolytischer Viren in der Krebstherapie stellt eine neuartige Behandlungsmöglichkeit in der Onkologie dar, da diese Viren malignes Gewebe infizieren, in diesem selektiv replizieren, dieses dabei lysieren und dementsprechend antitumorale Eigenschaften besitzen, wobei sich gleichzeitig die Nebenwirkungen für die Patienten bisher als ausgesprochen überschaubar erwiesen. Dennoch hat sich in der klinischen Überprüfung dieser Eigenschaften gezeigt, dass es für den Einsatz von Masern-Impfviren (MeV) als onkolytische Vektoren einige Beschränkungen gibt, die von primären Resistenzphänomenen bis zu einem Mangel an therapeutischem Effekt reichen. Daher sind wohlüberlegte Kombinationsstrategien erforderlich, die diese Problembereiche elegant lösen können.

Inhibitoren der Enzymgruppe der humanen Histon-Deacetylasen (HDACi) werden als Therapieoption für verschiedene Tumorentitäten in Betracht gezogen, da diese gezeigt haben, Krebszellen selbst zerstören zu können, diese an der Proliferation zu hindern und darüber hinaus zusätzliche immunmodulierende Eigenschaften besitzen. HDACi können dabei interessanterweise das angeborene zelluläre Immunsystem der Tumorzellen nach der Infektion mit onkolytischen Vektoren unterdrücken, sodass Histon-Deacetylase-Inhibitoren für die Kombination mit onkolytischen Viren hervorragend geeignet erscheinen.

Ziel dieser Arbeit war, das Potenzial des epi-virotherapeutischen Kombinationsansatzes des neuen HDAC-Inhibitor Resminostat (Res) zusammen mit dem onkolytischen Masernimpfvirus MeV-SCD (das für ein sog. Suizidgen kodiert) an einer Auswahl von drei humanen Hepatomzelllinien zu charakterisieren. Um zugrunde liegende Mechanismen aufzudecken, wurden Untersuchungen auf Ebene der Virusbiologie (wie primäre Infektionsraten oder auch Replikations-

kompetenz) durchgeführt. Darüber hinaus wurden Einflüsse der Kombinations-therapie auf Signalwege des angeborenen Immunsystems der Tumorzellen, aber auch Mechanismen des programmierten Zelltodes beobachtet.

Es konnte gezeigt werden, dass die epi-virotherapeutische Kombinations-behandlung (Res + MeV) einen verstärkten zytotoxischen/onkolytischen Effekt in den humanen Hepatomzelllinien erzielt, dies jeweils im Vergleich zu den entsprechenden Monotherapien, jedoch nicht in untransformierten, gesunden primären Hepatozyten (PHH). Dieser Effekt konnte zumindest partiell auf eine vermehrte Anzahl an apoptotischen Tumorzellen zurückgeführt werden. Primäre Infektionsraten der Hepatomzellen mit MeV konnten durch Zugabe von Resminostat gesteigert werden, ohne dabei die nachfolgende Virusreplikation und -ausbreitung negativ zu beeinflussen.

Auf molekularer Ebene zeigte sich Resminostat als potenter Inhibitor einer durch Stimulation mit humanem IFN- β (Interferon beta) induzierten Hochregulation von IFIT-1 (*interferon-induced protein with tetratricopeptide repeats*). Durch diese Resminostat-vermittelte transiente Immunmodulation kann wiederum eine erfolgreiche onkolytische Virotherapie potenziell gefördert werden.

Da sowohl Masern-Impfviren als auch Resminostat derzeit in zahlreichen klinischen Studien getestet werden, könnte dieser epi-virotherapeutische Kombinationsansatz als effektive Behandlungsmöglichkeit des fortgeschrittenen Leberkarzinoms zügig im klinischen Alltag zur Anwendung kommen.

Appendix

List of equations

EQUATION 1: DETERMINATION OF CELL COUNT USING A NEUBAUER COUNTING CHAMBER	33
EQUATION 2: CALCULATION OF VIRAL TITERS USING THE TCID ₅₀ METHOD WITH INCLUDED CONVERSION INTO PFU/ML UNITS.....	37

List of figures

FIGURE 1.1: CANCER-RELATED DEATHS 2012	1
FIGURE 1.2: PRINCIPLES OF ONCOLYTIC VIROTHERAPY USING THE EXAMPLE OF ONCOLYTIC MEASLES VACCINES.	4
FIGURE 1.3: PRIME-BOOST / SINGLE-SHOT PARADIGMS OF VIROTHERAPEUTIC APPLICATION SCHEMES.....	9
FIGURE 1.4: SCHEMATIC MORPHOLOGY OF MEASLES VIRUS:.....	13
FIGURE 1.5: MECHANISM OF ACTION OF MEV-SCD PRODRUG CONVERTASE SUPER-CYTOSINE DEAMINASE (SCD):.....	15
FIGURE 1.6: SELECTED APPLICATION SCHEMES OF MEV-CEA:.....	19
FIGURE 1.7: SELECTED APPLICATION SCHEMES OF MEV-NIS:.....	19
FIGURE 1.8: PRINCIPLES OF HISTONE DEACETYLASE INHIBITION.....	22
FIGURE 1.9: IMMUNOMODULATING EFFECTS OF RESMINOSTAT	26
FIGURE 2.1: REPRESENTATIVE NEUBAUER HAEMOCYTOMETER USED FOR CELL COUNTING.....	33
FIGURE 2.2: IMPROVED NEUBAUER CHAMBER GRID DETAIL:.....	34
FIGURE 2.3: SCHEME OF MEV TITRATION ON VERO CELLS:	36
FIGURE 2.4: SCHEMATIC CONSTRUCTION OF A FLOW CYTOMETER AS USED FOR ANALYSING MEV-GFP INFECTION RATES, CD46-EXPRESSION ON HEPATOMA CELLS AND ANALYSIS OF CELL CYCLE PHASES:.....	40
FIGURE 2.5: CORRECT ARRANGEMENT OF ACCESSORIES AND SUPPLIES IN A WESTERN BLOT "SANDWICH":.....	48
FIGURE 3.1: REMAINING TUMOR CELL MASSES AFTER SINGLE (MONOTHERAPEUTIC) TREATMENT WITH MEV-SCD:.....	52
FIGURE 3.2 CYTOTOXIC EFFECT OF RESMINOSTAT AS A MONOTHERAPEUTIC AGENT IN HEPATOMA CELL LINES	53
FIGURE 3.3: APPLICATION SCHEME FOR MEV-SCD AND RESMINOSTAT CO-TREATMENT IN HEPATOMA CELLS	54

FIGURE 3.4: BOOSTED CYTOTOXIC EFFECTS OBTAINED BY EPI-VIROTHERAPEUTIC CO-TREATMENT WITH MEV-SCD AND RESMINOSTAT	56
FIGURE 3.5: COMBINATION SETTING OF RES + MEV CO-TREATMENT (RESMINOSTAT PRE-TREATMENT 48 HBI):.....	57
FIGURE 3.6: PRIME-BOOST APPROACH FOR EPI-VIROTHERAPEUTIC TREATMENT:	59
FIGURE 3.7: TRIPLE-THERAPY: ADDITION OF PRODRUG 5-FC TO THE MEV/RES COMBINATION SETTING:.....	60
FIGURE 3.8: INFLUENCE OF RESMINOSTAT CO-TREATMENT ON MEV-GFP INFECTION IN HEPATOMA CELLS:.....	62
FIGURE 3.9: RESMINOSTAT ENHANCES RATES OF PRIMARY INFECTION OF HUMAN HEPATOMA CELLS BY MEASLES VACCINE VIROTHERAPEUTICS.	65
FIGURE 3.10: ALTERATIONS OF CD46 EXPRESSION LEVELS ON MEV-GFP AND/OR RESMINOSTAT-TREATED HUMAN HEPATOMA CELLS:.....	66
FIGURE 3.11: RESMINOSTAT DOES NOT IMPAIR REPLICATION OF MEV-SCD AND SUBSEQUENT SPREAD OF PROGENY VIRAL PARTICLES	67
FIGURE 3.12: EXPRESSION LEVELS OF ZFP64 (PHARMACODYNAMIC BIOMARKER FOR RESMINOSTAT ACTIVITY) IN HUMAN HEPATOMA CELL LINES AFTER EPI-VIROTHERAPEUTIC (RES + MEV) TREATMENT:.....	68
FIGURE 3.13: CELL CYCLE PROFILES OF HUMAN HEPATOMA CELLS UNDERGOING EPI-VIROTHERAPEUTIC CO-TREATMENT WITH MEV-SCD AND RESMINOSTAT:	70
FIGURE 3.14 IFN- β INDUCED EXPRESSION OF IFIT-1 IS SUPPRESSED BY RESMINOSTAT, WHEREAS PHOSPHORYLATION OF STAT1 IS NOT:.....	72
FIGURE 4.1: POSSIBLE INFLUENCES OF RESMINOSTAT ON INTERFERON (IFN) SIGNALING:	80

List of tables

TABLE 1.1: SELECTED CLINICAL TRIALS USING ONCOLYTIC VECTOR SYSTEMS AS MONOTHERAPEUTIC AGENTS.....	6
TABLE 2.1: COMMERCIAL CELL LINES USED FOR THE STUDIES IN THIS THESIS:	31
TABLE 2.2: PLATING/TREATMENT CONDITIONS FOR SAMPLE COLLECTION IN THE VIRAL GROWTH CURVES EXPERIMENTS.....	38
TABLE 2.3: CONDITIONS FOR FLUORESCENCE MICROSCOPY OF MEV-GFP EXPERIMENTS.....	39
TABLE 2.4: CELL CULTURE CONDITIONS IN CD46-EXPRESSION EXPERIMENTS.	42
TABLE 2.5: INGREDIENTS OF THE RESOLVING GEL USED FOR SDS-PAGE:.....	46
TABLE 2.6: INGREDIENTS OF THE 5% STACKING GEL USED FOR SDS-PAGE:.....	46
TABLE 2.7: LIST OF ANTIBODIES USED FOR WESTERN BLOTTING:.....	49

Index of abbreviations

5-FC	5-fluorocytosine
5-FU	5-fluorouracil
5-dFUTP	5-desoxyfluorouridine triphosphate
5-FdUMP	5-fluorodesoxyuridine monophosphate
5-FUMP	5-fluorouridine monophosphate
ANOVA	Analysis of variance
BSA	Bovine serum albumin
CAR	Coxsackie virus and adenovirus receptor
CD	Cluster of differentiation
CD	Cytosine deaminase
CD46	Cluster of differentiation, human membrane cofactor protein
CTCL	Cutaneous T-cell lymphoma
CTLA-4	Cytotoxic T-lymphocyte-associated Protein 4
DAMPs	danger-associated molecular patterns
DC	Dendritic cell
DHFU	Dihydrofluorouracil
DMEM	Dulbecco's Modified Eagle's Medium
DMSO	Dimethylsulfoxid
DNA	Desoxyribonucleic acid
DPD	dihydropyrimidine dehydrogenase
EDTA	Ethylendiamintetraacetic acid
EGF	Epidermal growth factor
eIF3	Eukaryotic initiation factor 3
EMA	European Medicines Agency
FACS	Fluorescence-activated cell sorting
FBS	Fetal Bovine Serum
FDA	U.S. Food and Drug Administration

GFP	Green fluorescent protein
GM-CSF	Granulocyte-macrophage colony-stimulating factor
H-1PV	Oncolytic rodent parvovirus
HAT	Histone acetyl transferases
HBV	Hepatitis B virus
HCC	Hepatocellular carcinoma
HCV	Hepatitis C virus
HDAC	Histone deacetylase
HDACi	Inhibitor of histone deacetylase
hDCT	Human dopachrome tautomerase
hpi	Hours post infection
HSP	Heat-shock-protein
HSV	Herpes simplex virus
HRP	Horseradish peroxidase
ICTV	International Committee on Taxonomy of Viruses
IFIT	IFN-induced proteins with tetratricopeptide repeats
IFN	Interferon
IL-6	Interleukin 6
IPS-1	IFN- β promoter stimulator 1
IRF-3/IRF-7	IFN regulatory factors 3/7
ISG	IFN stimulated gene
ISGF	IFN-stimulated gene factor
ISRE	IFN-stimulated response element
JAK	Janus kinase
JX-594	Pexastimogene devacirepvec, Pexa-Vec= oncolytic vaccinia virus encoding for GM-CSF
LC	Langerhans cell
MDA5	melanoma-differentiation-associated protein 5

MeV	Measles virus
MeV-Edm	Edmonston strain measles vaccine viruses
MeV	Oncolytic measles vaccine virus encoding for GFP
MeV-SCD	Oncolytic measles vaccine virus encoding for SCD
MFI	Means of fluorescence intensity
MOI	Multiplicity of infection
MeV-CEA	Oncolytic measles vaccine virus encoding for carcino-embryonic antigen
MeV-NIS	Oncolytic measles vaccine virus encoding for human thyroidal sodium iodide symporter
MYD88	Myeloid differentiation primary response gene 88
NCT	ClinicalTrials.gov identification number
NF- κ B	nuclear factor kappa-light-chain-enhancer of activated B cells
OD	Optical density
OV	Oncolytic virus
OV	Oncolytic virotherapy
PAMP	Pathogen-associated molecular pattern
PBS	Phosphate buffered saline
PD-1	Programmed cell death protein 1
PE	Phycoerythrin
pfu	Plaque-forming units
PHH	Primary human hepatocytes
PRDX1	Peroxiredoxin 1
Res	Resminostat
PVDF	Polyvinylidene difluoride
RIG-I	Retinoic acid-inducible gene 1
RNA	Ribonucleic acid
RNP	Ribonucleo-protein complex
SCD	Super-Cytosine Deaminase

SLAM	Signaling lymphocyte activation molecule (= CD150)
SPECT/CT	Single Photon Emission Computed Tomography
ssRNA	Single-stranded RNA
SAHA	Vorinostat (=suberanilohydroxamic acid)
SDS	Sodium dodecyl sulfate
SRB	Sulforhodamine B
STAT	Signal Transducer and Activator of Transcription
TCA	Trichloroacetic acid
TCID ₅₀	Tissue culture infective dose 50
TLR	Toll-like receptor
TNF- α	Tumor necrosis factor α
TSA	Trichostatin A
T-Vec	Talimogene Laherparepvec, oncolytic HSV virus encoding for GM-CSF (IMLYGIC®)
UPRT	Uracil phosphoribosyltransferase
VEGF	Vascular endothelial growth factor
VPA	Valproic acid
VSV	Vesicular Stomatitis Virus
WHO	World Health Organization
Zfp64	Zinc finger protein 64

References

1. Ferlay, J, Soerjomataram, I, Ervik, M, Dikshit, R, Eser, S, Mathers, C, *et al.* GLOBOCAN 2012 v1. 0, Cancer Incidence and Mortality Worldwide: IARC Cancer Base 2013; No. 11 [Internet]. Lyon, France: International Agency for Research on Cancer.
2. Stewart, BW, and Wild, C (2014). *World Cancer Report 2014*, World Health Organization.
3. Bosetti, C, Turati, F, and La Vecchia, C (2014). Hepatocellular carcinoma epidemiology. *Best practice & research Clinical gastroenterology* **28**: 753-770.
4. Pang, TC, and Lam, VW (2015). Surgical management of hepatocellular carcinoma. *World journal of hepatology* **7**: 245-252.
5. Peck-Radosavljevic, M (2014). Drug therapy for advanced-stage liver cancer. *Liver cancer* **3**: 125-131.
6. Llovet, JM, Ricci, S, Mazzaferro, V, Hilgard, P, Gane, E, Blanc, JF, *et al.* (2008). Sorafenib in advanced hepatocellular carcinoma. *N Engl J Med* **359**: 378-390.
7. Kelly, E, and Russell, SJ (2007). History of oncolytic viruses: genesis to genetic engineering. *Molecular therapy : the journal of the American Society of Gene Therapy* **15**: 651-659.
8. Greentree, LB (1983). Hodgkin's disease: therapeutic role of measles vaccine. *The American journal of medicine* **75**: 928.
9. Hansen, RM, and Libnoch, JA (1978). Remission of chronic lymphocytic leukemia after smallpox vaccination. *Archives of internal medicine* **138**: 1137-1138.
10. Dock, G (1904). The influence of complicating diseases upon leukemia. *Am J Med Sci* **127**: 563-592.
11. Pasquinucci, G (1971). Possible effect of measles on leukaemia. *Lancet* **1**: 136.
12. Gross, S (1971). Measles and leukaemia. *Lancet* **1**: 397-398.
13. Zygiert, Z (1971). Hodgkin's disease: remissions after measles. *Lancet* **1**: 593.
14. Taqi, AM, Abdurrahman, MB, Yakubu, AM, and Fleming, AF (1981). Regression of Hodgkin's disease after measles. *Lancet* **1**: 1112.
15. Bluming, AZ, and Ziegler, JL (1971). Regression of Burkitt's lymphoma in association with measles infection. *Lancet* **2**: 105-106.
16. Kirn, D, Martuza, RL, and Zwiebel, J (2001). Replication-selective virotherapy for cancer: Biological principles, risk management and future directions. *Nature medicine* **7**: 781-787.
17. Bell, J, and McFadden, G (2014). Viruses for Tumor Therapy. *Cell Host & Microbe* **15**: 260-265.
18. Lichty, BD, Breitbach, CJ, Stojdl, DF, and Bell, JC (2014). Going viral with cancer immunotherapy. *Nature reviews Cancer* **14**: 559-567.
19. Vacchelli, E, Eggermont, A, Sautes-Fridman, C, Galon, J, Zitvogel, L, Kroemer, G, *et al.* (2013). Trial watch: Oncolytic viruses for cancer therapy. *Oncoimmunology* **2**: e24612.

20. Miest, TS, and Cattaneo, R (2014). New viruses for cancer therapy: meeting clinical needs. *Nature reviews Microbiology* **12**: 23-34.
21. Woller, N, Gurlevik, E, Ureche, CI, Schumacher, A, and Kuhnel, F (2014). Oncolytic viruses as anticancer vaccines. *Frontiers in oncology* **4**: 188.
22. Cattaneo, R, Miest, T, Shashkova, EV, and Barry, MA (2008). Reprogrammed viruses as cancer therapeutics: targeted, armed and shielded. *Nature reviews Microbiology* **6**: 529-540.
23. Moehler, MH, Zeidler, M, Wilsberg, V, Cornelis, JJ, Woelfel, T, Rommelaere, J, *et al.* (2005). Parvovirus H-1-induced tumor cell death enhances human immune response in vitro via increased phagocytosis, maturation, and cross-presentation by dendritic cells. *Hum Gene Ther* **16**: 996-1005.
24. Mastrangelo, MJ, Maguire, HC, Jr., Eisenlohr, LC, Laughlin, CE, Monken, CE, McCue, PA, *et al.* (1999). Intratumoral recombinant GM-CSF-encoding virus as gene therapy in patients with cutaneous melanoma. *Cancer gene therapy* **6**: 409-422.
25. Hwang, T-H, Moon, A, Burke, J, Ribas, A, Stephenson, J, Breitbach, CJ, *et al.* (2011). A Mechanistic Proof-of-concept Clinical Trial With JX-594, a Targeted Multi-mechanistic Oncolytic Poxvirus, in Patients With Metastatic Melanoma. *Mol Ther* **19**: 1913-1922.
26. Diaz, RM, Galivo, F, Kottke, T, Wongthida, P, Qiao, J, Thompson, J, *et al.* (2007). Oncolytic immunovirotherapy for melanoma using vesicular stomatitis virus. *Cancer Res* **67**: 2840-2848.
27. Ruf, B, and Lauer, U (2015). Assessment of current virotherapeutic application schemes: "Hit hard and early" versus "Killing softly"? *Molecular Therapy — Oncolytics* **2**: 150018.
28. Garber, K (2006). China approves world's first oncolytic virus therapy for cancer treatment. *Journal of the National Cancer Institute* **98**: 298-300.
29. Russell, SJ, Peng, KW, and Bell, JC (2012). Oncolytic virotherapy. *Nature biotechnology* **30**: 658-670.
30. Kaufman, HL, Andtbacka, RHI, Collichio, FA, Amatruda, T, Senzer, NN, Chesney, J, *et al.* (2014). Primary overall survival (OS) from OPTiM, a randomized phase III trial of talimogene laherparepvec (T-VEC) versus subcutaneous (SC) granulocyte-macrophage colony-stimulating factor (GM-CSF) for the treatment (tx) of unresected stage IIIB/C and IV melanoma. *ASCO Meeting Abstracts* **32**: 9008a.
31. Garcia-Carbonero, R, Gil-Martin, M, Calvo, E, Prados, S, De la Portilla, F, Salazar, R, *et al.* (2014). A phase 1 mechanism of action study of intratumoral or intravenous administration of enadenotucirev, an oncolytic Ad11/Ad3 chimeric group B adenovirus in colon cancer patients undergoing resection of primary tumor. *ASCO Meeting Abstracts* **32**: TPS3112.
32. Burke, JM, Lamm, DL, Meng, MV, Nemunaitis, JJ, Stephenson, JJ, Arseneau, JC, *et al.* (2012). A first in human phase 1 study of CG0070, a GM-CSF expressing oncolytic adenovirus, for the treatment of nonmuscle invasive bladder cancer. *The Journal of urology* **188**: 2391-2397.

33. Kimball, KJ, Preuss, MA, Barnes, MN, Wang, M, Siegal, GP, Wan, W, *et al.* (2010). A phase I study of a tropism-modified conditionally replicative adenovirus for recurrent malignant gynecologic diseases. *Clinical cancer research : an official journal of the American Association for Cancer Research* **16**: 5277-5287.
34. Andtbacka, RHI, Curti, BD, Kaufman, H, Daniels, GA, Nemunaitis, JJ, Spitler, LE, *et al.* (2014). CALM study: A phase II study of an intratumorally delivered oncolytic immunotherapeutic agent, coxsackievirus A21, in patients with stage IIIc and stage IV malignant melanoma. *ASCO Meeting Abstracts* **32**: 3031.
35. Senzer, NN, Kaufman, HL, Amatruda, T, Nemunaitis, M, Reid, T, Daniels, G, *et al.* (2009). Phase II Clinical Trial of a Granulocyte-Macrophage Colony-Stimulating Factor–Encoding, Second-Generation Oncolytic Herpesvirus in Patients With Unresectable Metastatic Melanoma. *Journal of Clinical Oncology* **27**: 5763-5771.
36. Chang, KJ, Senzer, NN, Binmoeller, K, Goldsweig, H, and Coffin, R (2012). Phase I dose-escalation study of talimogene laherparepvec (T-VEC) for advanced pancreatic cancer (ca). *ASCO Meeting Abstracts* **30**: e14546.
37. Cripe, TP, Racadio, JM, Conner, J, Towbin, A, Brunner, MM, Stockman, BA, *et al.* (2013). A phase I dose-escalation study of intratumoral herpes simplex virus-1 mutant HSV1716 in pediatric/young adult patients with refractory non-central nervous system solid tumors. *ASCO Meeting Abstracts* **31**: 10047.
38. Ferris, RL, Gross, ND, Nemunaitis, JJ, Andtbacka, RHI, Argiris, A, Ohr, J, *et al.* (2014). Phase I trial of intratumoral therapy using HF10, an oncolytic HSV-1, demonstrates safety in HSV+/HSV- patients with refractory and superficial cancers. *ASCO Meeting Abstracts* **32**: 6082.
39. Galanis, E, Hartmann, LC, Cliby, WA, Long, HJ, Peethambaram, PP, and Barrette, BA (2010). Phase I trial of intraperitoneal administration of an oncolytic measles virus strain engineered to express carcinoembryonic antigen for recurrent ovarian cancer. *Cancer Res* **70**: 875-882.
40. Galanis, E, Atherton, PJ, Maurer, MJ, Knutson, KL, Dowdy, SC, Cliby, WA, *et al.* (2015). Oncolytic measles virus expressing the sodium iodide symporter to treat drug-resistant ovarian cancer. *Cancer Res* **75**: 22-30.
41. Russell, SJ, Federspiel, MJ, Peng, KW, Tong, C, Dingli, D, Morice, WG, *et al.* (2014). Remission of disseminated cancer after systemic oncolytic virotherapy. *Mayo Clinic proceedings* **89**: 926-933.
42. Geletneky, K, Huesing, J, Rommelaere, J, Schlehofer, JR, Leuchs, B, Dahm, M, *et al.* (2012). Phase I/IIa study of intratumoral/intracerebral or intravenous/intracerebral administration of Parvovirus H-1 (ParvOryx) in patients with progressive primary or recurrent glioblastoma multiforme: ParvOryx01 protocol. *BMC cancer* **12**: 99.
43. Desjardins, A, Sampson, JH, Peters, KB, Ranjan, T, Vlahovic, G, Watts, J, *et al.* (2014). Phase I study of the intratumoral administration of an oncolytic polio/rhinovirus recombinant (PVSRIPO) in recurrent glioblastoma (GBM). *ASCO Meeting Abstracts* **32**: TPS2106.

44. Forsyth, P, Roldan, G, George, D, Wallace, C, Palmer, CA, Morris, D, *et al.* (2008). A phase I trial of intratumoral administration of reovirus in patients with histologically confirmed recurrent malignant gliomas. *Mol Ther* **16**: 627-632.
45. Galanis, E, Markovic, SN, Suman, VJ, Nuovo, GJ, Vile, RG, Kottke, TJ, *et al.* (2012). Phase II trial of intravenous administration of Reolysin((R)) (Reovirus Serotype-3-dearing Strain) in patients with metastatic melanoma. *Molecular therapy : the journal of the American Society of Gene Therapy* **20**: 1998-2003.
46. Mita, AC, Sankhala, K, Sarantopoulos, J, Carmona, J, Okuno, S, Goel, S, *et al.* (2009). A phase II study of intravenous (IV) wild-type reovirus (Reolysin) in the treatment of patients with bone and soft tissue sarcomas metastatic to the lung. *ASCO Meeting Abstracts* **27**: 10524.
47. Molina, JR, Mandrekar, SJ, Dy, GK, Aubry, M-C, Allen Ziegler, KL, Dakhil, SR, *et al.* (2013). A randomized double-blind phase II study of the Seneca Valley virus (NTX-010) versus placebo for patients with extensive stage SCLC (ES-SCLC) who were stable or responding after at least four cycles of platinum-based chemotherapy: Alliance (NCCTG) N0923 study. *ASCO Meeting Abstracts* **31**: 7509.
48. Rudin, CM, Senzer, N, Stephenson, J, Loesch, D, Burroughs, K, Police, SR, *et al.* (2009). Phase I study of intravenous Seneca Valley virus (NTX-010), a replication competent oncolytic virus, in patients with neuroendocrine (NE) cancers. *ASCO Meeting Abstracts* **27**: 4629.
49. Lauer, U, Zimmermann, M, Sturm, J, Koppenhoefer, U, Bitzer, M, Malek, NP, *et al.* (2013). Phase I/II clinical trial of a genetically modified and oncolytic vaccinia virus GL-ONC1 in patients with unresectable, chemotherapy-resistant peritoneal carcinomatosis. *ASCO Meeting Abstracts* **31**: 3098.
50. Khan, KH, Young, A-M, Mateo, J, Tunariu, N, Yap, TA, Tan, DSP, *et al.* (2013). Phase I clinical trial of a genetically modified and oncolytic vaccinia virus GL-ONC1 with green fluorescent protein imaging (NCT009794131). *ASCO Meeting Abstracts* **31**: 3062.
51. Zeh, HJ, Downs-Canner, S, McCart, JA, Guo, ZS, Rao, UN, Ramalingam, L, *et al.* (2015). First-in-man Study of Western Reserve Strain Oncolytic Vaccinia Virus: Safety, Systemic Spread, and Antitumor Activity. *Mol Ther* **23**: 202-214.
52. Heo, J, Reid, T, Ruo, L, Breitbach, CJ, Rose, S, Bloomston, M, *et al.* (2013). Randomized dose-finding clinical trial of oncolytic immunotherapeutic vaccinia JX-594 in liver cancer. *Nature medicine* **19**: 329-336.
53. Park, BH, Hwang, T, Liu, TC, Sze, DY, Kim, JS, Kwon, HC, *et al.* (2008). Use of a targeted oncolytic poxvirus, JX-594, in patients with refractory primary or metastatic liver cancer: a phase I trial. *The lancet oncology* **9**: 533-542.
54. Breitbach, CJ, Burke, J, Jonker, D, Stephenson, J, Haas, AR, Chow, LQ, *et al.* (2011). Intravenous delivery of a multi-mechanistic cancer-targeted oncolytic poxvirus in humans. *Nature* **477**: 99-102.

55. Lee, J, Park, YS, Burke, J, Lim, HY, Lee, J, Kang, WK, *et al.* (2013). Phase Ib dose-escalation study of Pexa-Vec (pexastimogene devacirepvec; JX-594), an oncolytic and immunotherapeutic vaccinia virus, administered by intravenous (IV) infusions in patients with metastatic colorectal carcinoma (mCRC). *ASCO Meeting Abstracts* **31**: 3608.
56. Heo, J, Chao, Y, Jonker, DJ, Baron, AD, Habersetzer, F, Burke, J, *et al.* (2013). Phase IIb randomized trial of Pexa-Vec (pexastimogene devacirepvec; JX-594), a targeted oncolytic vaccinia virus, plus best supportive care (BSC) versus BSC alone in patients with advanced hepatocellular carcinoma who have failed sorafenib treatment (TRAVERSE). *ASCO Meeting Abstracts* **31**: TPS4161.
57. Bauerschmitz, GJ, Kanerva, A, Wang, M, Herrmann, I, Shaw, DR, Strong, TV, *et al.* (2004). Evaluation of a selectively oncolytic adenovirus for local and systemic treatment of cervical cancer. *International journal of cancer Journal internationale du cancer* **111**: 303-309.
58. Tesfay, MZ, Ammayappan, A, Federspiel, MJ, Barber, GN, Stojdl, D, Peng, KW, *et al.* (2014). Vesiculovirus neutralization by natural IgM and complement. *Journal of virology* **88**: 6148-6157.
59. Andtbacka, RHI, Collichio, FA, Amatruda, T, Senzer, NN, Chesney, J, Delman, KA, *et al.* (2013). OPTiM: A randomized phase III trial of talimogene laherparepvec (T-VEC) versus subcutaneous (SC) granulocyte-macrophage colony-stimulating factor (GM-CSF) for the treatment (tx) of unresected stage IIIB/C and IV melanoma. *ASCO Meeting Abstracts* **31**: LBA9008.
60. Kaufman, HL, Ruby, CE, Hughes, T, and Slingluff, CL, Jr. (2014). Current status of granulocyte-macrophage colony-stimulating factor in the immunotherapy of melanoma. *J Immunother Cancer* **2**: 11.
61. Herold, G (2014). *Innere Medizin 2014 : eine vorlesungsorientierte Darstellung ; unter Berücksichtigung des Gegenstandskataloges für die ärztliche Prüfung ; mit ICD 10-Schlüssel im Text und Stichwortverzeichnis*, Eigenverl.
62. Simons, E, Ferrari, M, Fricks, J, Wannemuehler, K, Anand, A, Burton, A, *et al.* (2012). Assessment of the 2010 global measles mortality reduction goal: results from a model of surveillance data. *Lancet* **379**: 2173-2178.
63. Tatsuo, H, Ono, N, Tanaka, K, and Yanagi, Y (2000). SLAM (CDw150) is a cellular receptor for measles virus. *Nature* **406**: 893-897.
64. de Vries, RD, Mesman, AW, Geijtenbeek, TB, Duprex, WP, and de Swart, RL (2012). The pathogenesis of measles. *Current opinion in virology* **2**: 248-255.
65. Noyce, RS, Bondre, DG, Ha, MN, Lin, LT, Sisson, G, Tsao, MS, *et al.* (2011). Tumor cell marker PVRL4 (nectin 4) is an epithelial cell receptor for measles virus. *PLoS Pathog* **7**: e1002240.
66. Muhlebach, MD, Mateo, M, Sinn, PL, Prufer, S, Uhlig, KM, Leonard, VH, *et al.* (2011). Adherens junction protein nectin-4 is the epithelial receptor for measles virus. *Nature* **480**: 530-533.
67. Nanche, D, Varior-Krishnan, G, Cervoni, F, Wild, TF, Rossi, B, Rabourdin-Combe, C, *et al.* (1993). Human membrane cofactor protein (CD46) acts as a cellular receptor for measles virus. *Journal of virology* **67**: 6025-6032.

68. Dorig, RE, Marcil, A, Chopra, A, and Richardson, CD (1993). The human CD46 molecule is a receptor for measles virus (Edmonston strain). *Cell* **75**: 295-305.
69. Seya, T, Ballard, LL, Bora, NS, Kumar, V, Cui, W, and Atkinson, JP (1988). Distribution of membrane cofactor protein of complement on human peripheral blood cells. An altered form is found on granulocytes. *Eur J Immunol* **18**: 1289-1294.
70. Cole, JL, Housley, GA, Jr., Dykman, TR, MacDermott, RP, and Atkinson, JP (1985). Identification of an additional class of C3-binding membrane proteins of human peripheral blood leukocytes and cell lines. *Proceedings of the National Academy of Sciences of the United States of America* **82**: 859-863.
71. Buckland, R, and Wild, TF (1997). Is CD46 the cellular receptor for measles virus? *Virus research* **48**: 1-9.
72. Anderson, BD, Nakamura, T, Russell, SJ, and Peng, KW (2004). High CD46 receptor density determines preferential killing of tumor cells by oncolytic measles virus. *Cancer Res* **64**: 4919-4926.
73. Jurianz, K, Ziegler, S, Garcia-Schuler, H, Kraus, S, Bohana-Kashtan, O, Fishelson, Z, *et al.* (1999). Complement resistance of tumor cells: basal and induced mechanisms. *Molecular immunology* **36**: 929-939.
74. Fishelson, Z, Donin, N, Zell, S, Schultz, S, and Kirschfink, M (2003). Obstacles to cancer immunotherapy: expression of membrane complement regulatory proteins (mCRPs) in tumors. *Molecular immunology* **40**: 109-123.
75. Rima, BK, and Duprex, WP (2011). New concepts in measles virus replication: getting in and out in vivo and modulating the host cell environment. *Virus research* **162**: 47-62.
76. Bankamp, B, Wilson, J, Bellini, WJ, and Rota, PA (2005). Identification of naturally occurring amino acid variations that affect the ability of the measles virus C protein to regulate genome replication and transcription. *Virology* **336**: 120-129.
77. Longley, DB, Harkin, DP, and Johnston, PG (2003). 5-Fluorouracil: mechanisms of action and clinical strategies. *Nature reviews Cancer* **3**: 330-338.
78. Graepler, F, Lemken, ML, Wybranietz, WA, Schmidt, U, Smirnow, I, Gross, CD, *et al.* (2005). Bifunctional chimeric SuperCD suicide gene -YCD: YUPRT fusion is highly effective in a rat hepatoma model. *World journal of gastroenterology : WJG* **11**: 6910-6919.
79. Berchtold, S, Lampe, J, Weiland, T, Smirnow, I, Schleicher, S, Handgretinger, R, *et al.* (2013). Innate immune defense defines susceptibility of sarcoma cells to measles vaccine virus-based oncolysis. *Journal of virology* **87**: 3484-3501.
80. Vermes, A, Guchelaar, HJ, and Dankert, J (2000). Flucytosine: a review of its pharmacology, clinical indications, pharmacokinetics, toxicity and drug interactions. *The Journal of antimicrobial chemotherapy* **46**: 171-179.

81. Kanai, F, Kawakami, T, Hamada, H, Sadata, A, Yoshida, Y, Tanaka, T, *et al.* (1998). Adenovirus-mediated transduction of Escherichia coli uracil phosphoribosyltransferase gene sensitizes cancer cells to low concentrations of 5-fluorouracil. *Cancer Res* **58**: 1946-1951.
82. Danenberg, PV (1977). Thymidylate synthetase - a target enzyme in cancer chemotherapy. *Biochimica et biophysica acta* **473**: 73-92.
83. Thorn, CF, Marsh, S, Carrillo, MW, McLeod, HL, Klein, TE, and Altman, RB (2011). PharmGKB summary: fluoropyrimidine pathways. *Pharmacogenetics and genomics* **21**: 237-242.
84. Kuriyama, S, Masui, K, Sakamoto, T, Nakatani, T, Kikukawa, M, Tsujinoue, H, *et al.* (1998). Bystander effect caused by cytosine deaminase gene and 5-fluorocytosine in vitro is substantially mediated by generated 5-fluorouracil. *Anticancer research* **18**: 3399-3406.
85. Nabel, GJ (2013). Designing tomorrow's vaccines. *N Engl J Med* **368**: 551-560.
86. Phuong, LK, Allen, C, Peng, KW, Giannini, C, Greiner, S, TenEyck, CJ, *et al.* (2003). Use of a vaccine strain of measles virus genetically engineered to produce carcinoembryonic antigen as a novel therapeutic agent against glioblastoma multiforme. *Cancer Res* **63**: 2462-2469.
87. Dingli, D, Peng, KW, Harvey, ME, Greipp, PR, O'Connor, MK, Cattaneo, R, *et al.* (2004). Image-guided radiovirotherapy for multiple myeloma using a recombinant measles virus expressing the thyroidal sodium iodide symporter. *Blood* **103**: 1641-1646.
88. Mader, EK, Maeyama, Y, Lin, Y, Butler, GW, Russell, HM, Galanis, E, *et al.* (2009). Mesenchymal stem cell carriers protect oncolytic measles viruses from antibody neutralization in an orthotopic ovarian cancer therapy model. *Clinical cancer research : an official journal of the American Association for Cancer Research* **15**: 7246-7255.
89. Alvarez-Breckenridge, CA, Yu, J, Price, R, Wei, M, Wang, Y, Nowicki, MO, *et al.* (2012). The Histone Deacetylase Inhibitor Valproic Acid Lessens NK Cell Action against Oncolytic Virus-Infected Glioblastoma Cells by Inhibition of STAT5/T-BET Signaling and Generation of Gamma Interferon. *Journal of virology* **86**: 4566-4577.
90. Noll, M, Berchtold, S, Lampe, J, Malek, NP, Bitzer, M, and Lauer, UM (2013). Primary resistance phenomena to oncolytic measles vaccine viruses. *International journal of oncology* **43**: 103-112.
91. Li, H, Peng, KW, and Russell, SJ (2012). Oncolytic measles virus encoding thyroidal sodium iodide symporter for squamous cell cancer of the head and neck radiovirotherapy. *Human gene therapy* **23**: 295-301.
92. Liu, C, Sarkaria, JN, Petell, CA, Paraskevaku, G, Zollman, PJ, Schroeder, M, *et al.* (2007). Combination of measles virus virotherapy and radiation therapy has synergistic activity in the treatment of glioblastoma multiforme. *Clinical cancer research : an official journal of the American Association for Cancer Research* **13**: 7155-7165.
93. Forbes, NE, Abdelbary, H, Lupien, M, Bell, JC, and Diallo, JS (2013). Exploiting tumor epigenetics to improve oncolytic virotherapy. *Frontiers in genetics* **4**: 184.

94. Naik, S, and Russell, SJ (2009). Engineering oncolytic viruses to exploit tumor specific defects in innate immune signaling pathways. *Expert opinion on biological therapy* **9**: 1163-1176.
95. Reikine, S, Nguyen, JB, and Modis, Y (2014). Pattern Recognition and Signaling Mechanisms of RIG-I and MDA5. *Frontiers in immunology* **5**: 342.
96. Akira, S, Uematsu, S, and Takeuchi, O (2006). Pathogen recognition and innate immunity. *Cell* **124**: 783-801.
97. Le Negrate, G (2012). Viral interference with innate immunity by preventing NF-kappaB activity. *Cellular microbiology* **14**: 168-181.
98. Fensterl, V, and Sen, GC (2011). The ISG56/IFIT1 gene family. *Journal of interferon & cytokine research : the official journal of the International Society for Interferon and Cytokine Research* **31**: 71-78.
99. Darnell, JE, Jr., Kerr, IM, and Stark, GR (1994). Jak-STAT pathways and transcriptional activation in response to IFNs and other extracellular signaling proteins. *Science (New York, NY)* **264**: 1415-1421.
100. Diamond, MS, and Farzan, M (2013). The broad-spectrum antiviral functions of IFIT and IFITM proteins. *Nature reviews Immunology* **13**: 46-57.
101. Shingai, M, Ebihara, T, Begum, NA, Kato, A, Honma, T, Matsumoto, K, *et al.* (2007). Differential type I IFN-inducing abilities of wild-type versus vaccine strains of measles virus. *Journal of immunology (Baltimore, Md : 1950)* **179**: 6123-6133.
102. Nanche, D, Yeh, A, Eto, D, Manchester, M, Friedman, RM, and Oldstone, MB (2000). Evasion of host defenses by measles virus: wild-type measles virus infection interferes with induction of Alpha/Beta interferon production. *Journal of virology* **74**: 7478-7484.
103. Ruf, B, Berchtold, S, Venturelli, S, Burkard, M, Smirnow, I, Prenzel, T, *et al.* (2015). Combination of the oral histone deacetylase inhibitor resminostat with oncolytic measles vaccine virus as a new option for epi-virotherapeutic treatment of hepatocellular carcinoma. *Molecular Therapy — Oncolytics* **2**: 15019.
104. Kazantsev, AG, and Thompson, LM (2008). Therapeutic application of histone deacetylase inhibitors for central nervous system disorders. *Nature reviews Drug discovery* **7**: 854-868.
105. Bolden, JE, Peart, MJ, and Johnstone, RW (2006). Anticancer activities of histone deacetylase inhibitors. *Nature reviews Drug discovery* **5**: 769-784.
106. Thiagalingam, S, Cheng, KH, Lee, HJ, Mineva, N, Thiagalingam, A, and Ponte, JF (2003). Histone deacetylases: unique players in shaping the epigenetic histone code. *Ann N Y Acad Sci* **983**: 84-100.
107. Lund, AH, and van Lohuizen, M (2004). Epigenetics and cancer. *Genes & development* **18**: 2315-2335.
108. Baylin, SB, and Ohm, JE (2006). Epigenetic gene silencing in cancer - a mechanism for early oncogenic pathway addiction? *Nature reviews Cancer* **6**: 107-116.
109. Bolden, JE, Shi, W, Jankowski, K, Kan, CY, Cluse, L, Martin, BP, *et al.* (2013). HDAC inhibitors induce tumor-cell-selective pro-apoptotic transcriptional responses. *Cell death & disease* **4**: e519.

110. Ellis, L, Atadja, PW, and Johnstone, RW (2009). Epigenetics in cancer: targeting chromatin modifications. *Molecular cancer therapeutics* **8**: 1409-1420.
111. Whittaker, SJ, Demierre, MF, Kim, EJ, Rook, AH, Lerner, A, Duvic, M, *et al.* (2010). Final results from a multicenter, international, pivotal study of romidepsin in refractory cutaneous T-cell lymphoma. *Journal of clinical oncology : official journal of the American Society of Clinical Oncology* **28**: 4485-4491.
112. Piekarz, RL, Frye, R, Turner, M, Wright, JJ, Allen, SL, Kirschbaum, MH, *et al.* (2009). Phase II multi-institutional trial of the histone deacetylase inhibitor romidepsin as monotherapy for patients with cutaneous T-cell lymphoma. *Journal of clinical oncology : official journal of the American Society of Clinical Oncology* **27**: 5410-5417.
113. Slingerland, M, Guchelaar, HJ, and Gelderblom, H (2014). Histone deacetylase inhibitors: an overview of the clinical studies in solid tumors. *Anti-cancer drugs* **25**: 140-149.
114. Lane, AA, and Chabner, BA (2009). Histone deacetylase inhibitors in cancer therapy. *Journal of clinical oncology : official journal of the American Society of Clinical Oncology* **27**: 5459-5468.
115. Marchion, D, and Munster, P (2007). Development of histone deacetylase inhibitors for cancer treatment. *Expert review of anticancer therapy* **7**: 583-598.
116. Hrabeta, J, Stiborova, M, Adam, V, Kizek, R, and Eckschlager, T (2014). Histone deacetylase inhibitors in cancer therapy. A review. *Biomedical papers of the Medical Faculty of the University Palacky, Olomouc, Czechoslovakia* **158**: 161-169.
117. Rudek, MA, Zhao, M, He, P, Hartke, C, Gilbert, J, Gore, SD, *et al.* (2005). Pharmacokinetics of 5-azacitidine administered with phenylbutyrate in patients with refractory solid tumors or hematologic malignancies. *Journal of clinical oncology : official journal of the American Society of Clinical Oncology* **23**: 3906-3911.
118. Griffiths, EA, and Gore, SD (2008). DNA methyltransferase and histone deacetylase inhibitors in the treatment of myelodysplastic syndromes. *Seminars in hematology* **45**: 23-30.
119. Cecconi, D, Donadelli, M, Dalla Pozza, E, Rinalducci, S, Zolla, L, Scupoli, MT, *et al.* (2009). Synergistic effect of trichostatin A and 5-aza-2'-deoxycytidine on growth inhibition of pancreatic endocrine tumour cell lines: a proteomic study. *Proteomics* **9**: 1952-1966.
120. Catalano, MG, Poli, R, Pugliese, M, Fortunati, N, and Boccuzzi, G (2007). Valproic acid enhances tubulin acetylation and apoptotic activity of paclitaxel on anaplastic thyroid cancer cell lines. *Endocrine-related cancer* **14**: 839-845.
121. Pei, X-Y, Dai, Y, and Grant, S (2004). Synergistic induction of oxidative injury and apoptosis in human multiple myeloma cells by the proteasome inhibitor bortezomib and histone deacetylase inhibitors. *Clinical Cancer Research* **10**: 3839-3852.

122. Badros, A, Burger, AM, Philip, S, Niesvizky, R, Kolla, SS, Goloubeva, O, *et al.* (2009). Phase I study of vorinostat in combination with bortezomib for relapsed and refractory multiple myeloma. *Clinical Cancer Research* **15**: 5250-5257.
123. Dasmahapatra, G, Lembersky, D, Son, MP, Attkisson, E, Dent, P, Fisher, RI, *et al.* (2011). Carfilzomib interacts synergistically with histone deacetylase inhibitors in mantle cell lymphoma cells in vitro and in vivo. *Molecular cancer therapeutics* **10**: 1686-1697.
124. Rasheed, W, Bishton, M, Johnstone, RW, and Prince, HM (2008). Histone deacetylase inhibitors in lymphoma and solid malignancies.
125. Camphausen, K, and Tofilon, PJ (2007). Inhibition of histone deacetylation: a strategy for tumor radiosensitization. *Journal of clinical oncology : official journal of the American Society of Clinical Oncology* **25**: 4051-4056.
126. Coradini, D, and Speranza, A (2005). Histone deacetylase inhibitors for treatment of hepatocellular carcinoma. *Acta pharmacologica Sinica* **26**: 1025-1033.
127. Brunetto, AT, Ang, JE, Lal, R, Olmos, D, Molife, LR, Kristeleit, R, *et al.* (2013). First-in-human, pharmacokinetic and pharmacodynamic phase I study of Resminostat, an oral histone deacetylase inhibitor, in patients with advanced solid tumors. *Clinical cancer research : an official journal of the American Association for Cancer Research* **19**: 5494-5504.
128. Venturelli, S, Armeanu, S, Pathil, A, Hsieh, CJ, Weiss, TS, Vonthein, R, *et al.* (2007). Epigenetic combination therapy as a tumor-selective treatment approach for hepatocellular carcinoma. *Cancer* **109**: 2132-2141.
129. Armeanu, S, Pathil, A, Venturelli, S, Mascagni, P, Weiss, TS, Gottlicher, M, *et al.* (2005). Apoptosis on hepatoma cells but not on primary hepatocytes by histone deacetylase inhibitors valproate and ITF2357. *Journal of hepatology* **42**: 210-217.
130. Kitazono, S, Fujiwara, Y, Nakamichi, S, Mizugaki, H, Nokihara, H, Yamamoto, N, *et al.* (2015). A phase I study of resminostat in Japanese patients with advanced solid tumors. *Cancer Chemother Pharmacol* **75**: 1155-1161.
131. Bitzer, M, Mais, A, Hauns, B, Asche, J, Herz, T, Pegoraro, S, *et al.* (2013). Subgroup analysis of prognostic factors for overall survival in the SHELTER trial evaluating resminostat in advanced hepatocellular carcinoma (HCC). *European Journal of Cancer* **Volume 49** 2.601.
132. Bitzer, M, Horgler, M, Giannini, EG, Ganten, TM, Worns, MA, Siveke, JT, *et al.* (2016). Resminostat in combination with sorafenib as second-line therapy of advanced hepatocellular carcinoma - The SHELTER Study. *Journal of hepatology*.
133. Walewski, J, Borsaru, G, Moicean, A, Hellmann, A, Janikova, A, Hauns, B, *et al.* (2012). Efficient HDAC inhibition and TARC reduction in patients with refractory Hodgkin's lymphoma treated with Resminostat PK/PD data from the Phase II SAPHIRE study. *Journal of the European Hematology Association* **97**: 83.

134. Schulze-Bergkamen, H, Jaeger, D, Kopp, H-G, Mayer, F, Bitzer, M, Mais, A, *et al.* (2013). Phase I dose escalation of the oral histone deacetylase inhibitor (HDACi) resminostat in combination with FOLFIRI in colorectal cancer (CRC) patients: The SHORE trial. *ASCO Meeting Abstracts* **31**: 3625.
135. Mandl-Weber, S, Meinel, FG, Jankowsky, R, Oduncu, F, Schmidmaier, R, and Baumann, P (2010). The novel inhibitor of histone deacetylase resminostat (RAS2410) inhibits proliferation and induces apoptosis in multiple myeloma (MM) cells. *British journal of haematology* **149**: 518-528.
136. Bitzer, M, Ganten, TM, Woerns, MA, Siveke, JT, Dollinger, MM, Scheulen, ME, *et al.* (2013). Resminostat in advanced hepatocellular carcinoma (HCC): Overall survival subgroup analysis of prognostic factors in the SHELTER trial. *ASCO Meeting Abstracts* **31**: e15088.
137. Hamm, S, Prenzel, T, and Henning, S (2015). ITOC2 – 031. Immunomodulatory characteristics of Resminostat, a novel HDAC inhibitor in phase II clinical development. *European Journal of Cancer* **51**: S11.
138. van Baren, N, and Van den Eynde, BJ (2015). Tumoral Immune Resistance Mediated by Enzymes That Degrade Tryptophan. *Cancer immunology research* **3**: 978-985.
139. Becker, JC, Andersen, MH, Schrama, D, and Thor Straten, P (2013). Immune-suppressive properties of the tumor microenvironment. *Cancer Immunol Immunother* **62**: 1137-1148.
140. Kumar, S, Gao, L, Yeagy, B, and Reid, T (2008). Virus combinations and chemotherapy for the treatment of human cancers. *Current opinion in molecular therapeutics* **10**: 371-379.
141. Harrington, KJ, Melcher, A, Vassaux, G, Pandha, HS, and Vile, RG (2008). Exploiting synergies between radiation and oncolytic viruses. *Current opinion in molecular therapeutics* **10**: 362-370.
142. Nguyen, TL, Wilson, MG, and Hiscott, J (2010). Oncolytic viruses and histone deacetylase inhibitors--a multi-pronged strategy to target tumor cells. *Cytokine & growth factor reviews* **21**: 153-159.
143. Nguyen, TL, Abdelbary, H, Arguello, M, Breitbart, C, Leveille, S, Diallo, JS, *et al.* (2008). Chemical targeting of the innate antiviral response by histone deacetylase inhibitors renders refractory cancers sensitive to viral oncolysis. *Proceedings of the National Academy of Sciences of the United States of America* **105**: 14981-14986.
144. Bridle, BW, Chen, L, Lemay, CG, Diallo, JS, Pol, J, Nguyen, A, *et al.* (2013). HDAC inhibition suppresses primary immune responses, enhances secondary immune responses, and abrogates autoimmunity during tumor immunotherapy. *Molecular therapy : the journal of the American Society of Gene Therapy* **21**: 887-894.
145. Noyce, RS, Bondre, DG, Ha, MN, Lin, LT, Sisson, G, and Tsao, MS (2011). Tumor cell marker PVRL4 (nectin 4) is an epithelial cell receptor for measles virus. *PLoS Pathog* **7**: e1002240.
146. MacTavish, H, Diallo, JS, Huang, B, Stanford, M, Le Boeuf, F, De Silva, N, *et al.* (2010). Enhancement of vaccinia virus based oncolysis with histone deacetylase inhibitors. *PloS one*, vol. 5. p e14462.

147. Otsuki, A, Patel, A, Kasai, K, Suzuki, M, Kurozumi, K, Chiocca, EA, *et al.* (2008). Histone deacetylase inhibitors augment antitumor efficacy of herpes-based oncolytic viruses. *Molecular therapy : the journal of the American Society of Gene Therapy* **16**: 1546-1555.
148. Cody, JJ, Markert, JM, and Hurst, DR (2014). Histone deacetylase inhibitors improve the replication of oncolytic herpes simplex virus in breast cancer cells. *PloS one* **9**: e92919.
149. Liu, TC, Castelo-Branco, P, Rabkin, SD, and Martuza, RL (2008). Trichostatin A and oncolytic HSV combination therapy shows enhanced antitumoral and antiangiogenic effects. *Molecular therapy : the journal of the American Society of Gene Therapy* **16**: 1041-1047.
150. Li, J, Bonifati, S, Hristov, G, Marttila, T, Valmary-Degano, S, Stanzel, S, *et al.* (2013). Synergistic combination of valproic acid and oncolytic parvovirus H-1PV as a potential therapy against cervical and pancreatic carcinomas. *EMBO molecular medicine* **5**: 1537-1555.
151. Kitazono, M, Goldsmith, ME, Aikou, T, Bates, S, and Fojo, T (2001). Enhanced adenovirus transgene expression in malignant cells treated with the histone deacetylase inhibitor FR901228. *Cancer Res* **61**: 6328-6330.
152. Höti, N, Chowdhury, W, Hsieh, JT, Sachs, MD, Lupold, SE, and Rodriguez, R (2006). Valproic acid, a histone deacetylase inhibitor, is an antagonist for oncolytic adenoviral gene therapy. *Molecular therapy : the journal of the American Society of Gene Therapy* **14**: 768-778.
153. Hayflick, L (1965). The limited in vitro lifetime of human diploid cell strains. *Experimental Cell Research* **37**: 614-636.
154. Bastidas, O (2013). Cell counting with Neubauer chamber. Celeromics, Tech. Rep.
155. Spearman, C (1908). THE METHOD OF 'RIGHT AND WRONG CASES' ('CONSTANT STIMULI') WITHOUT GAUSS'S FORMULAE. *British Journal of Psychology, 1904-1920* **2**: 227-242.
156. Kärber, G (1931). Beitrag zur kollektiven Behandlung pharmakologischer Reihenversuche. *Archiv f experiment Pathol u Pharmakol* **162**: 480-483.
157. Kolev, M, and Kemper, C (2014). Detection of Cell Membrane-Bound CD46 Using Flow Cytometry. In: Gadjeva, M (ed). *The Complement System*, vol. 1100. Humana Press. pp 329-339.
158. Nicoletti, I, Migliorati, G, Pagliacci, MC, Grignani, F, and Riccardi, C (1991). A rapid and simple method for measuring thymocyte apoptosis by propidium iodide staining and flow cytometry. *Journal of immunological methods* **139**: 271-279.
159. Skehan, P, Storeng, R, Scudiero, D, Monks, A, McMahon, J, Vistica, D, *et al.* (1990). New colorimetric cytotoxicity assay for anticancer-drug screening. *Journal of the National Cancer Institute* **82**: 1107-1112.
160. Vichai, V, and Kirtikara, K (2006). Sulforhodamine B colorimetric assay for cytotoxicity screening. *Nature protocols* **1**: 1112-1116.
161. Rampersad, SN (2012). Multiple applications of Alamar Blue as an indicator of metabolic function and cellular health in cell viability bioassays. *Sensors (Basel, Switzerland)* **12**: 12347-12360.

162. Bradford, MM (1976). A rapid and sensitive method for the quantitation of microgram quantities of protein utilizing the principle of protein-dye binding. *Analytical Biochemistry* **72**: 248-254.
163. Compton, SJ, and Jones, CG (1985). Mechanism of dye response and interference in the Bradford protein assay. *Analytical Biochemistry* **151**: 369-374.
164. Laemmli, UK (1970). Cleavage of Structural Proteins during the Assembly of the Head of Bacteriophage T4. *Nature* **227**: 680-685.
165. Clark, DP, and Pazdernik, NJ (2013). *Molecular Biology*, Academic Press.
166. Lampe, J, Bossow, S, Weiland, T, Smirnow, I, Lehmann, R, Neubert, W, et al. (2013). An armed oncolytic measles vaccine virus eliminates human hepatoma cells independently of apoptosis. *Gene Ther* **20**: 1033-1041.
167. Lange, S, Lampe, J, Bossow, S, Zimmermann, M, Neubert, W, Bitzer, M, et al. (2013). A novel armed oncolytic measles vaccine virus for the treatment of cholangiocarcinoma. *Human gene therapy* **24**: 554-564.
168. Volker, I, Bach, P, Coulibaly, C, Plesker, R, Abel, T, Seifried, J, et al. (2013). Intrahepatic application of suicide gene-armed measles virotherapeutics: a safety study in transgenic mice and rhesus macaques. *Human gene therapy Clinical development* **24**: 11-22.
169. Yurttas, C, Berchtold, S, Malek, NP, Bitzer, M, and Lauer, UM (2014). Pulsed versus continuous application of the prodrug 5-fluorocytosine to enhance the oncolytic effectiveness of a measles vaccine virus armed with a suicide gene. *Human gene therapy Clinical development* **25**: 85-96.
170. Katsura, T, Iwai, S, Ota, Y, Shimizu, H, Ikuta, K, and Yura, Y (2009). The effects of trichostatin A on the oncolytic ability of herpes simplex virus for oral squamous cell carcinoma cells. *Cancer gene therapy* **16**: 237-245.
171. Shulak, L, Beljanski, V, Chiang, C, Dutta, SM, Van Grevenynghe, J, Belgnaoui, SM, et al. (2014). Histone deacetylase inhibitors potentiate vesicular stomatitis virus oncolysis in prostate cancer cells by modulating NF-kappaB-dependent autophagy. *Journal of virology* **88**: 2927-2940.
172. Fields, BN, Knipe, DM, and Howley, PM (2007). *Fields' Virology*, Wolters Kluwer Health/Lippincott Williams & Wilkins.
173. Delpout, S, Noyce, RS, Siu, RW, and Richardson, CD (2012). Host factors and measles virus replication. *Current opinion in virology* **2**: 773-783.
174. Bressac, B, Galvin, KM, Liang, TJ, Isselbacher, KJ, Wands, JR, and Ozturk, M (1990). Abnormal structure and expression of p53 gene in human hepatocellular carcinoma. *Proceedings of the National Academy of Sciences* **87**: 1973-1977.
175. Workenhe, ST, Simmons, G, Pol, JG, Lichty, BD, Halford, WP, and Mossman, KL (2014). Immunogenic HSV-mediated oncolysis shapes the antitumor immune response and contributes to therapeutic efficacy. *Molecular therapy : the journal of the American Society of Gene Therapy* **22**: 123-131.
176. Kim, DR, Park, MY, Lim, HJ, Park, JS, Cho, YJ, Lee, SW, et al. (2012). Combination therapy of conditionally replicating adenovirus and histone deacetylase inhibitors. *International journal of molecular medicine* **29**: 218-224.

177. Lecouturier, V, Fayolle, J, Caballero, M, Carabaña, J, Celma, ML, Fernandez-Munoz, R, *et al.* (1996). Identification of two amino acids in the hemagglutinin glycoprotein of measles virus (MV) that govern hemadsorption, HeLa cell fusion, and CD46 downregulation: phenotypic markers that differentiate vaccine and wild-type MV strains. *Journal of virology* **70**: 4200-4204.
178. Welstead, GG, Hsu, EC, Iorio, C, Bolotin, S, and Richardson, CD (2004). Mechanism of CD150 (SLAM) down regulation from the host cell surface by measles virus hemagglutinin protein. *Journal of virology* **78**: 9666-9674.
179. Kotredes, KP, and Gamero, AM (2013). Interferons as inducers of apoptosis in malignant cells. *Journal of interferon & cytokine research : the official journal of the International Society for Interferon and Cytokine Research* **33**: 162-170.
180. Indraccolo, S (2010). Interferon-alpha as angiogenesis inhibitor: learning from tumor models. *Autoimmunity* **43**: 244-247.
181. Hervas-Stubbs, S, Perez-Gracia, JL, Rouzaut, A, Sanmamed, MF, Le Bon, A, and Melero, I (2011). Direct effects of type I interferons on cells of the immune system. *Clinical cancer research : an official journal of the American Association for Cancer Research* **17**: 2619-2627.
182. Dunn, GP, Koebel, CM, and Schreiber, RD (2006). Interferons, immunity and cancer immunoediting. *Nature reviews Immunology* **6**: 836-848.
183. Stojdl, DF, Lichty, BD, tenOever, BR, Paterson, JM, Power, AT, Knowles, S, *et al.* (2003). VSV strains with defects in their ability to shutdown innate immunity are potent systemic anti-cancer agents. *Cancer cell* **4**: 263-275.
184. Stewart, CE, Randall, RE, and Adamson, CS (2014). Inhibitors of the interferon response enhance virus replication in vitro. *PloS one* **9**: e112014.
185. Nusinzon, I, and Horvath, CM (2006). Positive and negative regulation of the innate antiviral response and beta interferon gene expression by deacetylation. *Molecular and cellular biology* **26**: 3106-3113.
186. Chang, HM, Paulson, M, Holko, M, Rice, CM, Williams, BR, Marie, I, *et al.* (2004). Induction of interferon-stimulated gene expression and antiviral responses require protein deacetylase activity. *Proceedings of the National Academy of Sciences of the United States of America* **101**: 9578-9583.
187. Nusinzon, I, and Horvath, CM (2003). Interferon-stimulated transcription and innate antiviral immunity require deacetylase activity and histone deacetylase 1. *Proceedings of the National Academy of Sciences* **100**: 14742-14747.
188. Pichlmair, A, Lassnig, C, Eberle, CA, Gorna, MW, Baumann, CL, Burkard, TR, *et al.* (2011). IFIT1 is an antiviral protein that recognizes 5'-triphosphate RNA. *Nature immunology* **12**: 624-630.
189. Liikanen, I, Monsurrò, V, Ahtiainen, L, Raki, M, Hakkarainen, T, Diaconu, I, *et al.* (2011). Induction of Interferon Pathways Mediates In Vivo Resistance to Oncolytic Adenovirus. *Molecular therapy : the journal of the American Society of Gene Therapy* **19**: 1858-1866.
190. Wojton, J, and Kaur, B (2010). Impact of tumor microenvironment on oncolytic viral therapy. *Cytokine & growth factor reviews* **21**: 127-134.

191. Mogensen, TH (2009). Pathogen Recognition and Inflammatory Signaling in Innate Immune Defenses. *Clinical Microbiology Reviews* **22**: 240-273.
192. Wang, C, Liu, X, Liu, Y, Zhang, Q, Yao, Z, Huang, B, *et al.* (2013). Zinc finger protein 64 promotes Toll-like receptor-triggered proinflammatory and type I interferon production in macrophages by enhancing p65 subunit activation. *J Biol Chem* **288**: 24600-24608.
193. Liu, TC, Galanis, E, and Kirn, D (2007). Clinical trial results with oncolytic virotherapy: a century of promise, a decade of progress. *Nature clinical practice Oncology* **4**: 101-117.
194. Prestwich, RJ, Errington, F, Ilett, EJ, Morgan, RS, Scott, KJ, Kottke, T, *et al.* (2008). Tumor infection by oncolytic reovirus primes adaptive antitumor immunity. *Clinical cancer research : an official journal of the American Association for Cancer Research* **14**: 7358-7366.
195. Steele, L, Errington, F, Prestwich, R, Ilett, E, Harrington, K, Pandha, H, *et al.* (2011). Pro-inflammatory cytokine/chemokine production by reovirus treated melanoma cells is PKR/NF-kappaB mediated and supports innate and adaptive anti-tumour immune priming. *Mol Cancer* **10**: 20.
196. Tang, D, Kang, R, Coyne, CB, Zeh, HJ, and Lotze, MT (2012). PAMPs and DAMPs: signal 0s that spur autophagy and immunity. *Immunological reviews* **249**: 158-175.
197. Guo, ZS, Liu, Z, and Bartlett, DL (2014). Oncolytic Immunotherapy: Dying the Right Way is a Key to Eliciting Potent Antitumor Immunity. *Frontiers in oncology* **4**: 74.
198. Grote, D, Cattaneo, R, and Fielding, AK (2003). Neutrophils contribute to the measles virus-induced antitumor effect: enhancement by granulocyte macrophage colony-stimulating factor expression. *Cancer Res* **63**: 6463-6468.
199. Myers, RM, Greiner, SM, Harvey, ME, Griesmann, G, Kuffel, MJ, Buhrow, SA, *et al.* (2007). Preclinical pharmacology and toxicology of intravenous MV-NIS, an oncolytic measles virus administered with or without cyclophosphamide. *Clin Pharmacol Ther* **82**: 700-710.
200. Zamarin, D, Holmgaard, RB, Subudhi, SK, Park, JS, Mansour, M, Palese, P, *et al.* (2014). Localized oncolytic virotherapy overcomes systemic tumor resistance to immune checkpoint blockade immunotherapy. *Science translational medicine* **6**: 226ra232.
201. Engeland, CE, Grossardt, C, Veinalde, R, Bossow, S, Lutz, D, Kaufmann, JK, *et al.* (2014). CTLA-4 and PD-L1 checkpoint blockade enhances oncolytic measles virus therapy. *Molecular therapy : the journal of the American Society of Gene Therapy* **22**: 1949-1959.

Publication list

Publications in peer-reviewed journals

1. Ruf, B, and Lauer, U (2015). Assessment of current virotherapeutic application schemes: “Hit hard and early” versus “Killing softly”? *Molecular Therapy — Oncolytics 2: 150018*.
2. Ruf, B, Berchtold, S, Venturelli, S, Burkard, M, Smirnow, I, Prenzel, T, et al. (2015). Combination of the oral histone deacetylase inhibitor resminostat with oncolytic measles vaccine virus as a new option for epi-virotherapeutic treatment of hepatocellular carcinoma. *Molecular Therapy — Oncolytics 2: 150019*.

Abstracts/Posters

1. Ruf, B, Berchtold, S, Venturelli, S, Smirnow, I, Prenzel, T, Henning, S, et al. (2015). Combination of the oral histone deacetylase inhibitor resminostat with oncolytic measles vaccine virus as a new option for epi-virotherapeutic treatment of hepatocellular carcinoma (HCC). *Z Gastroenterol 53: KG242. Meeting abstract of the annual conference of the German Society for Digestive and Metabolic Diseases (DGVS) 2015 in Leipzig, Germany*.
2. Ruf, B, Berchtold, S, Malek, NP, Venturelli, S, and Lauer, U (2014). “Epi-Virotherapy”: Combination therapy with the oral Histone-Deacetylase Inhibitor Resminostat® and the Oncolytic Measles Vaccine Virus MeV-SCD as a new option for the treatment of hepatocellular carcinoma. *Poster presentation at the annual research colloquium of the Faculty of Medicine in Tübingen, Germany*.

Oral presentations/scientific talks

1. Ruf, B, Berchtold, S, Venturelli, S, and Lauer, U (2015). Kombinationstherapie des oralen Histon-Deacetylase-Inhibitors Resminostat mit einem onkolytischen Masern-Impfvirus als neue epi-virotherapeutische Behandlungsoption für das Hepatozelluläre Karzinom (HCC). *Scientific talk at the annual conference of the German Society for Digestive and Metabolic Diseases (DGVS) 2015 in Leipzig, Germany.*
2. Ruf, B, Berchtold, S, Venturelli, S, and Lauer, U (2014). Combination therapy of the oral pan-Histone-Deacetylase-Inhibitor Resminostat® with oncolytic Measles Vaccine Virus as a new epi-virotherapeutic option for the treatment of hepatocellular carcinoma (HCC). *Invited talk at 4SC AG; Planegg-Martinsried, Germany.*

Erklärungen zum Eigenanteil

Erklärungen zum Eigenanteil der Publikationen

1. Ruf, B, and Lauer, UM (2015). **Assessment of current virotherapeutic application schemes: “Hit hard and early” versus “Killing softly”?** *Molecular Therapy Oncolytics 2: 150018*.

Herr Prof. Dr. Lauer war an der Konzeption der Studie beteiligt, er hat die Arbeit betreut, war in die Ausgestaltung der Abbildungen involviert und hat das Manuskript bearbeitet und korrigiert.

Herr Ruf hat die Datenbankrecherche und das Zusammentragen der virotherapeutischen Studien durchgeführt, hat die Übersichtsabbildungen erstellt und hat den ersten Entwurf für das Manuskript selbständig verfasst und in der Folge die Korrekturen des Manuskriptes bearbeitet und das Manuskript in die finale Fassung gebracht und abschließend das Manuskript zur Veröffentlichung eingereicht.

2. Ruf, B, Berchtold, S, Venturelli, S, Burkard, M, Smirnow, I, Prenzel, T, Henning, SW, Lauer, UM, (2015). **Combination of the oral histone deacetylase inhibitor resminostat with oncolytic measles vaccine virus as a new option for epi-virotherapeutic treatment of hepatocellular carcinoma.** *Molecular Therapy — Oncolytics 2: 150019*.

Frau Dr. Berchtold war an der Konzeption der Studie beteiligt, hat die Arbeit betreut und das Manuskript korrigiert. Frau Dr. Berchtold hat die RNA-Isolation durchgeführt, deren Ergebnisse in Abbildung 5 des Manuskriptes dargestellt sind, war an den Western-Blot-Versuchen beteiligt, die in Abbildung 7 gezeigt sind, und war verantwortlich für die TMRE-Versuche (Supplementary figure 1 B). Frau Dr. Berchtold steuerte ebenso die Daten zur Behandlung primärer Hepatozyten (Fig. 2, Abbildung rechts unten) bei.

Herr Dr. Dr. Venturelli war an der Konzeption der Zellzyklus-Versuche beteiligt (Fig. 6) und hat die Daten der xCELLigence-Versuche, die in Abbildung S1 (C + D) dargestellt sind, zur Verfügung gestellt. Zudem hat er das Manuskript korrigiert.

Herr Dr. Burkard war an den xCELLigence-Versuchen beteiligt (Supplementary figure 1 C + D) und hat deren Daten zur Verfügung gestellt.

Frau Smirnow (MTA) war zu Teilen jeweils an der Durchführung der Western-Blot und der xCELLigence-Versuche beteiligt, die in Abbildung 7 bzw. Abbildung S1 (C + D) gezeigt sind.

Herr Dr. Henning und Frau Dr. Prenzel waren verantwortlich für die Durchführung der RT-qPCR-Versuche, haben gemeinsam mit Frau Dr. S. Berchtold die zugehörigen Daten zur Verfügung gestellt, die in Abbildung 5 gezeigt werden. Beide haben das Manuskript korrigiert.

Herr Prof. Lauer war an der Konzeption der Studie beteiligt, hat die Arbeit betreut und hat das Manuskript korrigiert.

Herr Ruf hat die Versuche 1, 2, 3, 4, 6, 7, S1A und deren Auswertung durchgeführt und die dazugehörigen Abbildungen erstellt (zudem Supplementary figure 2). Herr Ruf war an der Konzeption der Studie beteiligt, hat die Literaturrecherche durchgeführt und hat den ersten Entwurf des Manuskriptes selbständig verfasst und hat in der Folge die Korrekturen des Manuskriptes bearbeitet und das Manuskript in die finale Fassung gebracht und abschließend das Manuskript zur Veröffentlichung eingereicht.

Erklärung zum Eigenanteil der Dissertationsschrift

Die vorliegende Arbeit wurde in der Medizinischen Universitätsklinik, Abteilung für Innere Medizin VIII, in der Arbeitsgruppe Virotherapie unter Betreuung von Herrn Prof. Dr. U.M. Lauer durchgeführt.

Die Konzeption der Studie erfolgte durch Herrn Prof. Dr. U.M. Lauer in Zusammenarbeit mit Frau Dr. S. Berchtold (wiss. Mitarbeiterin).

Sämtliche Versuche - mit unten stehenden Ausnahmen - wurden (nach Einarbeitung durch Frau I. Smirnow, MTA) von mir eigenständig durchgeführt.

Der RT-qPCR-Versuch, abgebildet in Figure 3.12, wurde von Frau Dr. S. Berchtold in Kooperation mit Frau Dr. T. Prenzel und Herrn Dr. S.W. Henning (*beide 4SC AG, Planegg-Martinsried*) durchgeführt. Frau Berchtold steuerte ebenso die Daten zur Behandlung primärer Hepatozyten (Fig. 3.4, letzte Zeile) bei und war gemeinsam mit Frau I. Smirnow an den Western-Blot-Versuchen mitbeteiligt.

Die statistische Auswertung erfolgte selbständig durch mich (nach entsprechender Beratung durch das Institut für Biometrie).

Ich versichere, das Manuskript selbständig (nach Anleitung durch Frau Dr. S. Berchtold und Prof. U.M. Lauer) verfasst zu haben und keine weiteren als die von mir angegebenen Quellen verwendet zu haben.

Tübingen, den

Danksagung

Ein herzliches Dankeschön möchte ich allen aussprechen, die mich auf dem Weg diese Arbeit anzufertigen unterstützt und zum guten Gelingen beigetragen haben.

Zu allererst möchte ich mich bei meinem Doktorvater, Herrn Prof. Dr. Ulrich M. Lauer, bedanken für die Überlassung des Themas, die freundliche Aufnahme in seine Arbeitsgruppe und die Bereitstellung der nötigen Mittel. Sein persönliches Engagement, sein wissenschaftliches Interesse und die intensive persönliche Förderung werden mir immer ein Vorbild sein.

Herrn Prof. Dr. Stefan Beckert und Herrn Prof. Dr. Jean Rommelaere vom DKFZ in Heidelberg danke ich für die Erstellung der Gutachten zu dieser Disseratationsschrift.

Nicht genug danken kann ich Frau Dr. Susanne Berchtold für die ganz außergewöhnliche persönliche Betreuung. Ihre Einsatzbereitschaft, Unermüdbarkeit und Geduld -wenn es um eines ihrer „Kinder“ geht- suchen sicherlich ihresgleichen.

Herr Dr. Markus Burkard, Herr Dr. Dr. Sascha Venturelli und Herr Christian Leischner hatten ebenfalls jederzeit ein offenes Ohr, waren stets bereit für anregende Diskussionen und haben einen großen Anteil an der Durchführung einzelner Versuche sowie der Erstellung des Papers.

Andrea Schenk, Irina Smirnow und Christine Geisler waren für mich Herz & Seele des Labors. Vielen Dank für die Organisationsarbeit, die Unterstützung bei zahlreichen Versuchen und eure Hilfe, immer wenn der „Bub“ nicht weiter wusste. Die herzliche Atmosphäre im Labor, aber auch die netten Kaffeepausen haben die Zeit bei euch ganz besonders gemacht.

Vielen Dank für die gute Zusammenarbeit auch den anderen Doktoranden der Arbeitsgruppe: Can Yurttas, Verena May, Eike Binz, Luisa Köllhofer, Franziska Herster, Silvia Gross, Tim-Patrick Ellerhoff und Gabriel Scheubeck.

Ebenso bedanke ich mich bei den Mitarbeitern der Firma 4SC in Martinsried, namentlich Frau Dr. Tanja Wulff und Herrn Dr. Stefan W. Henning, für die Einladung zur Vorstellung der Ergebnisse, für die gute Zusammenarbeit bei der Durchführung der qPCR-Versuche und die Hilfe bei der Ausarbeitung des Papers.

Außerhalb der Welt des Labors haben meine großartigen Freunde ganz maßgeblich zum Gelingen dieser Arbeit beigetragen, da sie für den nötigen Ausgleich gesorgt haben und auch immer ein Ansporn gewesen sind um durchzuhalten.

Mein ganz besonderer Dank gilt jedoch meiner Familie. Meinen Eltern, meiner Oma und meiner Schwester Kathi, die mich auf meinem bisherigen Lebensweg jederzeit und in jeder erdenklichen Form unterstützt haben. Ohne eure moralische Unterstützung, euer Verständnis und eure Zuneigung wäre all dies nicht möglich gewesen. Danke!